Calibration of Automatic Network Analysis and Computer Aided Microwave Measurement

Jeffrey S. Kasten

Center for Communications and Signal Processing
Department of Electrical and Computer Engineering
North Carolina State University

CCSP TR-90/2

Table of Contents

Chapter 1

Introduction

1.1 Motivation

Computer technology increases each year and we can associate this to the increased computational power. These increases are spawned by increased clock speeds and data rates that require knowledge of transmission line effects to successfully design and fabricate systems. It has come to the attention of an ever increasing number of people that we must include effects such as transmission line discontinuities or at the very least delay associated with the lines. There exist two methods of predicting these effects. One, the discontinuity can be studied analytically by calculating its parameters based on electromagnetic field theory; analytic modeling. Two, the discontinuity parameters are measured; empirical model. Analytic models provide a compact representation of the discontinuity yet they still require experimental verification. So regardless of the modeling method chosen, measurement of transmission line effects is required.

The discontinuity parameters can be described with scattering parameters (s parameters) and measurement of scattering parameters is a well define process. S parameters are measured with a network analyzer where by a single frequency sinu-

soid is applied to the network and energy reflected from and transmitted through the network define its s parameters. The introduction of the Automatic Network Analyzer (ANA), has given engineers the measurement tool needed to study transmission line effects with high degree of accuracy.

Inherent to ANA's is the ability to remove systematic error by measuring several known networks (standards). This process is referred to by several names; calibration, error correction or de-embedding. The calibration of automatic network analysis is a general concept that has direct application to the ANA's and in this study we consider its application to the measurement of Printed Circuit Board (PCB) discontinuities.

The ANA calibration is done with coaxial standards but PCB transmission line structures are microstrip or stripline. This requires adaption from coaxial to PCB structures and this introduces systematic error. The premise of PCB error correction is to determine the error associated with this adaption and remove it. An application of ANA calibration could produce this result, however, manufacturing of printed circuit boards imparts limitation.

First it is necessary to measure many different structures on several PCB's such that manufacturing variations can be included, this requires a large number of measurements. Additionally, PCB manufacturing does not allow insertion of calibration standards without physically altering the board, i.e. destructive measurements such as cutting the board and inserting conventional standards.

Again, emphasizing the number of measurements needed is large therefore we need a non-destructive calibration method. Fortunately PCB manufacturing offers an important property. They are manufactured with repeatable uniformity on an individual board. With this in mind we are motivated to investigate PCB calibration.

Calibration of automatic network analysis has been a popular research area over the last two decades. Fig. 1.1.1 is an indication of past research effort and potential research. The graph indicates three regions of popularity. First, the late 1960's when the automatic network analyzer was introduced, second early to mid 1970's study of ANA calibration methods and third, early 1980's to future, study of fixture calibration methods. Our intention is to contribute to the rapid growth of fixture calibration methods by developing methods that address printed circuit board fixture calibration. In the following section we provide an overview of this report.

1.2 Thesis Overview

The purpose of this report is two fold. First, two decades of research has introduce a considerable amount of information concerning calibration of network analysis. The purpose of Chapter 2 is to review calibration methods by organizing this information into two catagories; one and two port calibration. As an introduction to this, we discuss the history of the Automatic Network Analyzer. One port

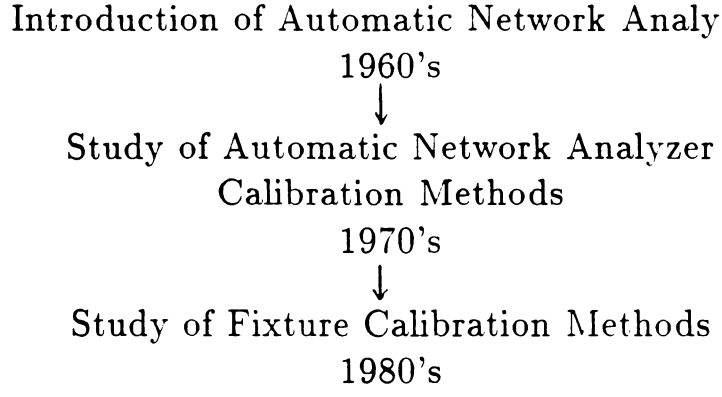

Figure 1.1.1: Graph representing research in calibration of automatic network analysis.

calibration is discussed and concludes with a discussion of previous authors choice of standards and their motivation. Two port calibration begins with a thorough review of ANA error models and concludes with fixture two port models and a discussion about fixture calibration standards. The second focus of this report is application of symmetrical arguments to printed circuit board fixture calibration.

Printed circuit board is a non-insertable measurement medium and is easily calibrated using symmetrical arguments. Chapter 3 defines symmetrical arguments and develops new calibration methods that exploit symmetry. Chapter 5 contains the results from experimental verification the algorithms developed in Chapter 3. Chapter 4 introduces SPANA: Signal Processing of Automatic Network Analysis; the computer program where algorithms are implemented and other various data manipulations are carried out. Finally, we conclude with summary of work accomplished and suggestions for future work in Chapter 6.

This report also contains three appendices. One contains a discussion of decascading error networks and lists the necessary transformations. Another is a user's manual for SPANA giving semantic information about commands that are available. The last appendix discusses the SPANA "shell" command where the reader is lead through an example shell subroutine to show how it can be modified.

1.3 Original Contributions

The original contributions reported here include:

i) the Through-Symmetry-Line de-embedding algorithm whereby symmetric arguments are used to synthesize either open or short circuit reflection coefficients,

ii) the development of Enhanced Through-Symmetry-Line de-embedding algorithm that calculates the complex characteristic impedance of the line standard using the experimentally determined propagation constant and the free-space capacitance of the line standard,

iii) the direct application of this enhancement to the Through-Reflect- Line de-embedding algorithm and Line-Reflect-Line algorithm,

iv) the development of Through-Symmetric Fixture de-embedding algorithm for use on second order symmetric fixtures, and

v) the development of the computer program SPANA for algorithm implementation and other data manipulations.

Chapter 2

Review of Calibration Theory

2.1 Literature Review

The determination of network parameters or network analysis is fundamental to the understanding and design of all microwave systems. It provides a tool for verification of theoretical research and gives design engineers data needed to complete their tasks.

Before the introduction of the network analyzer in the late 1960's, one-port impedance measurements dominated the measurement arena. Slotted lines and graphical interpretation maintained engineers until the development of the network analyzer. It was well understood that impedances could be measured through an unknown junction. If the unknown junction is lossless and represented by an effective impedance, then reflection coefficient measurements with a matched load and short circuit at the output of the junction give sufficient information to determine the unknown impedance. In 1953, Deschamps developed a graphical method to determine impedance if the junction is lossless. Through his result it was possible to determine the unknown impedance by synthesizing the matched load with several offset shorts [1]. A similar process for lossy junctions was introduced by

Storer et al. [2] in 1953, where by the junction parameters (input, output reflection coefficients, and transmission coefficient) could be determined by graphical means. Finally, in 1956 Wentworth and Barthel combined this previous work and introduced a simplified graphical calibration technique [3].

Graphical methods provide invaluable insight into processes that effect microwave measurement yet they are tedious and based on the users interpretation. To advance the state of the art in microwave measurement it was necessary to consider other methods for microwave measurement. In the mid 1960's, scattering parameters (s parameters) began finding use in the circuit design community replacing reflection and transmission coefficients. The need to measure two-port network parameters became increasingly necessary while existing one-port graphical methods provided no extension to two-port measurement. There is little doubt why an automatic means of microwave measurement is essential and history shows that two-port network analysis is inherently calibratable.

In the late 1960's Hackborn introduced the automatic network analyzer [5] (ANA) capable of measuring scattering parameters of two port networks. The ANA produced accurate s parameter measurements and offered calibration as a way to assure accuracy. Calibration was analytic and performed by computer control as compared to previous graphical methods and the automatic measurement significantly increased measurement speed. By modeling the network analyzer systematic error, Hackborn developed the foundation of calibration in use today.

Imperfections in the network analyzer were modeled as deviations from an ideal analyzer and referred to as error representation networks, see Fig. 2.1.1. Error for each ANA port was modeled with a corresponding scattering matrix with four complex parameters and easily represented with a signal flow diagram, see Fig. 2.1.2. Since graphical calibration used known standards e.g. matched load short circuits or offset short circuits, it would seem appropriate to measure similar standards with the new ANA in order to determine the error networks i.e. calibrate. This is exactly what Hackborn did.

First for one port calibration, he measured reflection coefficients with the error network terminated with an ideal short circuit, offset short and sliding matched load. These three measurements were sufficient to determine the error network and repeating this procedure for the second port gave six calibration terms (error s parameters or products . This result was sufficient for one port measurements on either ANA port but for full two port measurements two additional calibration terms needed to be calculated. A measurement of forward and reverse transmission coefficients with the error networks connected together (through connection) completed the two port calibration procedure. Finally, the removal of the error involved an iterative solution of nonlinear equations based on the signal flow diagram of the device placed between the port error networks. Soon after this work was published, Kruppa and Sodomsky revealed that Hackborn's iterative solution was in fact explicit [8].

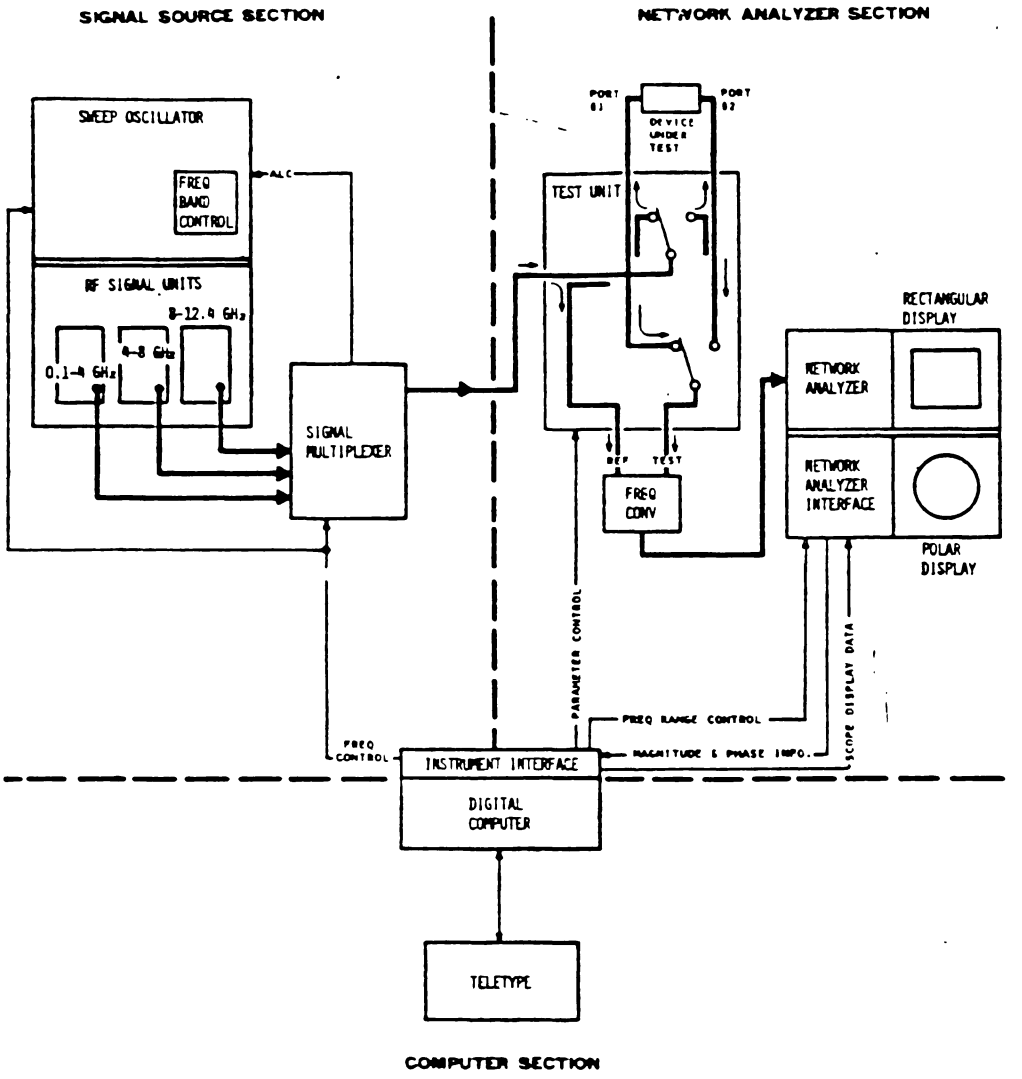

Figure 2.1.1: Automatic Network Analyzer (ANA) for measuring scattering of two port networks, after Hackborn, 1968.

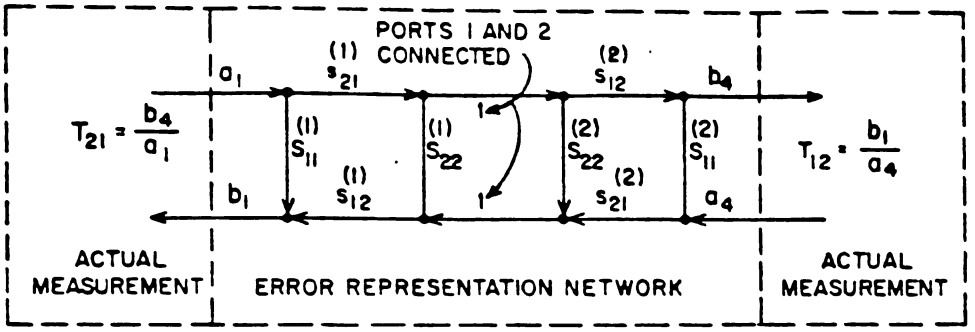

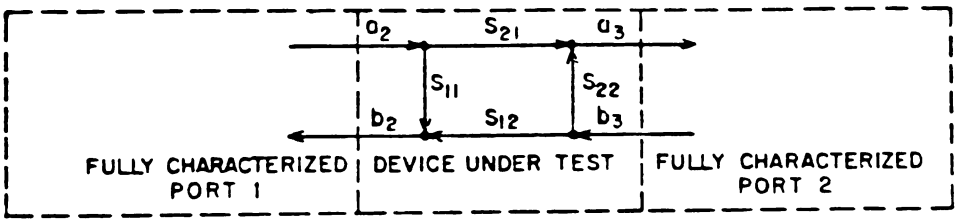

Figure 2.1.2: Signal flow graph representation of the ANA measurement error. Error networks corrupt ideal ANA, after Hackborn, 1968.

Since the introduction of Hackborn's ANA many authors have considered its use and studied network analyzers of different component topologies. Hackborn's error models have stood the test of time only receiving minor improvements. His contributions include one and two port error models represented by signal flow diagrams and calibration algorithm for removing these errors.

The history of network analysis calibration shows a significant change as methods of network analyzer calibration became widely accepted. At this point, authors began considering fixture calibration rather than ANA calibration since many devices to be measured were in transmission media that was of dissimilar geometry than the analyzer i.e. planar devices and coaxial analyzers. One and two port error models were still valid only the physical interpretation of the error terms changed. This resulted in direct application of network analyzer calibration methods to fixture measurements. However this was only moderately successful and new procedures were developed.

2.1.1 Introduction to Calibration of Network Analysis

For a thorough study of the calibration of network analysis, we need to investigate subtopics that form the calibration process. First we must look at one port measurements and discuss general methods of accomplishing one port calibration followed by a review of previous investigators. Second we expand one port results to two port and discuss the motivation of major contributors who evolved the

Hackborn error model.

2.1.2 The One Port Error Model

The measurement of reflection coefficients or impedance at microwave frequencies requires the determination of systematic error and then removing it i.e. calibrating. Here we state one port calibration in a general fashion and then review calibration methods developed by previous authors. The Hackborn one port error model shown in Fig. 2.1.3, has been examined by many authors. The measured reflection coefficient ρ_M is related to the desired reflection coefficient ρ_L by the familiar bilinear transform.

$$\rho_M = \frac{e_{00} - \rho_L \Delta e}{1 - \rho_L e_{11}} \tag{2.1.1}$$

Rearranging,

$$\rho_L = \frac{e_{00} - \rho_M}{\Delta e - e_{11}\rho_M} \tag{2.1.2}$$

$$\Delta e = e_{00}e_{11} - e_{01}e_{10} \tag{2.1.3}$$

we can see that the desired reflection coefficient is altered by the error network which is comprised of scattering parameters e_{00}, e_{11}, and the product $e_{01}e_{10}$. Two methods exit for calculating the error network; classical three termination and redundant terminations, or the impedance associated with ρ_L can be determine without calculating the error network by using properties of the bilinear transform. Let us consider these in more detail.

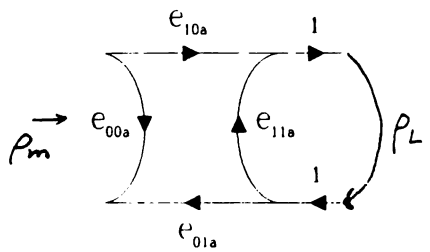

Figure 2.1.3: Signal flow graph for one port error network. Desired load reflection coefficient ρ_l is masked by error coefficients e_{ij} and ρ_m is the measured reflection coefficient.

Classical Result of One Port Calibration

Classical one port calibration is the calculation of these terms based on measurements made with three known terminations (standards) connected to the reference plane. The standards have associated reflection coefficients Γ_1, Γ_2 and Γ_3 and corresponding measured reflection coefficients M_1, M_2 and M_3. These reflection coefficients along with equation 2.1.2 form three simultaneous equations for the error terms with the solution:

$$e_{11} = \frac{A - 1}{A\Gamma_3 - \Gamma_2} \tag{2.1.4}$$

$$e_{01}e_{10} = \frac{(M_2 - M_1)(1 - e_{11}\Gamma_1)(1 - e_{11}\Gamma_2)}{\Gamma_2 - \Gamma_1} \tag{2.1.5}$$

and

$$e_{00} = M_1 - \frac{e_{01}e_{10}\Gamma_1}{1 - e_{11}} \tag{2.1.6}$$

with

$$A = \left(\frac{\Gamma_2 - \Gamma_1}{\Gamma_3 - \Gamma_2}\right)\left(\frac{M_3 - M_1}{M_2 - M_1}\right) \tag{2.1.7}$$

A final measurement and evaluation of 2.1.2 with the desired load in place yields the error corrected reflection coefficient. When a sweep frequency measurement is required, these error terms are calculated for each frequency thereby providing an error corrected reflection coefficient versus frequency.

Use of Redundant Standards

Three standards are necessary and sufficient but sensitive to experimental error. In 1974 Bauer and Penfield developed the use of redundant standards to improve

the calibration accuracy [9]. Although their results utilized impedance parameters it is a simple task to apply redundancy here.

An estimate of the error terms can be obtained by rearranging 2.1.2 such that an error function is formed

$$\epsilon_i = \rho_{Mi} - e_{00} + \rho_{Li}(\Delta e - e_{11}\rho_{Mi}) \tag{2.1.8}$$

with $i = 1, 2, 3, \ldots, N$ the number of standards and Δe as in 2.1.3. A least squares minimization of 2.1.8 yields the error terms which are then used to calculate the error corrected reflection coefficient given by 2.1.2.

Use of Bilinear Transformation Properties

Perhaps the most deviation from classical result is the use of bilinear transformation properties to determine one port impedance. Although this is not a calibration it does produce a result which corrects for measurement errors. Because bilinear transform does not use a scattering parameter signal flow diagram of the error network, it saves a remarkable amount of algebraic manipulation with regards to the classical simultaneous equations. If Z_1, Z_2 and Z_3 are the impedances corresponding to the standard reflection coefficients used above and M_1, M_2 and M_3 are the associated measured reflection coefficients then by using the crossratio property of the bilinear transform [10],

$$\left(\frac{Z - Z_1}{Z - Z_3}\right)\left(\frac{Z_2 - Z_3}{Z_2 - Z_1}\right) = \left(\frac{M - M_1}{M - M_3}\right)\left(\frac{M_2 - M_3}{M_2 - M_1}\right) \tag{2.1.9}$$

we can directly find the load impedance Z from the measure of its reflection coefficient M.

$$Z = \frac{Z_1 - Z_3 Q}{1 - Q} \tag{2.1.10}$$

$$Q = \frac{\frac{M - M_1}{M - M_3}\frac{M_2 - M_3}{M_2 - M_1}}{\frac{Z_2 - Z_3}{Z_2 - Z_1}} \tag{2.1.11}$$

The classical corrected reflection coefficient can be used to determine this impedance however the converse is not true because the reflection coefficient is a function of the output impedance of the error network which we do not know.

Classical one port, redundancy, and bilinear transform methods encompass the published results of this area of microwave measurement. The classical one port is frequently discussed by previous authors and it is directly extendable to two port calibration. This extention will be discussed in subsequent sections, but first, discussion of one port calibration standards will conclude the one port methods.

2.1.3 One Port Calibration Standards

Previous authors introduced three known terminations for use with the classical one port calibration. The investigators were motivated to use their standards for various reasons. In 1968, Hackborn introduced the one port model and his choice for standards was influenced by need. A direct short circuit, offset short, and a sliding load were used [5]. He chose the sliding matched load because it compensates for an imperfect load. Since then authors have studied the sliding load in great detail [6,7].

In 1971, Kruppa and Sodomsky used open and short circuits, and a matched load [8]. Their apparent motivation was the simplicity these ideal standards offer to the calibration equations. In 1973, Da Silva and McPhun replaced the sliding load with a direct short circuit and two offset shorts [11]. A short circuit was convenient and required less space. Similarly, Shurmer was motivated to avoid the sliding load. His standards included an open circuit, direct short, and offset short [12]. Gould et al. used matched load, short circuit, and mismatch load standards and they were placed directly at the reference plane. Gould chose these standards because their characteristics vary slightly with frequency therefore reducing the need for accurate frequency measurements [13]. In 1974, Kása analyzed the sliding termination and found that it was possible to use a known load with two different sliding terminations [6].

In each case, the authors have indicated that the standard terminations where known either by an ideal assumption or appropriate model. For example, short circuits or offset shorts are assumed ideal with reflection coefficients of $\Gamma = -1$ or $\exp j\theta$. An open circuit standard is assumed ideal or the parasitic capacitance associated with fringing electric field is determined. Of course this capacitance is geometric and frequency dependent and can be difficult to determine. To improve calibration accuracy we need to increase the certainty of the standards used.

In 1978, Da Silva and McPhun examined redundant measurements as a method to reduce the uncertainty of their standards i.e. combinations of short and offset

short circuit terminations, or open and offset open circuit terminations [14]. Their motivation was straight forward; offset standards require knowledge of the propagation constant of the offset line. A fourth standard (one redundant standard) gave sufficient information to determine the line propagation constant and if a fifth standard was used, it was possible to determine the reflection coefficient of an unknown termination such as an imperfect open circuit.

From this summary, it should be noted that we can use any combination of at least three standards and the choice is influenced by the accuracy of the standards. Many of these authors provided an extension of their one port result to a two port calibration procedure with Hackborn leading the way. Moreover, with a similar format as one port calibration methods, we will discuss two port calibration.

Two port calibration, containing additional error terms, has undergone changes since the Hackborn model. First, let's examine the Hackborn two port model then discuss the motivation of authors that followed him, and finally, look at the most recent model.

2.1.4 ANA Two Port Error Models

Common to all two port calibration methods is the attempt to model system imperfections with error networks. These networks, being system dependent, have taken on different descriptions to suit the system designer. Hackborn extended his one port model to two port by connecting the reference ports together and

measuring forward and reverse transmission from port one to two. Fig. 2.1.4 shows the signal flow graph his through connection. These measurements were sufficient to calibrate his ANA giving a total of eight error terms, six one port error terms and two transmission terms. This eight term result is derived assuming that no leakage path exits between ports, an assumption which seems intuitively impossible.

In 1973 Shurmer introduced the concept of leakage and developed a six term two port error model [12], or simply a "one path" model. Shurmer's motivation was straight forward, his network analyzer was not automatic. That is, he used two hardware configurations, one for reflection and another for transmission measurements. This required a reversal of input-output connections of a device under test (dut) to measure its s parameters. Fig. 2.1.5 shows the "one path" model introduced by Shurmer. If leakage was important for this model why not Hackborn's eight term model? Rehnmark, in 1974, introduced the ten term model by including forward and reverse leakage in the Hackborn model [15], see Fig. 2.1.6.

Automatic network analyzers used today model system error with a twelve term model which is a Shurmer one path for each direction. This idea was introduced in 1978 by Fitzpatrick and is shown in Fig. 2.1.7 [16]. However, it is not the most comprehensive model that exists. Digressing for a moment, we need to briefly discuss components that are used in constructing an automatic network analyzer to fully understand this comprehensive model.

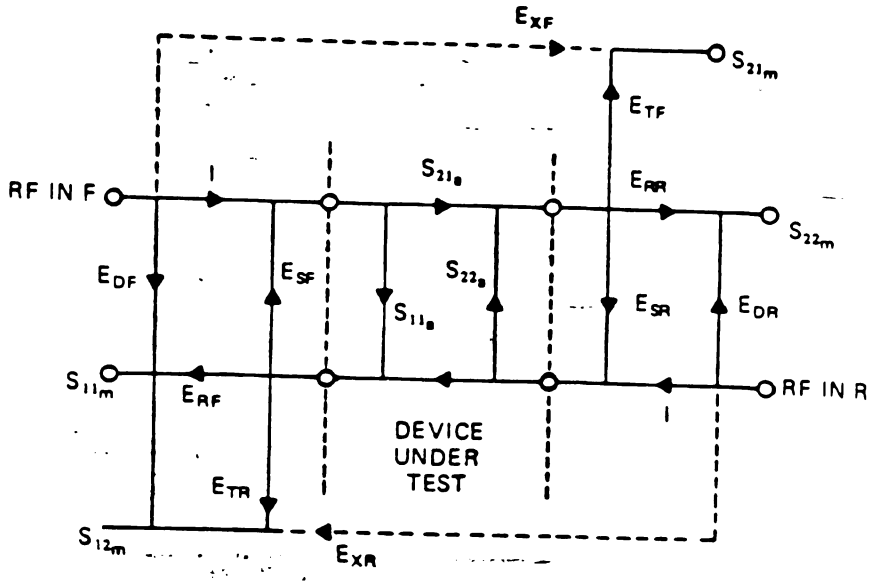

Figure 2.1.4: Through connection of the eight term error model. Each port is described with four s parameters, $S_{ij}^{1,2}$, after Hackborn, 1968.

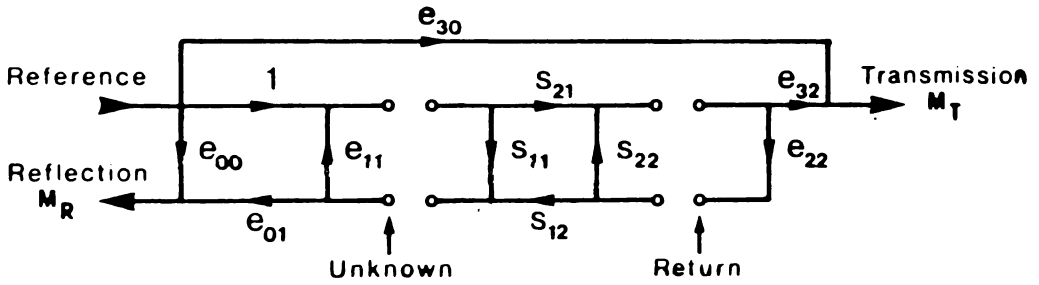

Figure 2.1.5: One path error model. Six error terms, e_{ij} embed the device s parameters, S_{ij} and for full characterization the device must be reversed.

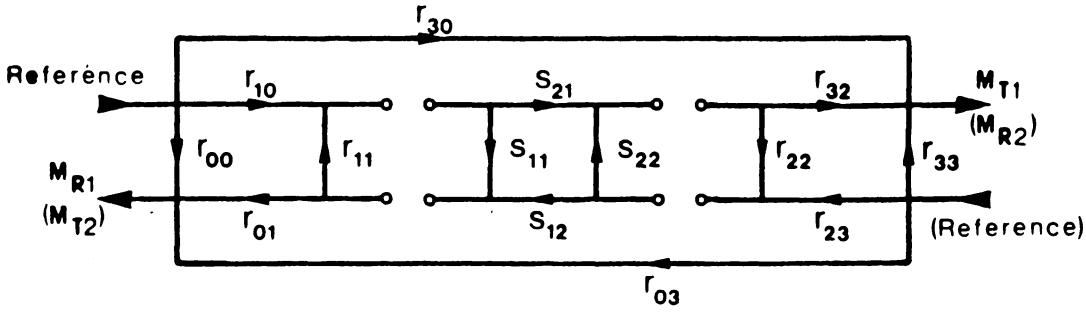

Figure 2.1.6: Ten term error model. Extension of Hackborn model by including the leakage to and from each port, e_{30} and e_{03}, after Rehnmark, 74.

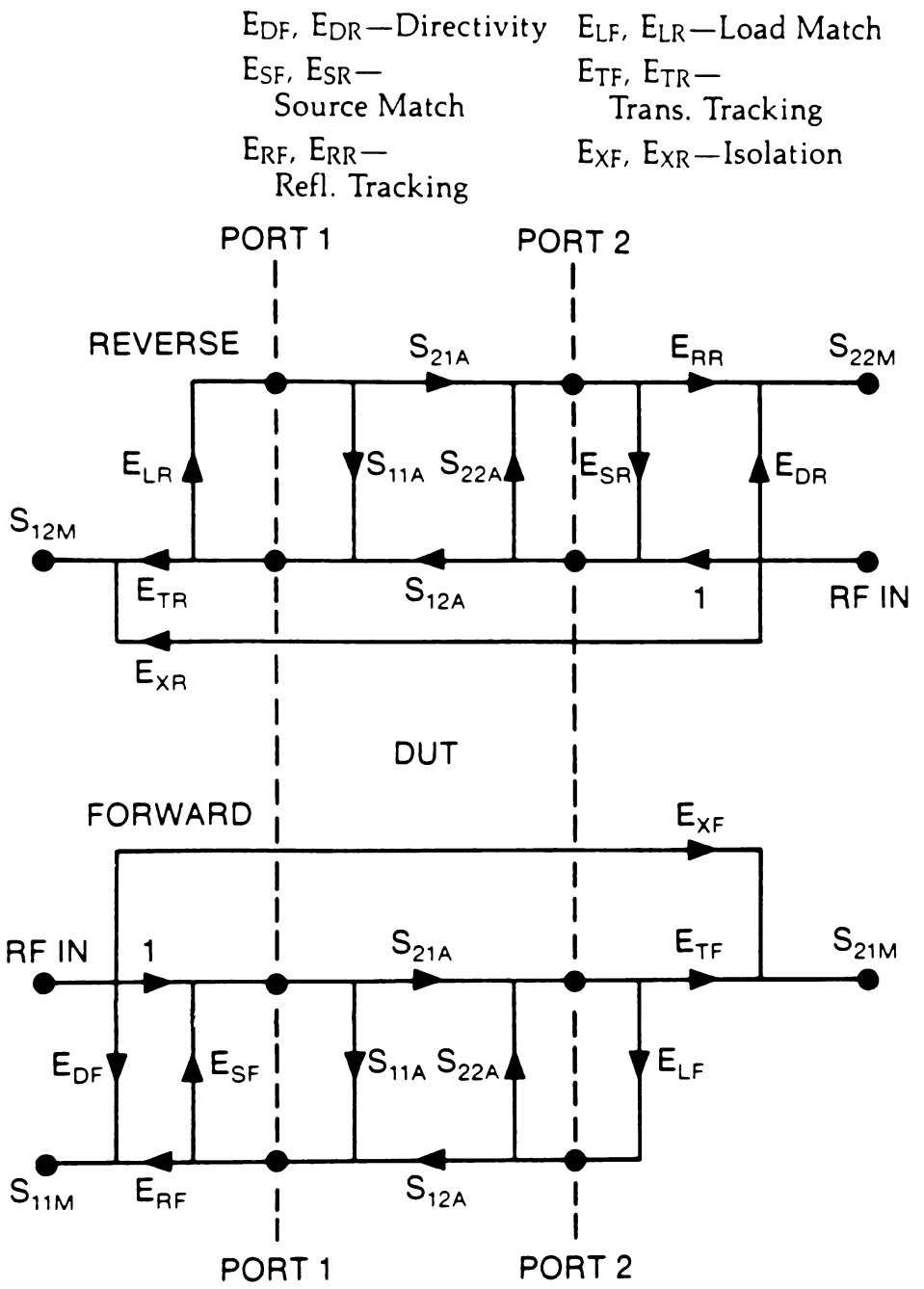

Figure 2.1.7: Twelve term error model. Introduce by Fitzpatrick, this model is a dual "one path". Full characterization of the device is done without interchanging ports.

True automatic network analysis frees the user from interchanging the dut connections. This useful feature is possible by redirecting the microwave source between measurement ports and possibly using one complex ratio detector to determine amplitude and phase information for both ports. Under this condition two switches are needed as shown in Fig. 2.1.8. In 1979, Saleh examined this test set indicating that the measurement port impedances looking into P1 and P2 can be functions of the switch positions [17]. In other words, a general error model would require terms that model each s parameter measured, Fig. 2.1.9, and a solution of systems of nonlinear equations would be necessary for calibration. Fortunately, test sets can be designed that do not require this general model. For example, by using two detectors it is accurate to use the twelve term model mentioned above.

Up to this point, we have discussed two port error models needed for calibrating network analysis. Each author has developed a calibration method based upon their model yet they have chosen from the "available" one port standards. We find that new standards were introduced after these models had become widely accepted and calibration of network analysis began focusing on fixture calibration. The next level of discussion applies these models to fixture calibration with the assumption that the network analyzer has been calibrated using one of the above models. This is important to note since it will be shown that fixture error models are comparatively simple with regards to the number of error terms. In fact,

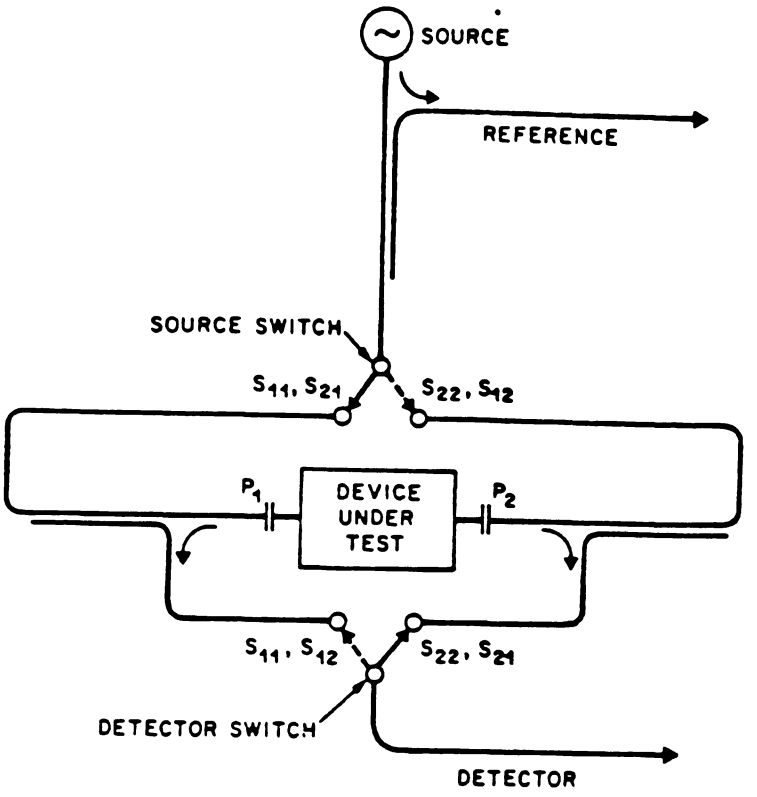

Figure 2.1.8: Automatic Network Analyzer using source and detector switches. In general, impedance looking into **P1** and **P2** is not constant therefore requiring error models for each s parameter.

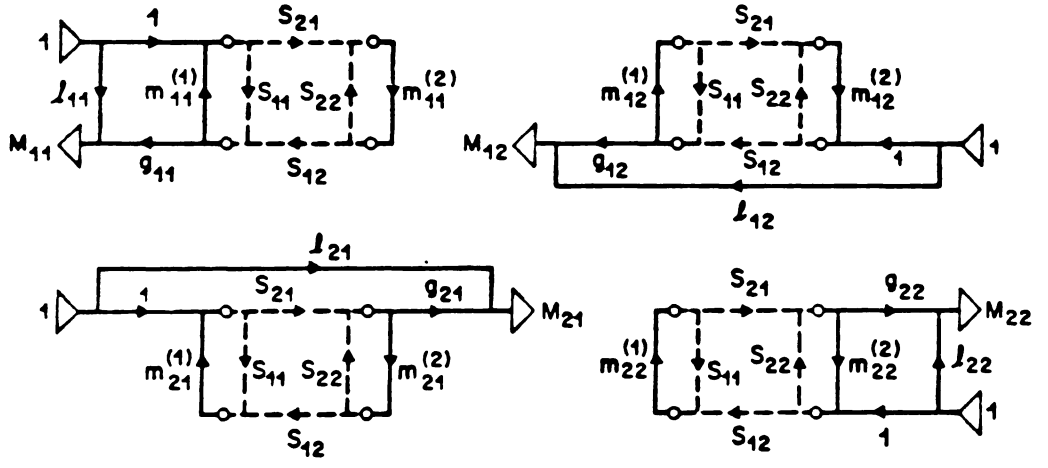

Figure 2.1.9: Sixteen term error model. Error models are used for each s parameter measured, after Saleh, 79.

Chapter 3 develops new calibration methods that exploit the simplicity of fixture error models.

2.1.5 Fixture Two Port Error Models

The s parameter measurement of an arbitrary two port network can be divided into two tiers. First we have the calibration of the network analyzer, i.e. measurement and calculation of ANA error terms, and second we need to interface our arbitrary network to the network analyzer. This interface or adaptor is commonly referred to as the fixture. For example, if we were interested in measuring the s parameters of a microstrip transmission line we need a fixture to adapt from a coaxial ANA to microstrip and then back again, Fig. 2.1.10. Fixturing introduces error into our measurement and modeling and additional calibration measurements we can remove this error. This fixture calibration is sometimes referred to as de-embedding because the device to be measured is embedded within the fixture. From this point on the terms calibration and de-embedding will be interchangeable.

Fig. 2.1.11 shows the fixture error model. It is composed of two error networks one for each measurement port, error networks **A** and **B**. As we have seen from the classical one port calibration, there are six independent error terms for this model and we can use one port calibration standards to calculate them. This result is accurate if forward and reverse transmission through the fixture are equal. Fig. 2.1.12 shows a signal flow graph for the fixture error, and application of Mason's

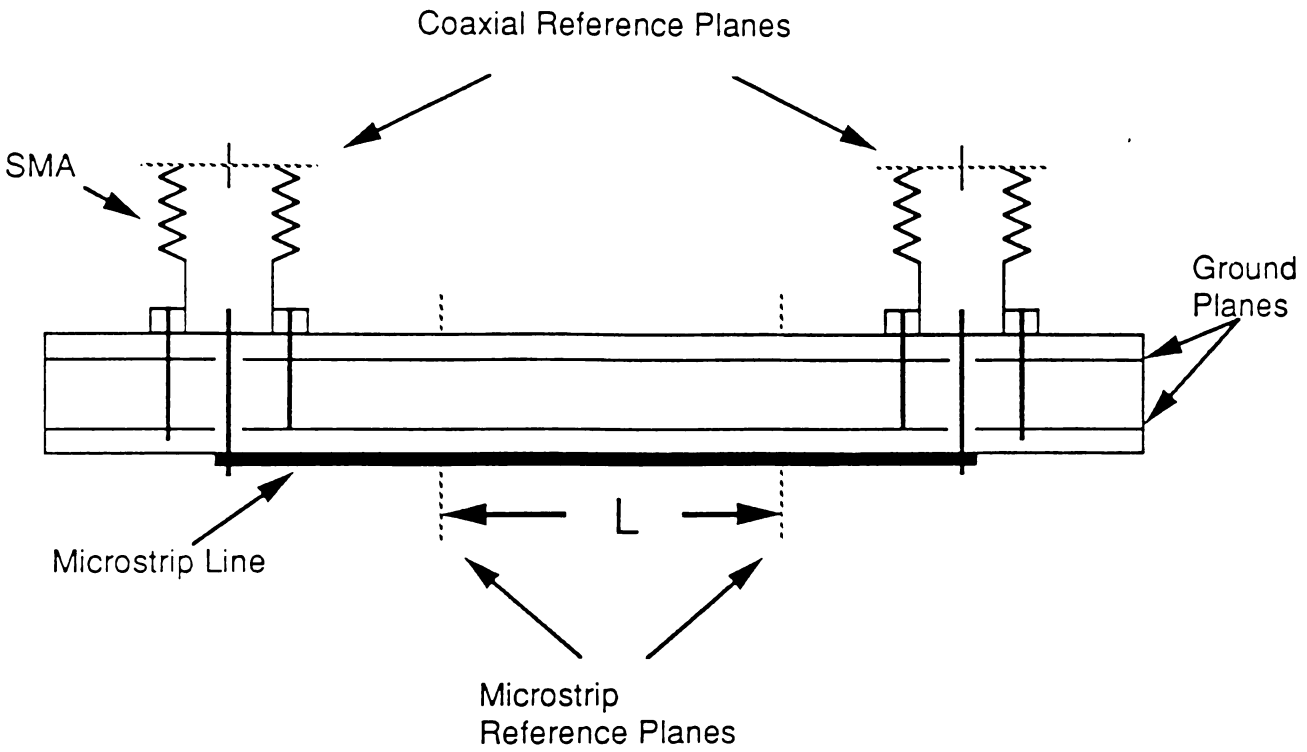

Figure 2.1.10: Example of microstrip two port fixture.

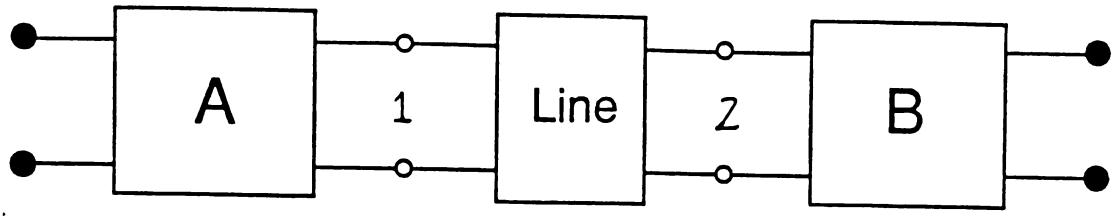

Figure 2.1.11: Block diagram of a two port fixture, **A** and **B** contain the fixture error networks and the measurement planes are fixture ports 1 and 2.

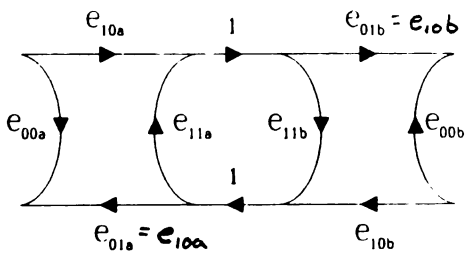

Figure 2.1.12: Six term signal flow graph with error terms, e_{ij}.

rule verifies this fact. In general, a fixture is passive and non magnetic therefore must have equivalent forward and reverse transmission coefficients. This is the only difference between Hackborn's ANA two port error model and the six term fixture model. The ANA, however, can only be minimally modeled by the eight term two port model. Additionally, fixtures can be constructed such that port to port coupling is much smaller than that internal to the ANA and we do not need to modify the fixture error model. The disadvantage with fixture de-embedding is that its geometry can be very different from one port calibration standards discussed above.

Unfortunately many fixtures encountered in microwave measurement can not use the classical one port calibration standards and there exits a need for unique two port fixture standards or de-embedding standards. To strengthen this point, consider a microstrip fixture. We have seen that it is advantageous to use a matched load standard since it allows direct measurement of one error term. This of course assumes we know its reflection coefficient. In microstrip we can not fabricate an effective matched load and a sliding termination is physically impractical so we must use other standards. Similarly an open circuit standard is difficult to model so we need to avoid it as well.

2.1.6 Fixture Two Port De-embedding Standards

How can we de-embed planar fixtures? Most classical one port standards can not be used so we need to introduce standards unique to two port de-embedding. It is well known that we can calculate the two port parameters of a transmission line of different geometries. By measuring our fixture with a known two port (transmission line) inserted between the fixture error networks we introduce a distributed de-embedding standard.

In 1975 Franzen and Speciale introduced distributed standards for calibrating their ANA. Although their result is not a two-tier approach it is significant because they were the first to introduce distributed standards. Their technique was conveniently called Through-Short-Delay or TSD [18].

At this point we would like to briefly outline the next discussion of various fixture calibration procedures. First we will look at the standards used and consider the authors motivation and second we will examine the disadvantages we can encounter when using them.

TSD - Through-Short-Delay

TSD is based on both reflection and transmission measurements and it offers two advantages. First, a matched load standard in not required and second it uses mechanically simple standards. In addition, Franzen and Speciale found that an addition delay line could be used to insure consistency within their measurements.

TSD is not without disadvantage. The delay standard was assumed lossless and nonreflecting i.e. the propagation constant was pure delay and the impedance was that of the measurement system or 50 ohms. Also, TSD although not mentioned by these two, requires information from two delays; the through connection and the actual delay. If the phase difference between these two is near zero or 180 degrees the algorithm will fail to return a valid result. This is a limitation of any de-embedding technique that uses a delay type standard. Franzen and Speciale did not apply their results to a planar fixture but their work is significant. In 1976, Bianco et al. considered the planar problem first hand by applying distributed standards to a microstrip fixture [19].

Line-Offset Open-Line

Bianco used a total of three distributed standards; two delay lines and one offset open circuit for de-embedding standards. Just as with TSD, the delay lines were nonreflecting but they were not assumed lossless, in fact, the propagation constant and open circuit reflection coefficient could be determined for the microstrip line. The mechanics of their de-embedding required a separate measurement for each inserted delay line and a one port measurement with the error networks terminated with the offset open circuit. Of course their algorithm was subjected to the 180 degree bandwidth limitation with an added problem. When two delays are used it is assumed uniform and they have equivalent characteristic impedances. It is interesting to note that this result was reintroduced in 1979 by Engen and Hoer

under the familiar name Thru-Reflect-Line [20].

TRL - Thru-Reflect-Line

TRL as developed by Engen and Hoer used only one delay standard with a through connection and an arbitrary reflection to calibrate their network analyzer. The delay standard could be arbitrary, that is, its propagation constant need not be known, however, the line was assumed nonreflecting. The reflection standard could be any repeatable reflecting load and they suggested either an open or short circuit. Again, this result was stated by Bianco but Engen was the first to consider algorithm singularities associated with distributed standards.

Neither the Bianco or Engen work had been applied directly to a fixture. Benet, in 1982, introduced the universal MMIC test fixture that required several distributed standards for calibration yet they chose yet another calibration algorithm.

Open-Short-Five Offset Lines

Benet developed the open-short-five offset line calibration using a one tier approach [21]. As discussed before, the one tier calibration is usually centered on the twelve term ANA error model, that is, six for each direction of measurement. To determine the six terms Benet measured the fixture's response with open and short circuits at the fixture reference plane and then a minimum of three offset thru lines were inserted and measured. By approximation the offset lines caused

the measured reflection of the fixture to scribe a circle and at the center was an additional error term. Two additional offset lines were used to allow a least squares fit of the circle to these measurements. Returning to the open and short circuit error equations, he showed that two additional error terms could be determined. Finally, by approximation he determined the propagation constant of the thru lines and the remaining error terms. Benet's contribution showed that insertable distributed standards could be used to calibrate a test fixture. Next we will see that a two tier de-embedding method obtains a similar result and requires fewer assumptions.

Open-Short-Modeled Through Line

Under some circumstances the fixture can not be calibrated using insertable standards such as a transistor test fixture. Here the fixture can not be separated to insert the de-embedding standards. In 1982 Vaitkus and Scheitlin proposed a method of de-embedding such a fixture by considering a two tier de-embedding method. The ANA was first calibrated using OSL and its twelve term error model and then fixture de-embedding measurements were done. Their standards were an open and short circuit and a modeled through line [22]. The error model was simply a one port error network for each fixture port and two leakage terms to compensate for a leakage path around the transistor chip. This is a simplification of Rehnmark's ten term ANA error model. Vaitkus and Scheitlin exploited the passive nature of the fixture and the assumption that forward and reverse leakage

would be identical. This allowing them to reduce the total number of error terms to seven. Comparing this de-embedding result with Benet's, simplification is possible if a two tier calibration/de-embedding method is applied because the fixture offers a reduced number of error terms.

A through line standard had been previously used by others but Vaitkus differed by using a modeled through line and determined its equivalent circuit by optimization. A bond wire through line connected the fixture ports together and the equivalent circuit was optimized to fit the measured fixture s parameters. A similar procedure was performed on the bond wire short circuits. Vaitkus and Scheitlin produced results using a through line standard but a general examination of Open-Short-Through line was introduced later by Vaitkus himself [23] in 1986. Rather than model the through line, he assumed knowledge of line propagation constant, short circuit inductance, and open circuit capacitance.

Double Through Line

In 1987, Pennock et al. introduced a de-embedding technique for characterizing transitions between novel transmission media [24]. Their motivation was a lack of conventional standards and a need to reduce the total needed. In 1976, Bianco et al. eluded to the fact that transition parameters could be determined to within a multiplicative constant if only two through line standards are used [19]. They also showed that measurement of an additional through line was a linear combination of the first two and the constant could not be determined. Pennock exploited

the multiplicative constant and proceeded to use two line standards for their de-embedding.

Their fixture error model was the commonly used six term two port error model and we know that to completely characterize it we need three standards. Pennock showed that the Bianco constant was a ratio of two error terms. In fact, this ratio is nearly equal to unity for reasonable transitions and Pennock proceeded to de-embed the fixture under this assumption.

This result is not without problems. First, as stated before distributed standards must avoid $\lambda/2$ singularities and second, the line must be reflectionless. Additionally, the line attenuation constant is known or assumed equal (lossless line).

TTT – Triple Through

In 1988, Meys introduced a fixture de-embedding method that uses an auxiliary two port and matched load for standards [25]. Beginning with the standard two port error model, the **A** and **B** error networks are connected together and measured. Also, the auxiliary two port **C** is cascaded to either side of **A** and **B** to form the measured two ports **BC** and **CA**. These and the **AB** two port provide necessary but not sufficient information to determine the error networks. The reflection coefficient for the auxiliary two port terminated with a matched load is sufficient to determine the error networks.

The use of a matched load is undesirable but Meys points out that if the **C**

two port exhibits low SWR we can assume its reflection coefficient is zero and eliminate the matched load requirement. Since distributed standards are not used TTT is inherently broad-band.

Results of Eul and Schiek

In 1988, Eul and Schiek examined the conventional two port measurement system from a linear algebraic point of view. Their worked showed results noted by previous authors such as a need for at least three de- embedding two ports for complete characterization and previous de-embedding techniques. Their main contribution was the study of redundancy [26]. When three standards are inserted between the error networks and subsequently measured, the total number of unique measured quantities is twelve, yet there are only eight error terms linearly independent. This redundant information can be used to reduce the required knowledge of the standards used and as a result they proposed several de-embedding methods Thru-Match-Reflect is one example.

TMR – Thru-Match-Reflect

Thru-Match-Reflect uses a through connection, a matched load (or any other known reflection coefficient) and an arbitrary reflection. It offers the broad-band advantage of these standards however we need a prior knowledge of at least one standard i.e. the matched load. The reader is referred to [26] for discussion of the calibration algorithm used with these standard combinations.

2.2 Conclusion

The review of calibration theory encompassed one port measurements, automatic network analyzer error models and calibration methods and finally fixture de-embedding. It is clear that calibration of network analysis has been an ever changing study covering much of our recent history. It contains a variety of methods because the results of one may not be applicable to another or someone has a unique de-embedding requirement. It is important to note that when approaching a calibration dilemma one should look at the problem from a know/unknown point of view. In other words, consider the total number of unknowns in the measurement system and then decide on the variety of standards that are available. We feel that this review has provided the insight into calibration methods and hopefully given the reader a "what if we use ..." attitude towards their calibration of network analysis. The next chapter approaches new calibration methods and embodies this philosophy.

Chapter 3

Calibration Using a Symmetric Fixture

3.1 Introduction

As we have seen from Chapter 2, it is clear that a calibration can take many forms. Naturally, we feel that another calibration topic remains untouched; exploitation of the symmetrical nature of measurement fixtures. As with past calibration methods, there was a need for something "new" and we are similarly motivated with this study.

Chapter 3 concentrates on discussing advantages of symmetry arguments, reviewing symmetrical de-embedding methods, and the development of two new symmetrical de-embedding algorithms. In addition, we will re- examine TRL calibration and develop a practical enhancement.

3.2 Motivation for Using Symmetrical Arguments

When considering the history of calibration of network analysis, two directions have been pursued by the measurement community. On one hand, there was a need to compensate for imperfections in calibration standards, and on the other hand, calibration accuracy is directly related to the certainty of standards and if

at all possible choose the minimum necessary. A symmetrical argument allows a reduction in required standards thereby improving the certainty. In fact, later in this chapter we show that it is possibly to reduce the total number of standards to one. With this in mind, when can we use a symmetric argument or when is a fixture symmetric?

3.3 Evolution from an Asymmetric to Symmetric Fixture

A symmetric fixture is a special case of the general asymmetric fixture. In Fig. 3.3.1, we see the conventional two port error network and its corresponding signal flow graph. It is composed of two error networks **A** and **B** and in general, the individual signal paths S_{ija} and S_{ijb} are unique forcing fixture s parameters S_{ijf} to be unequal to each other. This represents an asymmetric fixture.

A fixture is symmetric if the port 1 and 2 reflection coefficients are equal and the fixture is reciprocal, i.e. if $S_{11f} = S_{22f}$ and $S_{21f} = S_{12f}$. Reciprocity is true when the fixture is passive and non-magnetic and these symmetrical equalities are possible with two orders of symmetry; first and second order.

Using Mason's non-touching loop rule [38] we see that the fixture s parameters are related to the individual error terms,

$$S_{11f} = S_{11a} + \frac{S_{21a}S_{12a}S_{11b}}{1 - S_{22a}S_{11b}} \tag{3.3.1}$$

$$S_{22f} = S_{22b} + \frac{S_{22a}S_{21b}S_{12b}}{1 - S_{22a}S_{11b}} \tag{3.3.2}$$

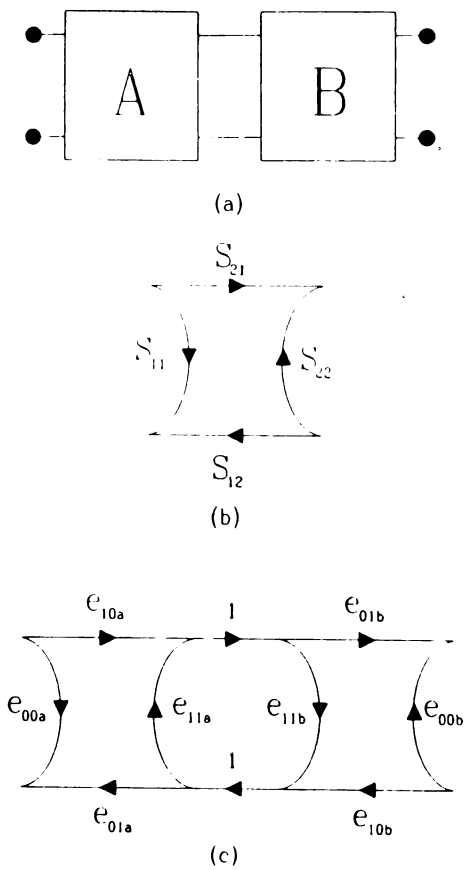

Figure 3.3.1: Two port error model for an asymmetric fixture (a). Fixture error can be described with eight error term S_{ija} and S_{ijb}. Port 1 and 2 are the calibrated ANA measurement ports. S_{ijf} are the measured fixture s parameters.

$$S_{21f} = \frac{S_{21a}S_{21b}}{1 - S_{22a}S_{11b}} \tag{3.3.3}$$

and

$$S_{12f} = \frac{S_{12a}S_{12b}}{1 - S_{22a}S_{11b}} \tag{3.3.4}$$

Equating 3.3.1 and 3.3.2 and applying reciprocity we find one equation in six complex unknowns.

$$S_{11a}(1 - S_{22a}S_{11b}) + S_{11b}S_{21a}^2 = S_{22b}(1 - S_{22a}S_{11b}) + S_{11b}S_{21a}^2 \tag{3.3.5}$$

This is the symmetry condition equation representing an under determined system. This implies that symmetry can be produced with an infinite number of six error parameters. Fortunately, symmetry corresponds to the physical nature of the fixture which limits the symmetric solutions to two; first and second order symmetry.

3.3.1 First Order Symmetric Fixture

A first-order symmetric fixture has identical fixture halves that are asymmetric, see Fig. 3.3.2. The port two error network, **B**, is now a port reverse of **A**, or $\mathbf{B} = \mathbf{A}^R$. This is true if $S_{11a} = S_{22b}$, $S_{22a} = S_{11b}$ and $S_{21a}^2 = S_{21b}^2$. Moreover, these conditions satisfy the symmetry condition equation 3.3.5. A "coaxial to microstrip" – "microstrip to coaxial" fixture is an example of first order fixturing. Most important, the signal flow graph shows that the symmetry reduces the number of error terms to three, that of the **A** network only. In other words, symmetry

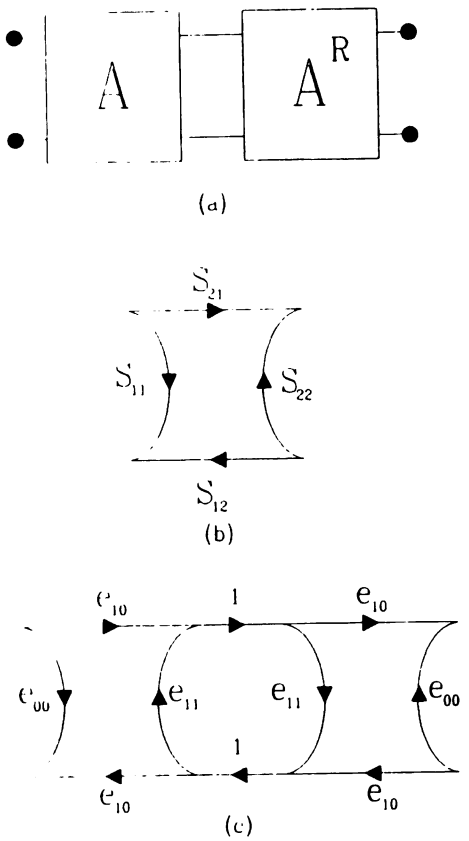

Figure 3.3.2: Two port error model for a first order symmetric fixture (a). Fixture error networks are described by three s parameters S_{ija}. S_{11f} and S_{21f} are the measured fixture s parameters.

allows a reduced number of error terms for a two port fixture, and this reduction is strictly a function of the manufacturing repeatability with direct application to printed circuit board measurements.

3.3.2 Second Order Symmetric Fixture

If the fixture halves are identical and symmetric, the fixture is second order symmetric. This implies that network **B** is equal to **A** or all reflection s parameters, S_{iia} or S_{iib}, are equal,($= S_{11}$) and all transmission s parameters are equal, S_{ija} or S_{ijb}, ($= S_{21}$), see Fig. 3.3.3. A second order fixture satisfies the symmetry condition equation 3.3.5 and a lumped element transistor test fixture is an example of second order fixturing.

3.4 Review of Symmetrical Methods

Previous authors have examined symmetric fixtures. In 1982, Souza et. al. used a microstrip first order fixture to develop a method to calculate the fixture half. Their results are based on further assumptions. First, the microstrip line used in the fixture is reflectionless (50 ohm characteristic impedance) and second the fixture half has a low return loss [27]. However, this result can not be applied to a fixture that introduces significant error. If the fixture microstrip line impedance is different from 50 ohms, both assumptions are invalid.

In 1983, Pollard and Lane indirectly used a first order symmetry assumption

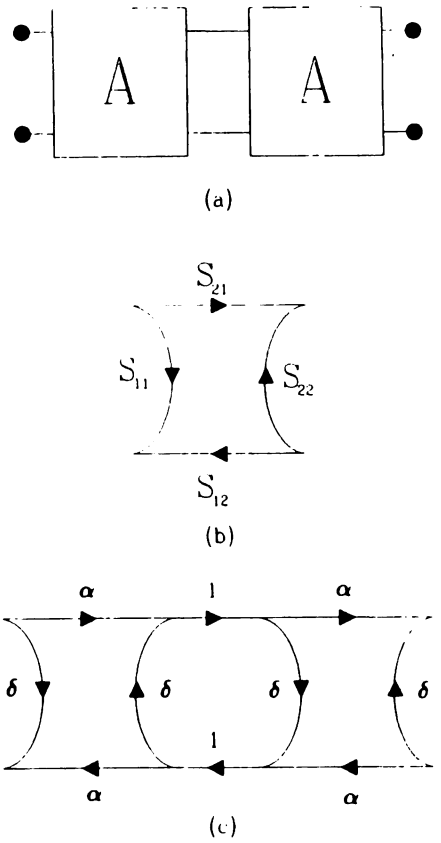

Figure 3.3.3: Two port error network for a second order symmetric fixture. Fixture error is described with two s parameters S_{11} and S_{21}.

by modelling their fixture half with a pi equivalent circuit with different shunt capacitances [35]. Their calibration standards are an open and short circuit and a through connection. The fixture input impedance equations for the open and short standards give sufficient information to extract the pi equivalent parameters if second order frequency terms are neglected. As with the Souza result, they use assumptions in addition to symmetry. Their result is invalid when the fixture is considerably long or can not be modeled with a lumped element circuit. In 1986, Ehlers was the first to apply symmetry without additional fixture assumptions.

Ehlers studied a finline first order symmetric fixture. The standards include a through connection and either a matched load or a reflectionless transmission line [37]. He pointed out that a symmetric fixture requires two standards for calibration. This is true only if the matched load or a reflectionless transmission line can be fabricated. If neither are accurately possible (as is the case for microstrip fixtures) then an additional standard is needed. For the finline example his result is adequate.

Most recently, in 1989, Enders developed an iterative de-embedding method that uses three line standards to determine the parameters of a first order fixture [36]. His result affirms the belief that symmetry is useful for calibrating fixtures and in the next section we will apply symmetrical arguments and distributed calibration standards. A second order fixturing was examined by Martin and Dukeman in 1987. They found that a second order fixture requires only one standard;

a through connection [31]. Their result uses extensive matrix renormizations that need not be done and in a following section a similar result based on signal flow theory is developed.

3.5 Development of Through-Symmetry-Line – TSL Using First Order Symmetry

3.5.1 TRL to TSL

As we have seen before, the calibration of a planar measurement fixture, e.g. microstrip and stripline, requires distributed standards. The preferred method for planar fixture de-embedding is Thru-Reflect-Line (TRL) or Line-Reflect-Line (LRL) because the distributed standards are easily modeled and constructed. A typical microstrip fixture, shown in Fig. 3.5.1, is a first order symmetric fixture. Identical coax to microstrip transitions and identical microstrip line lengths are the requirements for symmetry. These can be achieved into low microwave frequencies and at higher frequencies through careful design.

Because first order symmetry allows the fixture to be represented with three error terms, three standards are needed. Symmetry permits synthesis of TRL reflection standards thereby eliminating their need. TRL standards are shown in Fig. 3.5.2; through connection, an reflection and a reference transmission line of length l. The reflection is arbitrary and is typically a short circuit. For the

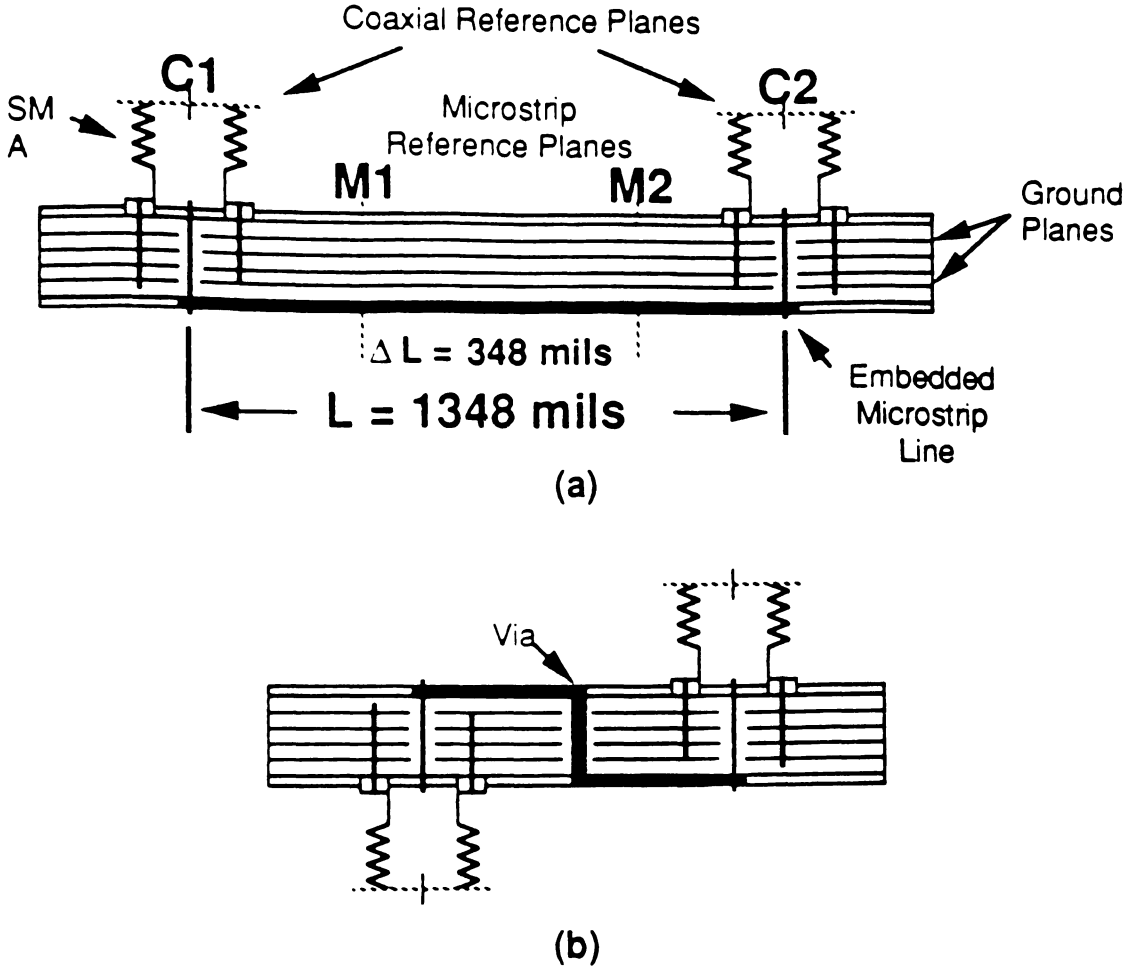

Figure 3.5.1: Typical microstrip fixture.

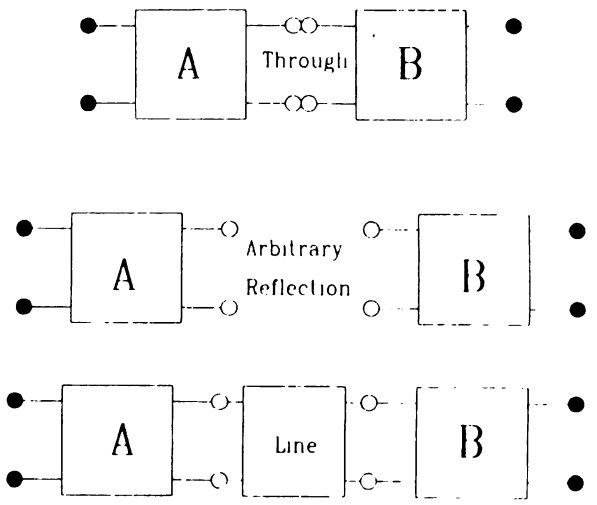

Figure 3.5.2: TRL calibration standards. (a) Through connection, (b) Arbitrary reflection, Γ, placed at each fixture port and (c) Line connection.

symmetrical through connection, we can calculate the reflection coefficient with the microstrip ports terminated in ideal open or short circuits. Either synthesized reflection coefficient can be applied to the TRL algorithm. Conforming to the naming of de- embedding methods we will refer this substitution as Through-Symmetry- Line or TSL.

3.5.2 Synthesize Reflection Standards

The TSL standards are a through and line connections, Fig. 3.5.3. These are similar to Souza et al. [27] however their result is based on symmetry and a low fixture return loss assumption. Note, the symmetry reflection coefficients can be used with the LRL algorithm with similar results. Next we will expound the derivation of ideal open and short circuit reflection coefficients.

Referring to the signal flow graphs of Fig. 3.5.4, we consider the through connection s parameters given by, $S_{11f}(= S_{22f})$ and $S_{21f}(= S_{12f})$, and the actual parameters of the **A** network being δ, α and γ for $S_{11a}, S_{21a} = S_{12a}$ and S_{22a} respectively. In addition, the input reflection coefficient with an ideal short circuit placed at port 1b of **A** is

$$\rho_{sc} = \delta - \frac{\alpha^2}{1+\gamma} \tag{3.5.1}$$

Before we used Mason's rule to relate the fixture parameters to the individual network parameters 3.3.1 – 3.3.4 here a similar result is given for the first order

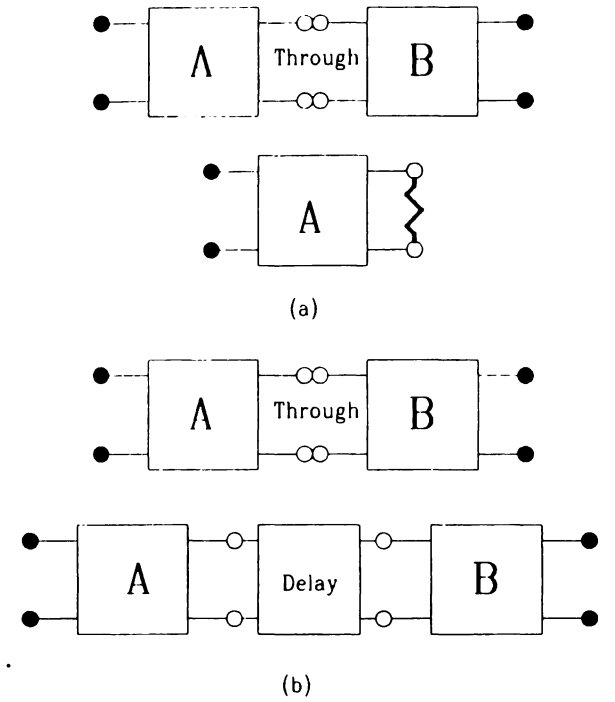

Figure 3.5.3: TSL calibration standards. (a) Through connection and (b) Line connection. TRL reflection standard is synthesized using symmetry.

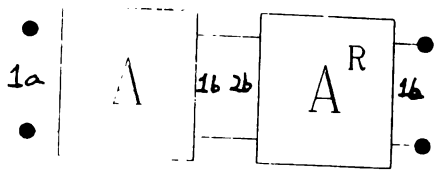

(a)

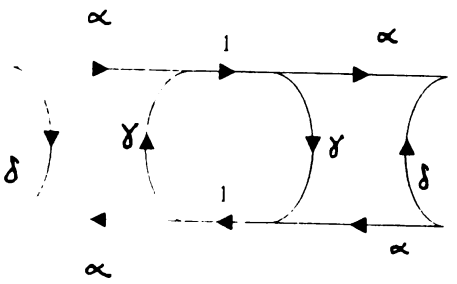

(b)

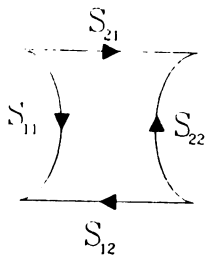

(c)

Figure 3.5.4: TSL signal flow graphs. (a) Measured fixture s parameters, (b) Fixture error model described by parameter δ, α and γ and (c) Signal flow graph with ideal short circuit placed at fixture port 1b.

symmetric fixture.

$$S_{11f} = \delta + \frac{\alpha^2\gamma}{1-\gamma^2} \tag{3.5.2}$$

$$S_{21f} = \frac{\alpha^2}{1-\gamma^2} \tag{3.5.3}$$

Combining (3.5.1), (3.5.2) and (3.5.3), the short circuit reflection coefficient can be expressed as a function of fixture s parameters (measured).

$$\rho_{sc} = S_{11f} - S_{21f} \tag{3.5.4}$$

A similar results holds for an ideal open circuit placed at port 1b.

$$\rho_{oc} = S_{11f} + S_{21f} \tag{3.5.5}$$

Naturally, TSL can reduce the number of standards needed and requires fewer connections to the microstrip ports improving the repeatability of this connection. Moreover, ρ_{sc} and ρ_{oc} can be derived for any fixture that exhibits first or second order symmetry including other planar measurement fixtures. Since these reflection coefficients are derived mathematically, it is possible to "insert" ideal open and short circuits within a non-insertable medium such as a dielectric loaded waveguide. The reader is directed to Chapter 5 for experimental verification of a symmetrically synthesized short circuit. In the next section will discuss an enhancement to TSL that is directly applicable to TRL and LRL as well.

3.6 Enhanced Through-Symmetry-Line – ETSL (ETRL)

3.6.1 Motivation: Failure of TRL Assumptions

The development of ETSL, hence ETRL, is necessary because of assumptions inherent to the TRL algorithm. As introduced in 1979 by Engen and Hoer [20], the algorithm requires the characteristic impedance of the line standard to be equal to the measurement system impedance. If not then we its value has to be determined. Also, the algorithm assumes a pure real characteristic impedance with no frequency dependence. If the fixture to be calibrated is composed of dispersive transmission lines, e.g. microstrip, it becomes necessary to determine the complex characteristic impedance Z_c as a function of frequency. We present a method that enhances the TSL algorithm by determining the characteristic impedance; Enhanced Through-Symmetry-Line – ETSL. For the sake of discussion we will consider an embedded microstrip fixture. Application of ETSL to an embedded microstrip fixture follows in Chapter 5.

An approximate value of Z_c can be made using time domain reflectometry (TDR), however, TDR can not determine frequency variations of the microstrip characteristic impedance which can vary by as much as 5 percent from DC to 10 GHz for a typical microstrip line [32]. Also, accurate modeling of Z_c is complicated by several factors; accepted models predict different frequency variations; material parameters may not be known; and ideal microstrip geometry may be corrupted

by dielectric coverings such as a passivation or solder resist layer as in the case of printed circuit boards, see Fig. 3.6.1. ETSL determines the complex characteristic impedance using the free- space capacitance of the microstrip geometry and an experimentally determined propagation constant, $\gamma = \alpha + j\beta$.

The impedance calculated in this fashion, if used in the conventional TRL algorithm, compensates for the algorithm assumptions. By using a free-space capacitance explicit knowledge of the dielectric parameters i.e. relative dielectric constant and loss tangent are not necessary. Also, we can determine characteristic impedances of geometries that are atypical such as embedded microstrip or any uniform TEM transmission line. Additionally, by incorporating the propagation constant we embody the effect loss has on the characteristic impedance (complex Z_c). In short, this method can be used to determine characteristic impedances of any arbitrary uniform TEM transmission line. In the next section we will develop the characteristic impedance algorithm with microstrip being the transmission line.

3.6.2 Calculation of Complex Characteristic Impedance

Microstrip lines are non-homogeneous transmission lines that support a quasi-TEM mode [32]. However the TSL algorithm requires the equivalent TEM mode characteristic impedance. For uniform TEM transmission lines the characteristic impedance is related to the free- space capacitance and the effective dielectric

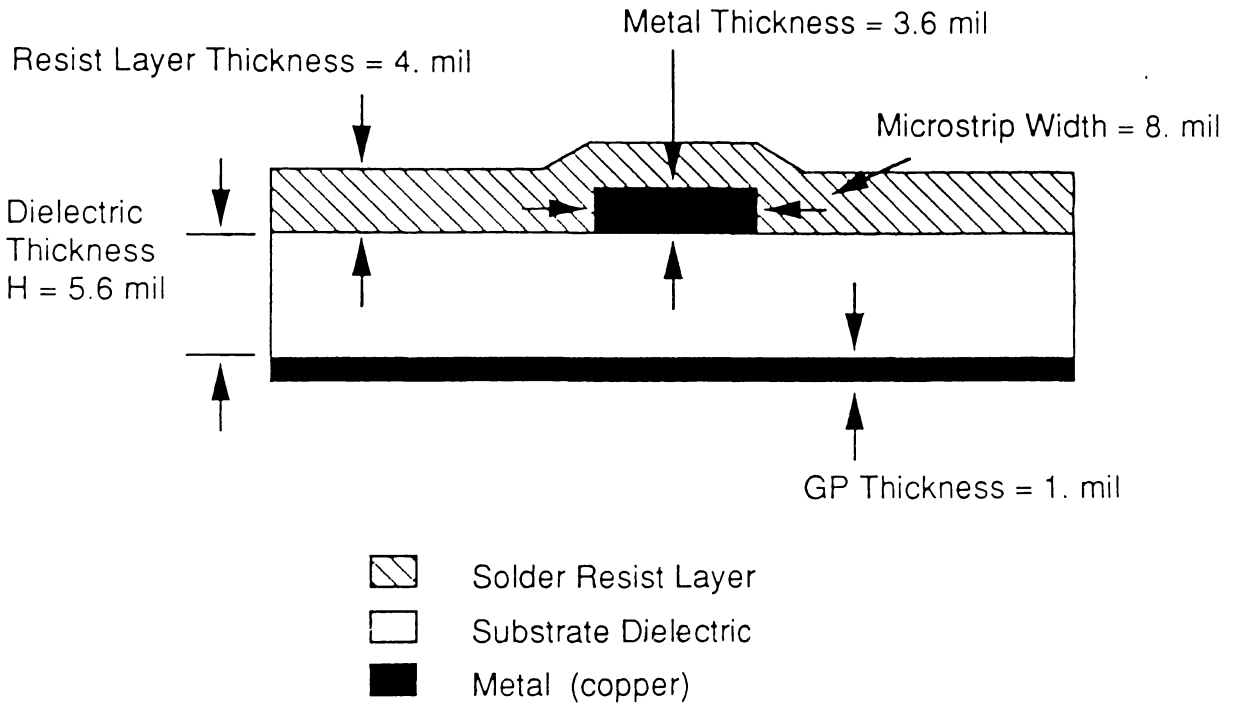

Figure 3.6.1: Embedded microstrip encountered in printed circuit board technology.

constant by [33]

$$Z_c = \frac{Z_0}{\sqrt{\epsilon_e}} \tag{3.6.1}$$

with

$$Z_0 = \frac{1}{C_0 c} \tag{3.6.2}$$

where Z_c is the dielectric loaded characteristic impedance of the line, Z_0 is its free-space characteristic impedance, C_0 is the free-space capacitance, c is the velocity of light and ϵ_e is the effective dielectric constant. C_0 is a geometrical dependent factor and is the capacitance of the structure in a dielectric-free medium. It is well known that the effective dielectric constant is related to the propagation constant γ by [28]

$$\epsilon_e = \frac{-\gamma^2 c^2}{\omega^2} \tag{3.6.3}$$

where $\gamma = \alpha + j\beta$ is available from measurement as a by product of the TRL algorithm. Recently, Mondal and Chen reported that the TRL algorithm can be used to determine the propagation constant of the TRL line standard. That is [29]

$$\gamma = \frac{\ln\left(\frac{A \pm \sqrt{A^2 - 4}}{2}\right)}{l} \tag{3.6.4}$$

where

$$A = T11_t \cdot T22_l + T11_l \cdot T22_t - T21_t \cdot T12_l - T12_t \cdot T21_l \tag{3.6.5}$$

Tij_l and Tij_t are the chain scattering parameters for the line and through calibration standards respectively, and l is the length of the line standard. Conversion

from s to t parameters is given by,

$$\begin{pmatrix} T_{11} & T_{12} \\ T_{21} & T_{22} \end{pmatrix} = \frac{1}{S_{21}} \begin{pmatrix} -\Delta & S_{11} \\ -S_{22} & 1 \end{pmatrix} \tag{3.6.6}$$

where

$$\Delta = S_{11}S_{22} - S_{12}S_{21} \tag{3.6.7}$$

This result can be derived for any fixture, symmetric or otherwise, and it is a natural progression to incorporate this information to determine the complex characteristic impedance. Combining (3.6.1)- (3.6.3) and taking the negative root

$$Z_c = \frac{j\omega}{c^2 C_0 \gamma} \tag{3.6.8}$$

The negative root is chosen because the result must be positive when the line is lossless and the impedance is positive pure real. This characteristic impedance is used to overcome impedance assumptions of TRL and is applicable to the TSL algorithm. The reader is directed to Chapter 5 where this derivation is experimentally verified with a fifty ohm coaxial example. Also, Chapter 5 contains complex microstrip characteristic impedance calculated with the verified algorithm. Next we examine singularities that arise when distributed standards are used and expand on the effect these singularities have on calculating the propagation constant.

3.6.3 Calculation of Propagation Constant

Inherent to the TRL algorithm is the need to separate the error networks with a transmission line. The line standard must be sufficiently long to produced a mea-

surable phase difference between through and line fixtures. Naturally, at lower frequencies this becomes this difference is limited by the network analyzer measurement resolution. Additionally, if the electrical length of the line is near 180 degrees it appears transparent. TRL returns invalid results in either case. Intuitively the "farthest" we can be from 180 degrees (or zero) would be a phase difference of 90 degrees and reliable propagation constants can be extracted from 20 to 160 phase differences [30]. By choosing line standards with electrical lengths within this range the characteristic impedance can be determined with no effect from the singularities.

3.6.4 Modifying TSL Algorithm

Again, the TRL (TSL) algorithm requires a reflectionless line. This is achieved by transforming each calibration measurement from the measurement reference impedance to Z_c. Application of TRL then determines the S parameters of the error network referenced to Z_c. To complete calibration the s parameters of the error network are returned to the measurement reference impedance system, (usually 50 ohms).

3.7 Development of Through-Symmetric Fixture – TSF Using Second Order Symmetry

What if the fixture is second order symmetric? Again, we define second order symmetry as a first order fixture with symmetric halves. As we have just seen, symmetry can be used to reduce the number of standards needed. When second order symmetry is valid the two port error network is represented with two error terms. Naturally, this allows us to use fewer de-embedding standards, in fact, a second order fixture requires only one measurement configuration, a through connection, thus in conformance with the practice of naming calibration procedures, we designate the new technique Through Symmetric Fixture – TSF method.

Fig. 3.7.1 shows the signal flow graph for the fixture s parameters S_{ijf} and the corresponding two port error model. Each error is identical and symmetric therefore the scattering matrix of each is

$$[S_{ija}] = \begin{bmatrix} \delta & \alpha \\ \alpha & \delta \end{bmatrix} \tag{3.7.1}$$

The goal of TSF is to determine the error terms (α and δ) and based on Mason's non-touching loop rule, unlike the matrix renormalizations used by Martin and Dukeman [31]. S parameter measurements of the through connection yield two independent quantities, S_{11f} and S_{21f}, as $S_{11f} = S_{22f}$ and $S_{12f} = S_{21f}$ because of symmetry and reciprocity. This is sufficient to determine S_{ija}. For clarity, we will let the subscript ijt (t - through) represent the measured fixture s parameters ijf.

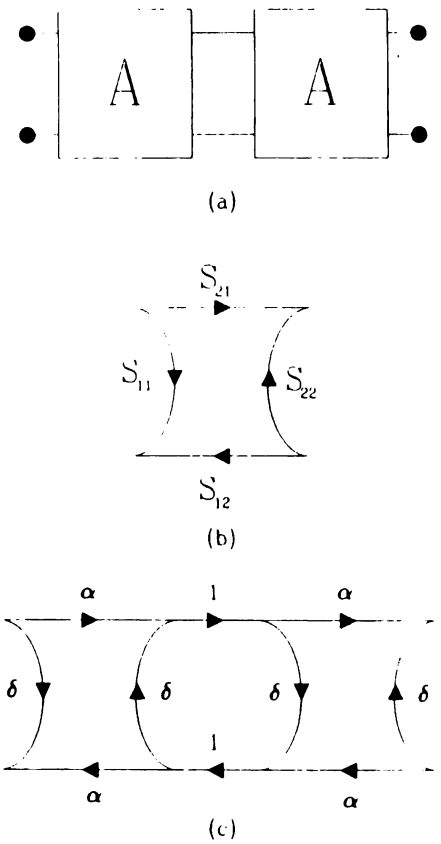

Figure 3.7.1: Signal flow graphs used by TSF. (a) Measured fixture s parameters and (b) fixture error network described by s parameters δ and α.

The signal flow graph provides two algebraic relationships for the known quantities as functions of the error terms,

$$S_{11t} = \delta + \frac{\alpha^2 \delta}{1 - \delta^2} \tag{3.7.2}$$

$$S_{21t} = \frac{\alpha^2}{1 - \delta^2} \tag{3.7.3}$$

Rearranging

$$\delta = \frac{S_{11t}}{1 + S_{21t}} \tag{3.7.4}$$

$$\alpha = \sqrt{S_{21t} \frac{b^2 - S_{11t}^2}{b^2}} \tag{3.7.5}$$

where

$$b = 1 + S_{21t} \tag{3.7.6}$$

The square root gives two possible solutions and the root choice depends upon the electrical length (L_e) of the through connection. The positive root is valid when

$$n\lambda < L_e < \frac{(2n+1)\lambda}{2} \tag{3.7.7}$$

where

$$n = 0, 1, 2, \cdots \tag{3.7.8}$$

otherwise the negative root is correct. This choice of roots is based on a physical constraint. The α term is the transmission coefficient of the error network and at low frequency the phase of α must be negative therefore the positive root choice in this interval.

Equation 3.7.4 contains a singularity that limits the bandwidth of TSF. When the fixture S_{21t} is nearly equal to -1 equation 3.7.4 will return invalid results for δ this can occur when the fixture is $\frac{n\lambda}{2}$. This singularity can be avoided if the length of the fixture is constructed such that it is not an integer half wavelength long at any frequency in a desired measurement range. TSF can be used on a lumped-element transistor test fixture where this restriction does not exist. Similar singularity restrictions exist when other distributed de-embedding techniques are employed. The reader is directed to Chapter 5 where TSF is experimentally verified.

3.8 Conclusion

In Chapter 3, we have presented new de-embedding algorithms. By using symmetric arguments, it is possible to reduce the required calibration standards. It was shown that reflection standards can be synthesized from a through measurement. Also, the complex characteristic impedance of uniform TEM transmission lines can be determined if the transmission line free-space capacitance is known. Taking this impedance into account, we can enhance the TSL or TRL algorithms.

Computer implementation of these algorithms is necessary for verification purposes. The next chapter develops SPANA or Signal Processing of Automatic Network Analysis a command level program useful for algorithm implementation and other computer aided data manipulation.

Chapter 4

SPANA: Computer Program for Computer Aided Microwave Measurement

4.1 Introduction to SPANA

Computer processing of microwave measurements is necessary to free the engineer from the costly measurement time. It is very reasonable to assume that computer processing is needed since a single two port measurement can produce sixty four kilobytes (64K) of data. SPANA (Signal Processing for Automatic Network Analysis) has been developed to meet the needs of automatic microwave measuring systems.

SPANA is a tool to be used for processing measured S parameter data and its prime use is to implement de-embedding algorithms. SPANA also performs various tasks such as input/output of data, data format conversions, and others. Written in FORTRAN in a modular fashion, SPANA is conducive to future expansion.

SPANA is by the simplest definitions an operating system and the operations are carried out by using a command language. These commands allow the user to interact with the data freely. One of the most important assets of SPANA is that a series of commands can be sequentially read from a command file; a macro.

SPANA is adaptable to outside programmers since it maintains all data I/O and frees the programmer to concentrate on the processing of data.

4.2 Structure

SPANA has two program levels and each level has the capability to inform the user if a syntax error occurs. At the top is the command interpreter and its task is to determine which command is to be executed. The next layer is the actual command function which may in turn nest several sub-layers to complete the function. When a command is completed, control is returned back to the command interpreter for subsequent command processing. It is important to note that SPANA is not a menu driven program but rather a command interpreter. Commands available in SPANA are given in the next section.

4.3 Tools available in SPANA

To use SPANA, data is input to the program by "GETing" a measurement set. After this it is available for processing by executing other commands. Finally, the results of data manipulation can be "PUT" to a file. For example, calibration using TSF requires a measurement for the through standard and the embedded device. Two "GETs" and a call to DMB2 (with appropriate TYPE) will calculate the error networks and the de-embedded device. "PUTting" these results will save them for later use. Below is a list of the functions and a brief discription of their

purpose. The reader is directed to Appendix B for a complete discussion of the semantics of each command and Appendix C where the "SHELL" command is example for the potential programmer.

	Function	Purpose
1.	**HELP**	On-line help
2.	**GET**	Input data
3.	**PUT**	Output data
4.	**DISP**lay	Display data statistics
5.	**DEL**ete	Delete data
6.	**PTOR**	Polar to Rectangular conversion
7.	**RTOP**	Rectangular to Polar conversion
8.	**STOY**	S parameters to Y parameters
9.	**SYM**metrize	Symmetrize data
10.	**PUL**l	Reduce size of data
11.	**WIN**dow	Smoothing of data
12.	**STRiP**	Produce X-Y data file
13.	De-embed **DMB2**	Two-Port error correction
14.	De-embed **DMB3**	Three-Port error correction
15.	**BuiLD**	Produce error standard
16.	**SIGMA**	Statistical calculations
17.	**GAIN**	Two-port gain calculations
18.	**PIE**	Conversion from S to pi equivalent circuit
19.	**INTP**	Linear interpolation between data points
20.	**STOP**	Exit SPANA

4.4 Conclusion

This chapter introduces SPANA with its purpose to aid microwave measurements. The ability to execute command macros is essential to extensive measurement calculations and SPANA can be modified by adding command to the interpreter and writing the appropriate sub-layers.

Chapter 5

Results and Discussion

5.1 Introduction

In this chapter the calibration techniques developed in Chapter 3 are verified. Through-Symmetry-Line and Enhanced Through-Symmetry-Line are applied to an embedded microstrip fixture commonly encountered in Printed Circuit Board technology. The error networks determined from these methods are removed from a PCB via and a pi equivalent circuit is imposed on the via measurements. Finally, Through-Symmetric Fixture is applied to a second order symmetric fixture and the results are compared directly with measured fixture halves and a de-embedded low pass filter. The use of scattering parameters is common to all results. With exception to TSF and a coaxial verification, a frequency range of 45 Mhz to 10 Ghz is used for the TSL and ETSL measurements.

5.2 Verification of the Through-Symmetry-Line De-embedding Method

5.2.1 Introduction

In the following sections the Through Symmetry Line calibration method is applied to a PCB embedded microstrip fixture. As discussed before, this fixture is non-insertable and cannot be compared with a direct measurement of the error networks. The symmetry verification and comparison of a synthesized and measured short circuit are given with discussion and finally TSL is applied to de-embed the PCB via.

5.2.2 Measurement and Fixture Design

Coaxial ports are used on all measurements to allow connection to the Automatic Network Analyzer (HP 8510. which is integrated within a computer controlled measurement setup show in Fig. 5.2.1. After the two port s parameters are measured, the data was transferred to a MicroVax where they were processed by SPANA. The two-tier nature of this measurement i.e. Coaxial calibration then post measurement de- embedding is convenient with this measurement system.

Keeping with symmetrical arguments of Chapter 3, the first order symmetric fixture is shown in Fig. 5.2.2 along with a detail of the embedded microstrip cross section Fig. 5.2.3 used throughout the chapter. The microstrip dimensions are

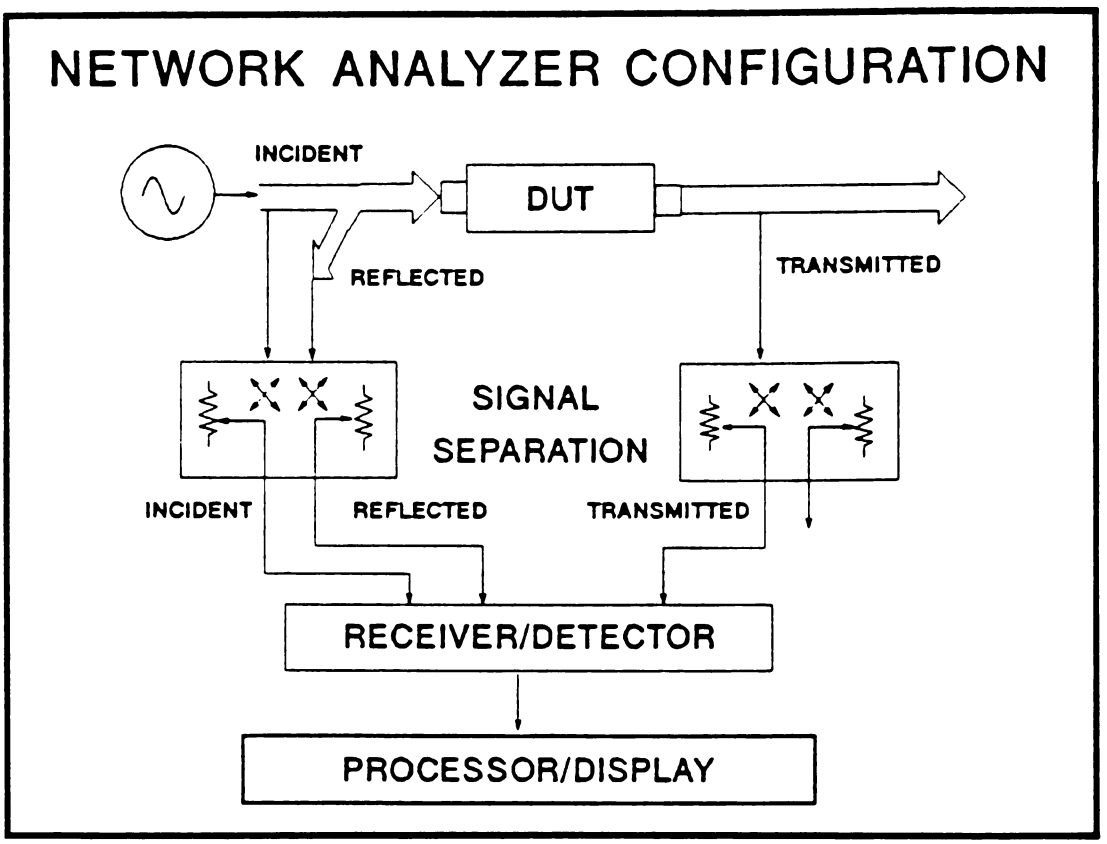

Figure 5.2.1: S parameter measurement setup. The HP 8510 measures the device s parameters under control of the controller, then the data is transmitted to the MicroVax for further processing.

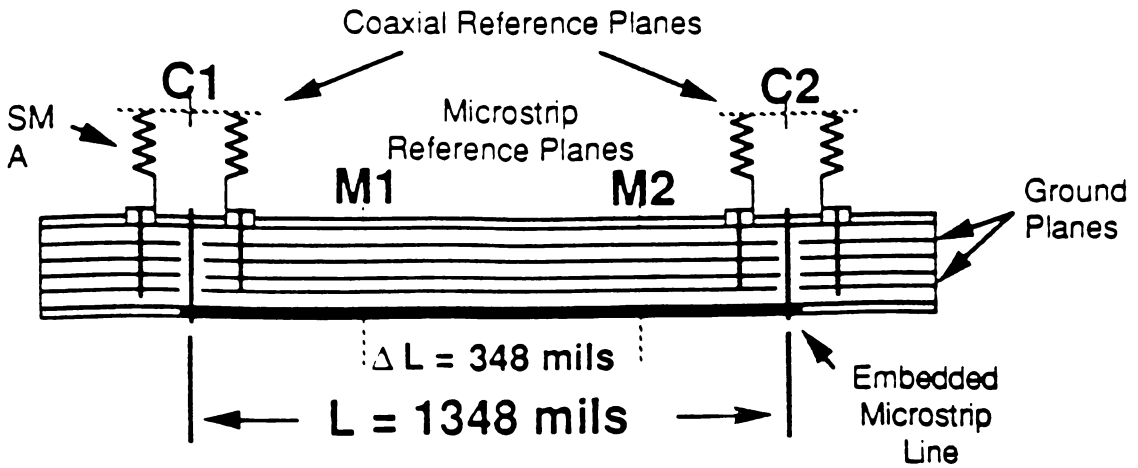

Figure 5.2.2: First order symmetric fixture used throughout Chapter 5. **C1** and **C2** are the calibrated coaxial measurement planes and **M1** and **M2** are the microstrip reference planes. Embedded structures are inserted at **M1** and **M2**.

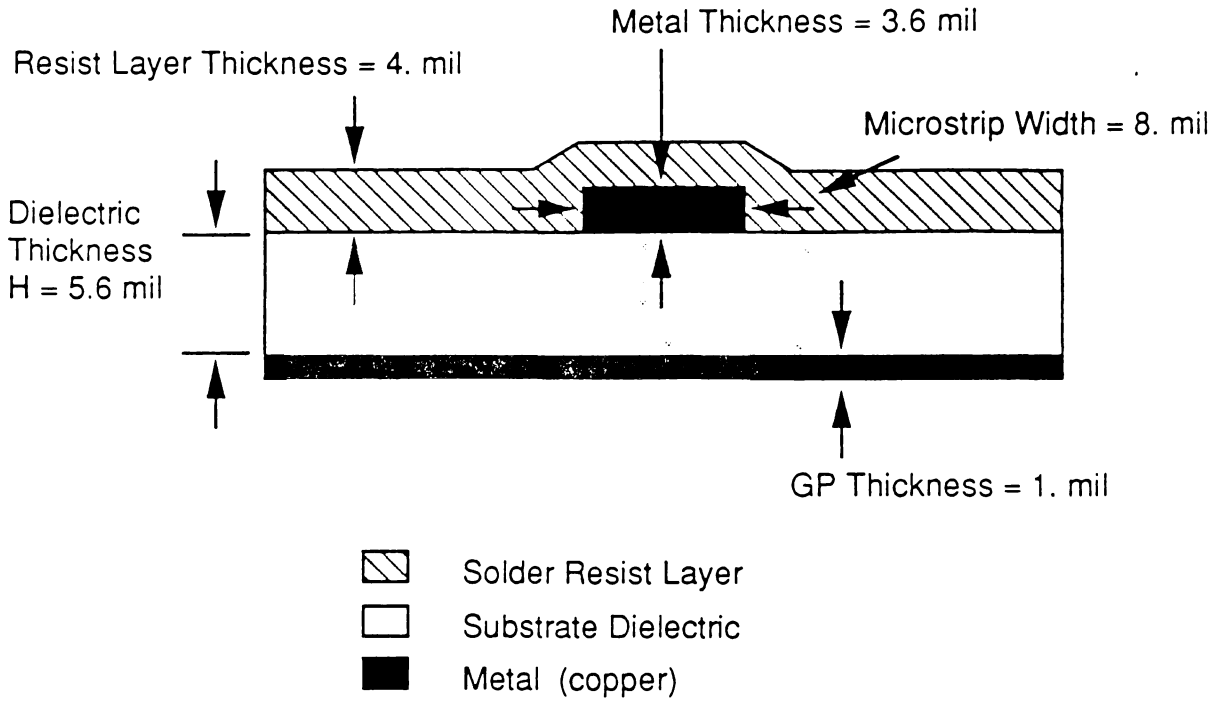

Figure 5.2.3: Detail cross section of the embedded microstrip.

width(w)=8 mils, height(h)=5.6 mils, metal thickness(t)=3.6 mils and the covering dielectric layer (solder resist layer) is approximately 4 mils thick. The length(l) of the microstrip portion of the fixture is 1000 mils. These physical dimensions (except length) were used because PCB manufacturing resources required them. Note, these dimensions were intended to result in a 50 ohm characteristic impedance and as we will see this is not the case. The microstrip length can be arbitrarily chosen with only coaxial connector clearance restricting the minimum value.

The network analyzer is calibrated to the coaxial reference planes **C1** and **C2** using the network analyzer Open Short Load calibration procedure. The fixture is connected to the coaxial reference planes and a full two port s parameter measurement is made. The magnitude and phase of the fixture s parameters S_{11f}, S_{22f} and S_{21f} are shown in Fig. 5.2.4, 5.2.5 and 5.2.6 with the exception of S_{12f} which is identical to S_{21f} and has been omitted.

Symmetry requires that the S_{iif} parameters be equal and from Fig 5.2.4-5.2.6 this is true with minor deviations at frequencies were the fixture is resonant (f=.8, 4.5 and 8 GHz). These resonances are are associated with discontinuity capacitances and for discussion, we may model the fixture with discontinuity capacitances at either coaxial port and a uniform transmission line between them, Fig. 5.2.7. These capacitances reduce the electrical length of the line and when the effective line length is an odd multiple of half wavelengths, the S_{iif} values exhibit minima. Sensitivity of the fixture symmetry at these frequencies is due to differences in

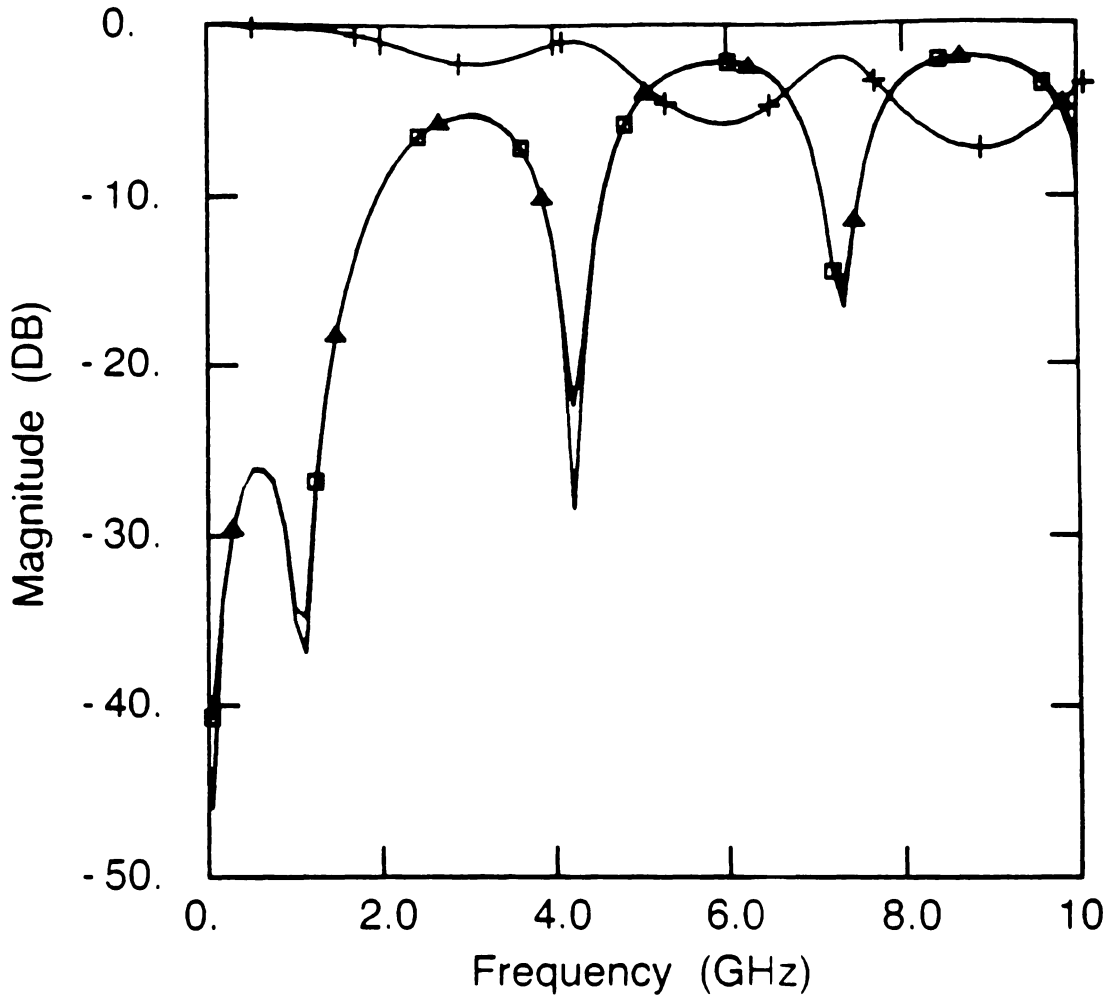

Figure 5.2.4: Embedded microstrip fixture s parameters. Magnitude of (□) S_{11f}, (+) S_{21f} and (△) S_{22f}.

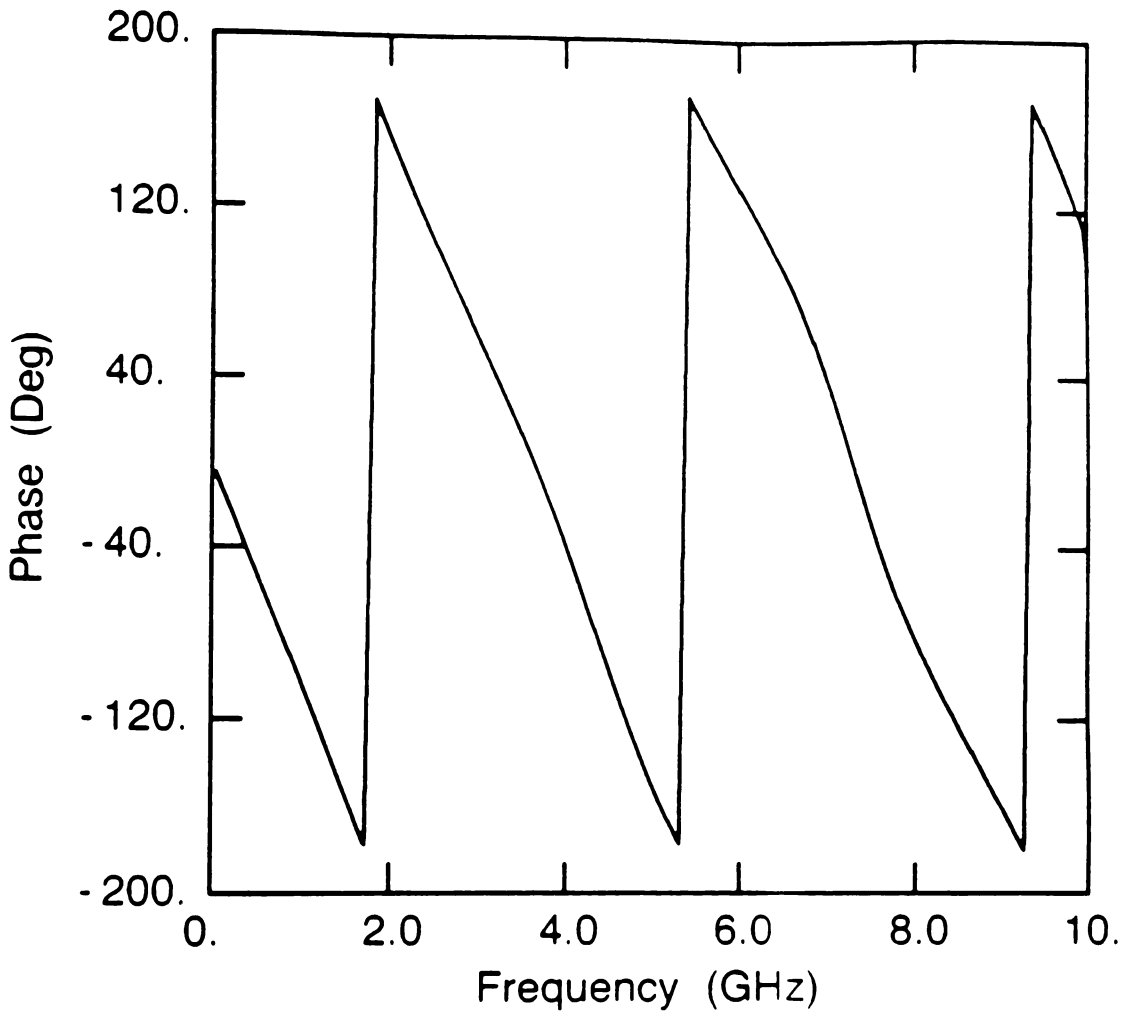

Figure 5.2.5: Cont. Embedded microstrip fixture s parameters. Phase of S_{21f}.

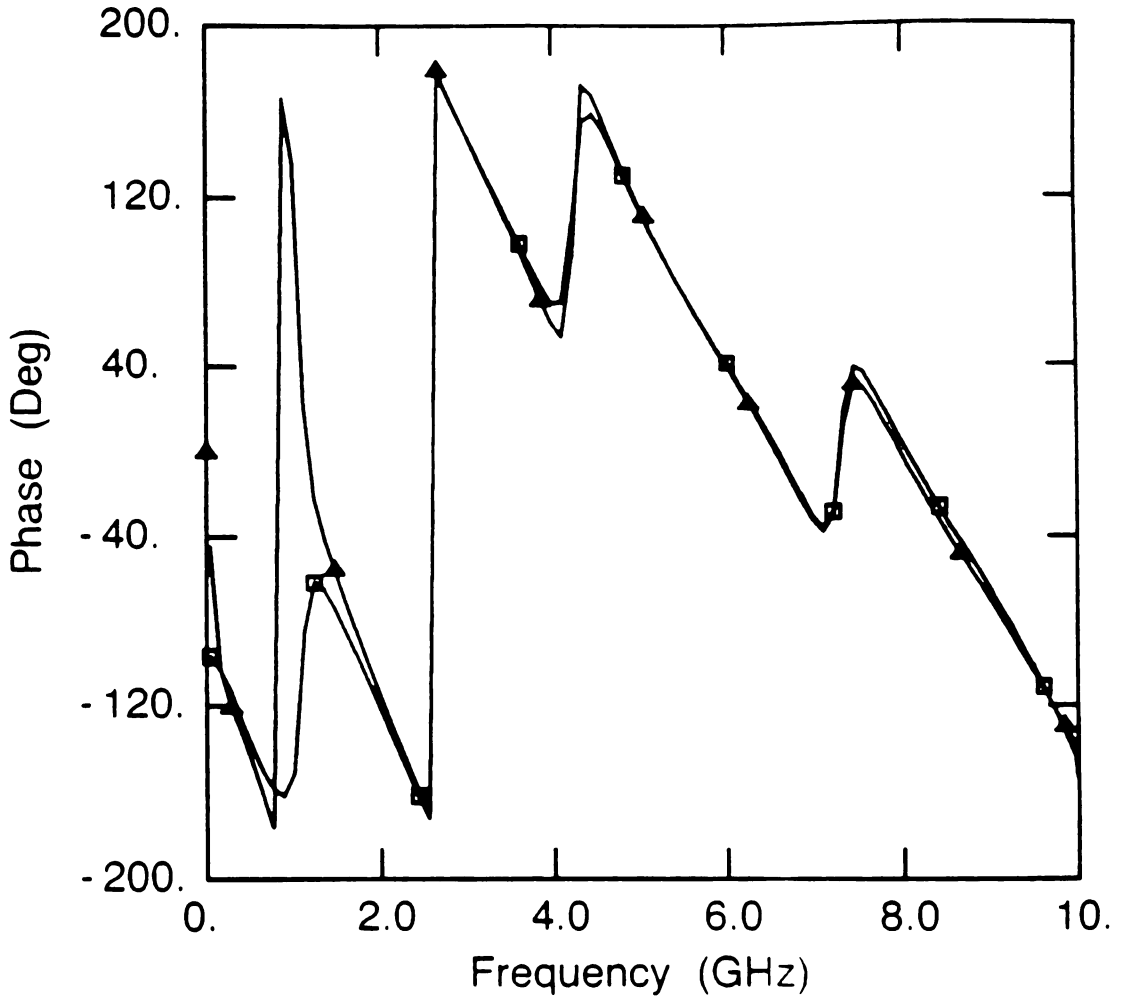

Figure 5.2.6: Cont. embedded microstrip fixture s parametes. Phase of (□) S_{11f} and (△) S_{22f}.

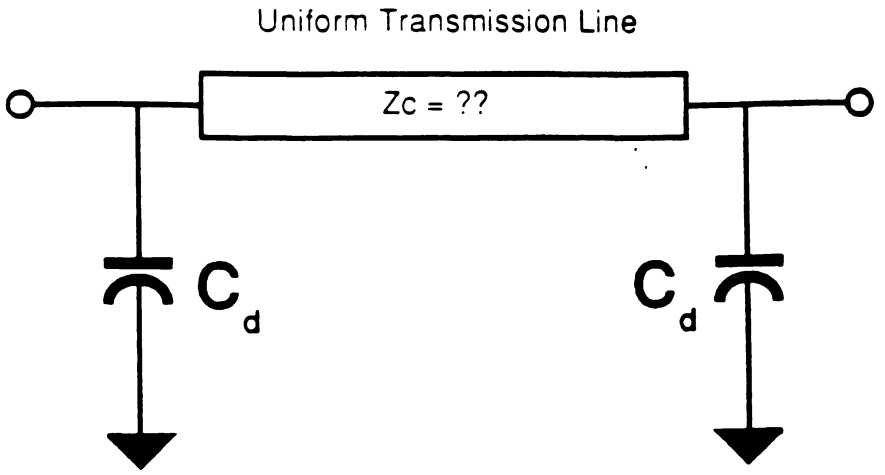

Figure 5.2.7: Approximate model for fixture. The fixture transmission line is effectivly terminated with equal discontinuity capacitances C_d.

the discontinuity capacitances. Additionally, at other frequencies reflection from the microstrip line dominate the reflection terms. When designing a symmetrical fixture, one can apply common sense arguments, such as reduce the discontinuity capacitance and use short lengths of microstrip. The symmetry of the network is exemplified by the synthesized short circuit verification.

5.2.3 Synthesis of Open and Short Circuit Reflection Coefficients

The Through Symmetry Line algorithm synthesizes the reflection standard needed in the TRL calibration method by using symmetry. To verify this is possible a low inductance short circuit was placed at the microstrip reference plane **M1**, shown on Fig. 5.2.2. The measured short circuit reflection coefficient is compared in magnitude and phase with the synthesized value in Fig. 5.2.8 and 5.2.9. In addition, the synthesized open circuit is also shown. The magnitude minimum is slightly different between measured and calculated. This minimum corresponds to the resonance of the discontinuity capacitance with the inductive input impedance of the short circuit terminated microstrip. Moreover, the physical short has a parasitic inductance that will lower the resonant frequency from the ideal synthesized short. In fact, it may be possible to extract an inductance value from this frequency shift. In any event, the TRL reflection standard can be synthesized and the next section presents results using TSL.

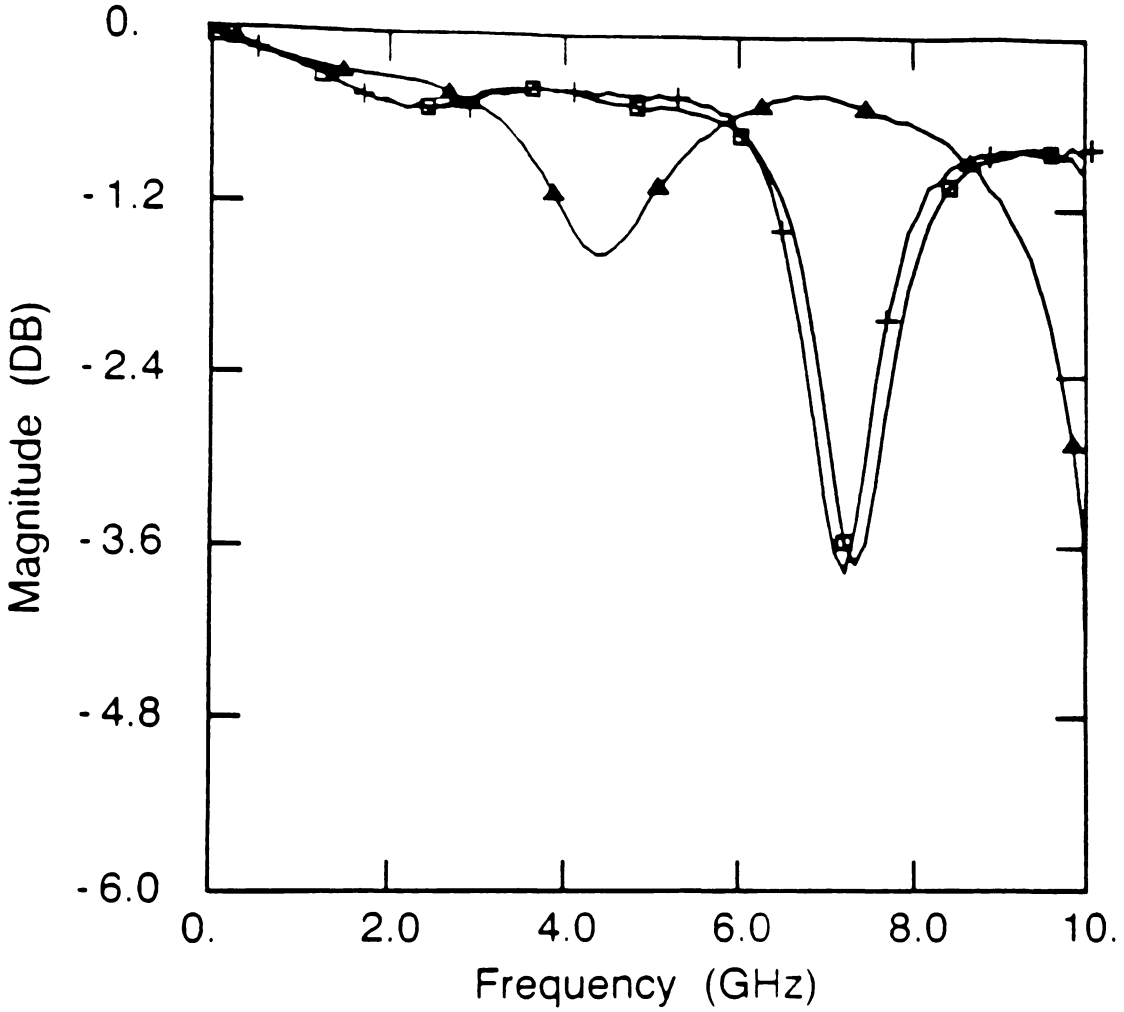

Figure 5.2.8: Magnitude comparison of synthesized and measured short circuit at microstrip reference plane. (+) Measured short circuit reflection coefficient, (□) synthesized and (△) synthesized open circuit reflection coefficient.

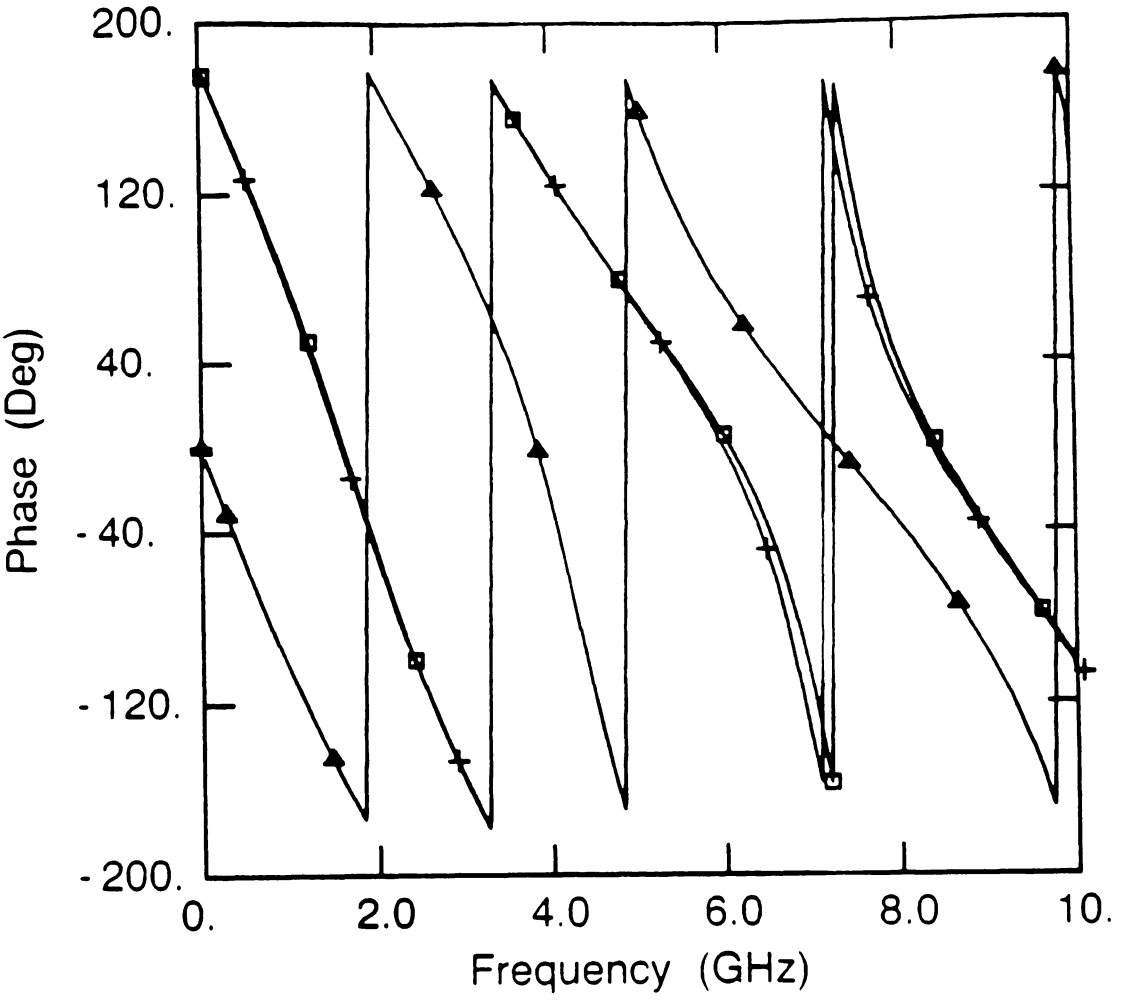

Figure 5.2.9: Phase comparison of synthesized and measured short circuit at microstrip reference plane. (□) Phase of synthesized short circuit reflection coefficient, (+) measured short circuit and (△) synthsized open circuit.

5.2.4 TSL De-embedding Results

The TSL algorithm was used to determine the pi equivalent circuit of a PCB via and to do so we need to remove it from the fixture. In effect, the via is inserted at the microstrip reference planes. As discussed before, PCB measurements are non-insertable so we must replicate the through fixture with the line standard and finally the device under test (DUT) inserted.

Fig. 5.2.10 shows the standards and the device to be de-embedded. The line length was 1348 mils giving a length difference, Δl, between the through and line standards of 348 mils. The useful measurement range for $\Delta l = 348$ is within the 45 MHz to 10 GHz measurement range, with the first TRL singularity near 10 GHz. The exact calculation of this singularity is not possible because the frequency variation of the effective dielectric constant and we can only approximate its magnitude. However the singularity does correspond to the Δl being an electrical half wavelength.

A printed circuit board via is a plated hole through the PCB connecting a fixture halve on each side of the board and can be modeled with a pi equivalent circuit as given by Wang et al. [31]. The via cross section and equivalent pi circuit are shown in Fig. 5.2.11. After applying the TSL algorithm to the embedded via measurement we can extract the pi equivalent circuit from the de-embedded via s parameters, see Appendix A for complete discussion of error removal by de-cascading. This extraction is done by converting the via s parameters to ad-

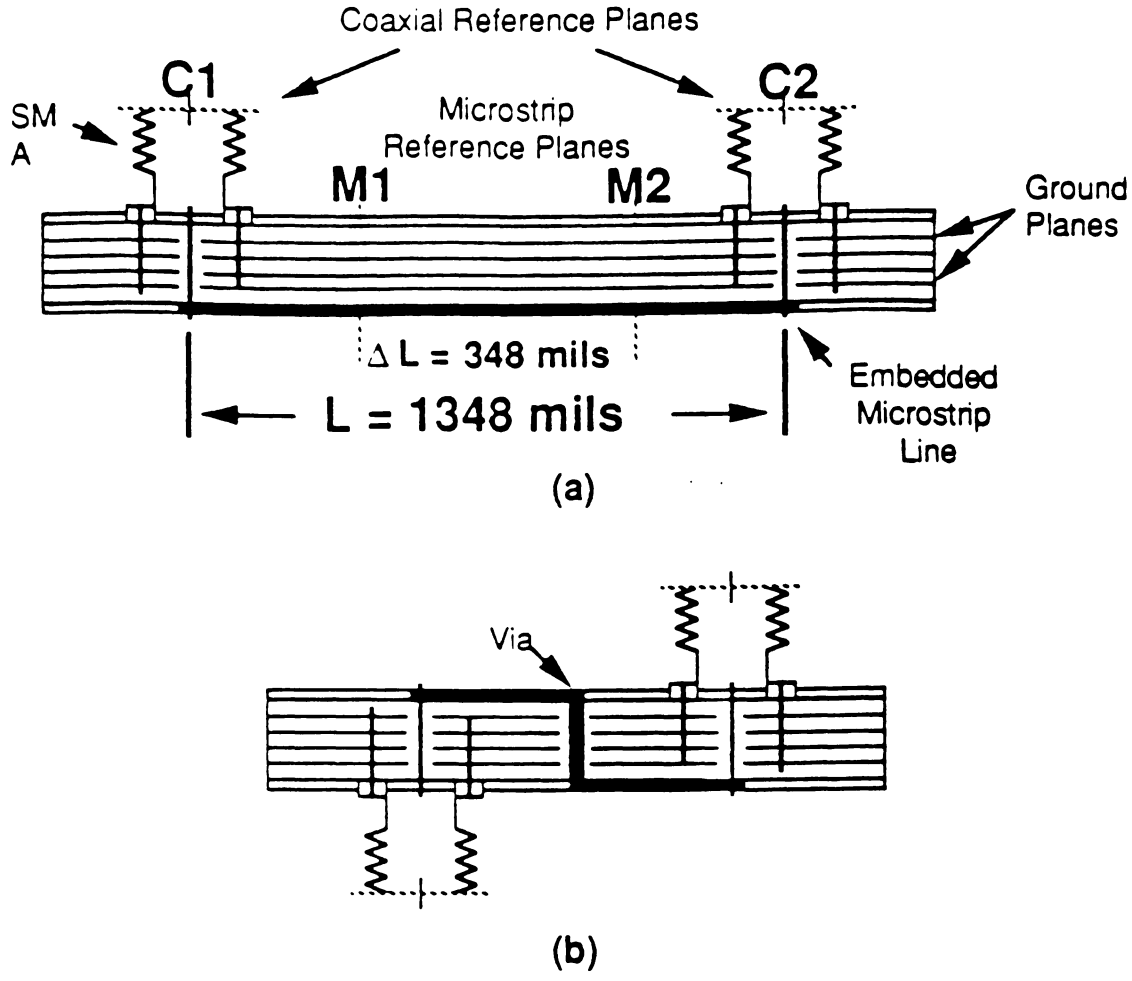

Figure 5.2.10: Diagram of the fixture with line standard inserted (a) and via (b).

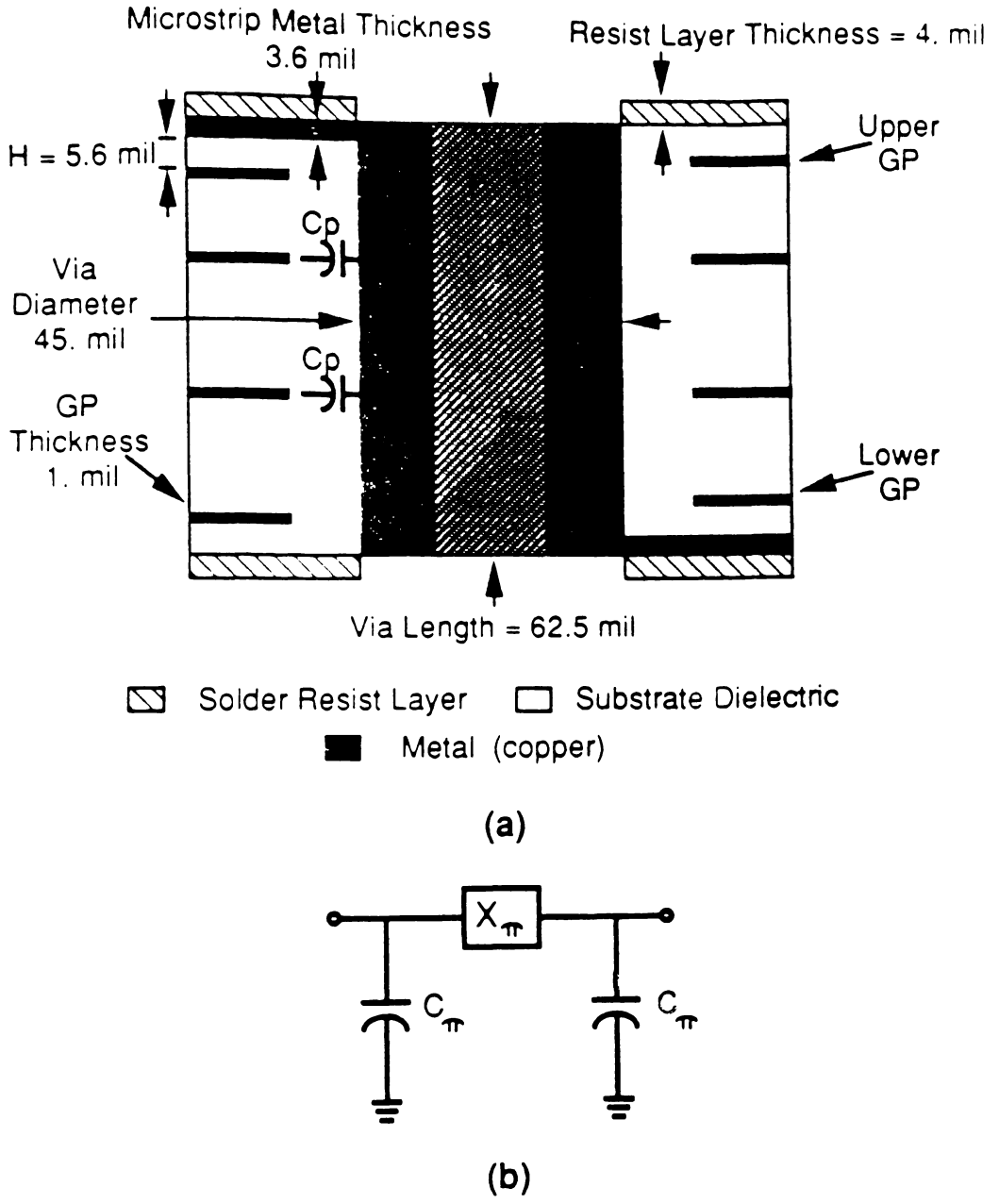

Figure 5.2.11: Detail cross section of printed circuit board via (a) and the pi equivalent circuit (b).

mittance parameters, which form a pi equivalent circuit, and then inverting these admittances. The resulting shunt capacitance (in pico Farads) and series inductive reactance (in ohms) are shown in Fig. 5.2.12 and Fig. 5.2.13 respectively.

When interpreting the TSL results, we should consider the fact that we have imposing a pi equivalent model to the via and at higher frequencies this result will decrease in accuracy. The series reactance behaves as an inductor through two GHz and the capacitance is constant to five. The increasing capacitance (with frequency) is associated with the increased energy stored in the fringe electric fields and the non-ideal inductance arises from resonances with other parisitic capacitances (C_p, 5.2.11).

A final note about the characteristic impedance of the line standard used in TSL. As mentioned in Chapter 3, the TRL algorithm requires that the line standard be reflectionless or we need to determine the impedance. The TSL results were determined using Time Domain Reflectometry (TDR) and found to be 57 ohms. This is different from the manufactures 50 ohm design goal but its effect can be removed as described in ETSL section.

5.2.5 Conclusion

The Through-Symmetry-Line de-embedding method has been used to calculate the pi equivalent circuit of a printed circuit board via. The close agreement between measured and synthesized short circuits verifies that a symmetrical argument can

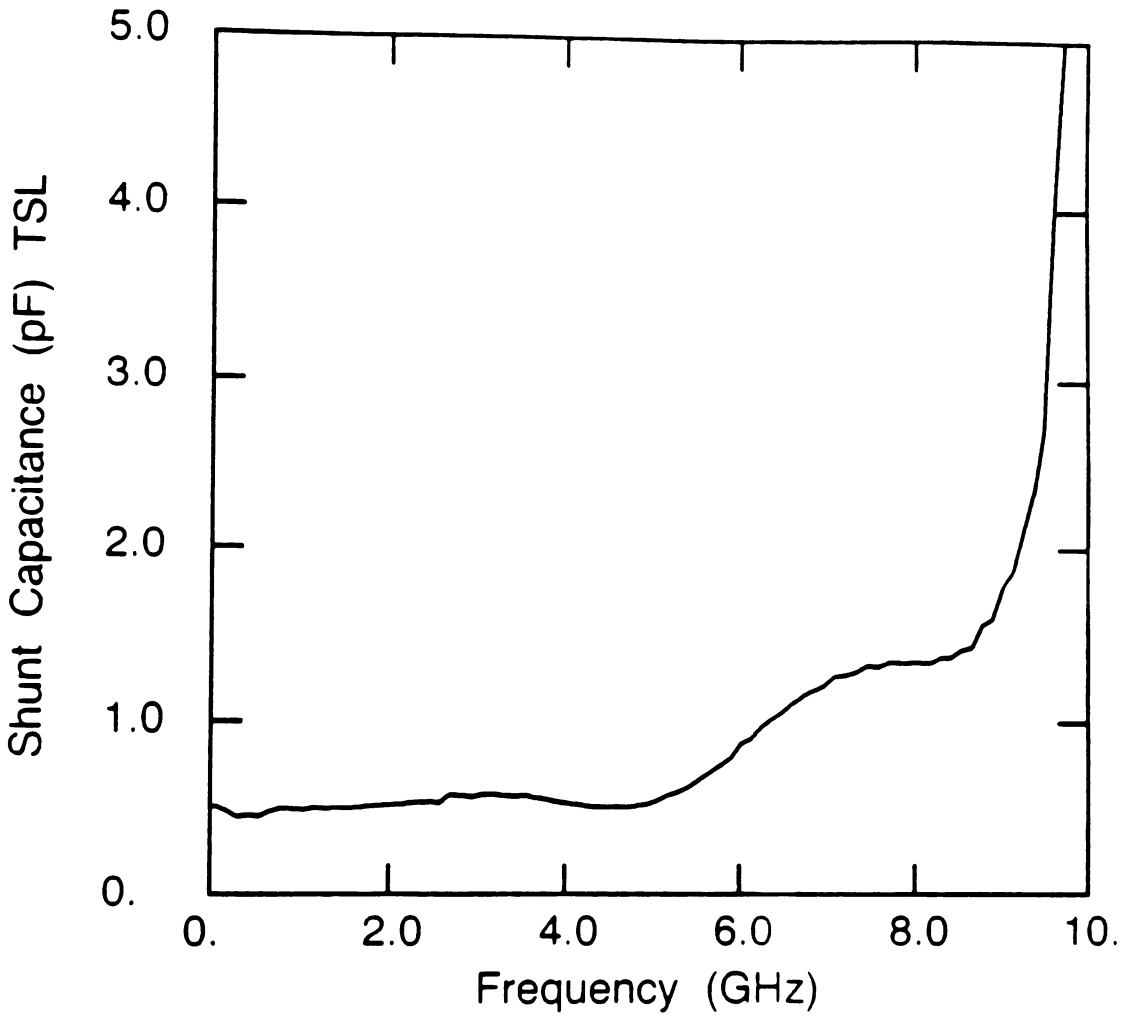

Figure 5.2.12: Shunt capacitance for a via pi equivalent circuit.

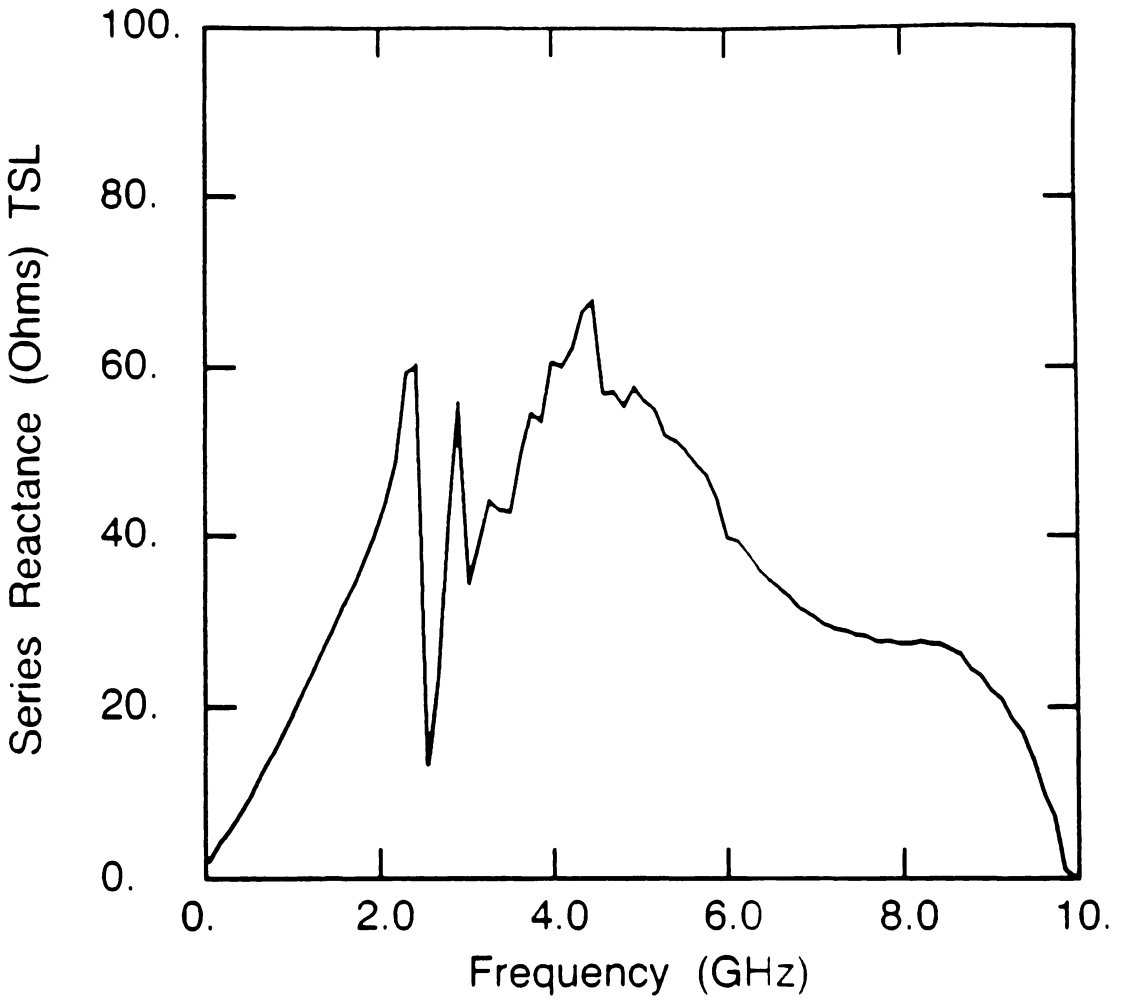

Figure 5.2.13: Series inductive reactance for a via pi equivalent circuit.

be used to modify the TRL algorithm to TSL.

5.3 Verification of the Enhanced Through-Symmetry-Line De-embedding Method

5.3.1 Introduction

This section contains verification of the impedance enhancement to TSL and its use in the new ETSL algorithm. Verification is done by calculating the impedance of a precision 50 ohm air line as well as other transmission line parameters including dielectric and propagation constants.

5.3.2 Coaxial Transmission Line Parameters

Fixturing for this verification is shown in Fig. 5.3.1. It includes two fixture halves each composed of APC-7 to female SMA and a male SMA to APC-7 adaptors. The through connection is the connection of the fixture halves and the air line was inserted between the halves for a line connection. The air line length is 10.21 cm and the air dielectric allows accurate calculation of the half wavelength singularities. These are $f = 1.4691i$ GHz, where $i = 1, 2, 3, \cdots$.

This fixturing was chosen for two reasons. First, the precision air line connections were APC-7 requiring a similar mating connector. Secondly, it was desirable to have a fixture of a non-zero length thus allowing direct application to the mi-

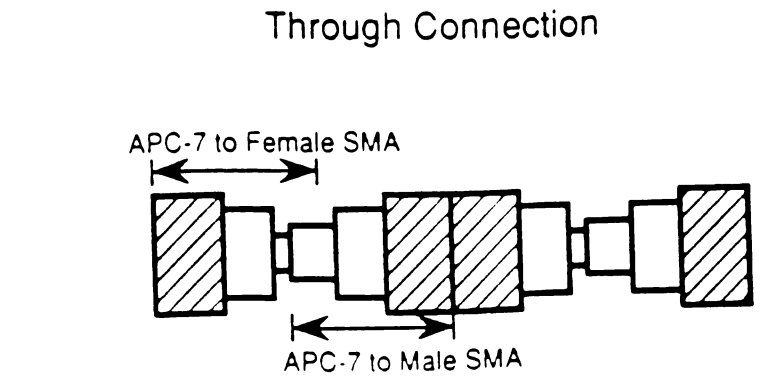

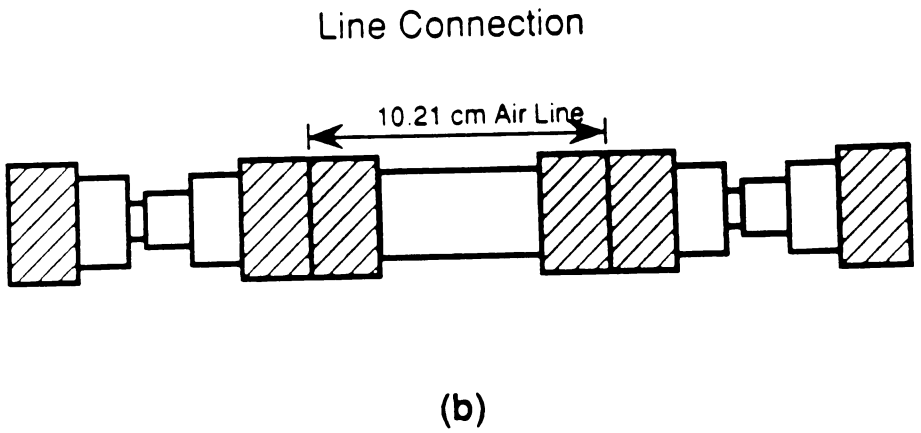

Figure 5.3.1: Coaxial fixturing used to verify TSL impedance enhancement. (a) Through connection and (b) 10.21 cm precision 50 ohm air line inserted in fixture.

crostrip fixture used in the previous TSL results. Next we will present the coaxial transmission line parameters.

Attenuation Constant (α)

The through and line connections were measured over a 15 to 3000 MHz frequency range and the propagation constant was calculated. Fig. 5.3.2 shows the attenuation constant, α, with per meter units. Several observations can be made. It is clear over this frequency range that we encounter two of the predicted halve wavelength singularities since the per meter attenuation values are unrealistically high. These constitute invalid regions. The second observation is low attenuation values within valid regions. This is typical of precision coaxial lines. Finally, we see that at low frequencies (below 200 MHz) we cannot measure significant phase difference between the through and line connection.

Propagation Factor (β)

The calculated propagation factor, $\beta = \frac{\beta}{\beta_0}$, has been normalized with respect to a free-space propagation factor, $\beta_0 = \frac{2\pi f}{c}$ where c is the speed of light, to reveal its accuracy. The precision air line should have a free-space propagation factor and the normalized β should be unity. This result is shown in Fig. 5.3.3.

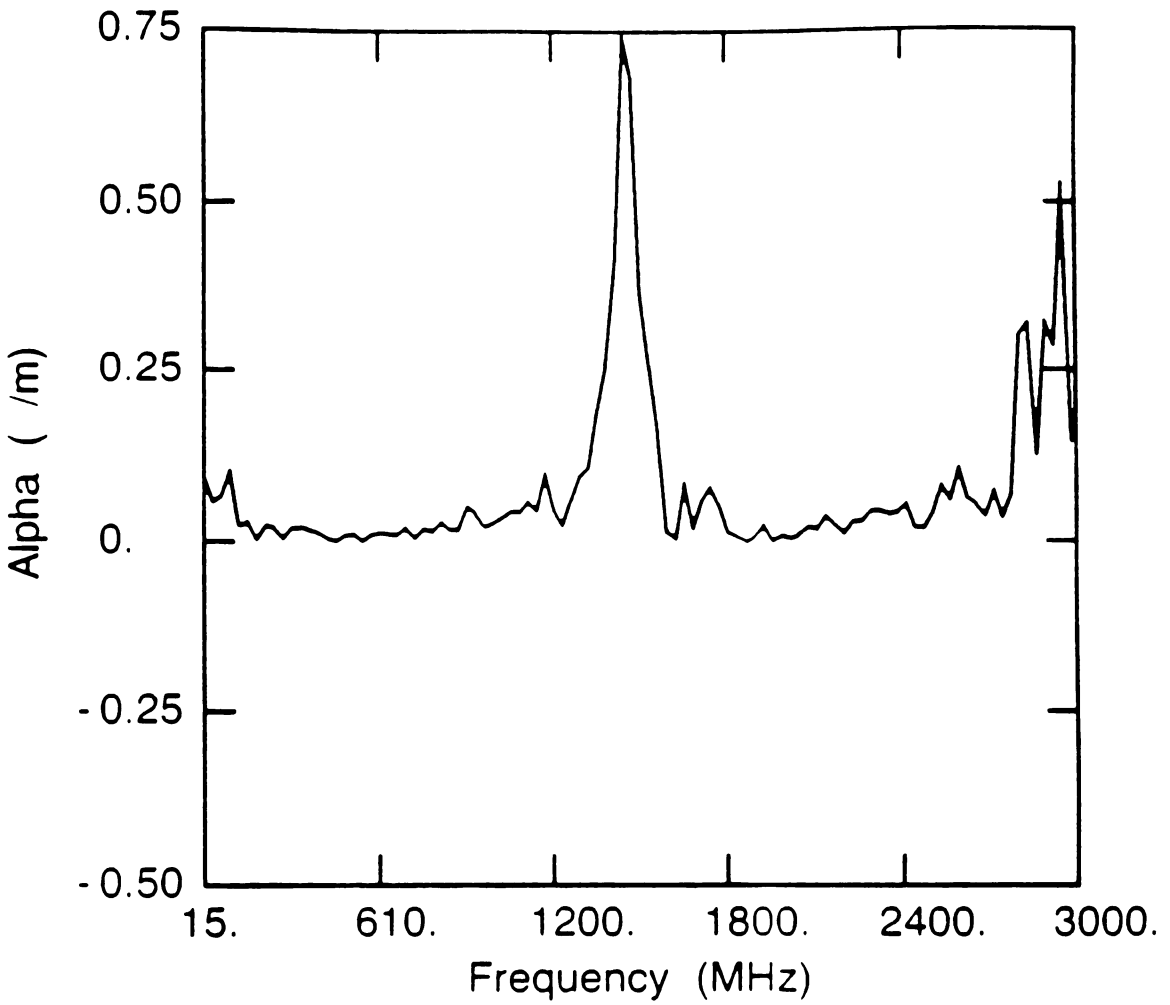

Figure 5.3.2: Attenuation factor, α, for the precision air line. Calculated using 3.6.4.

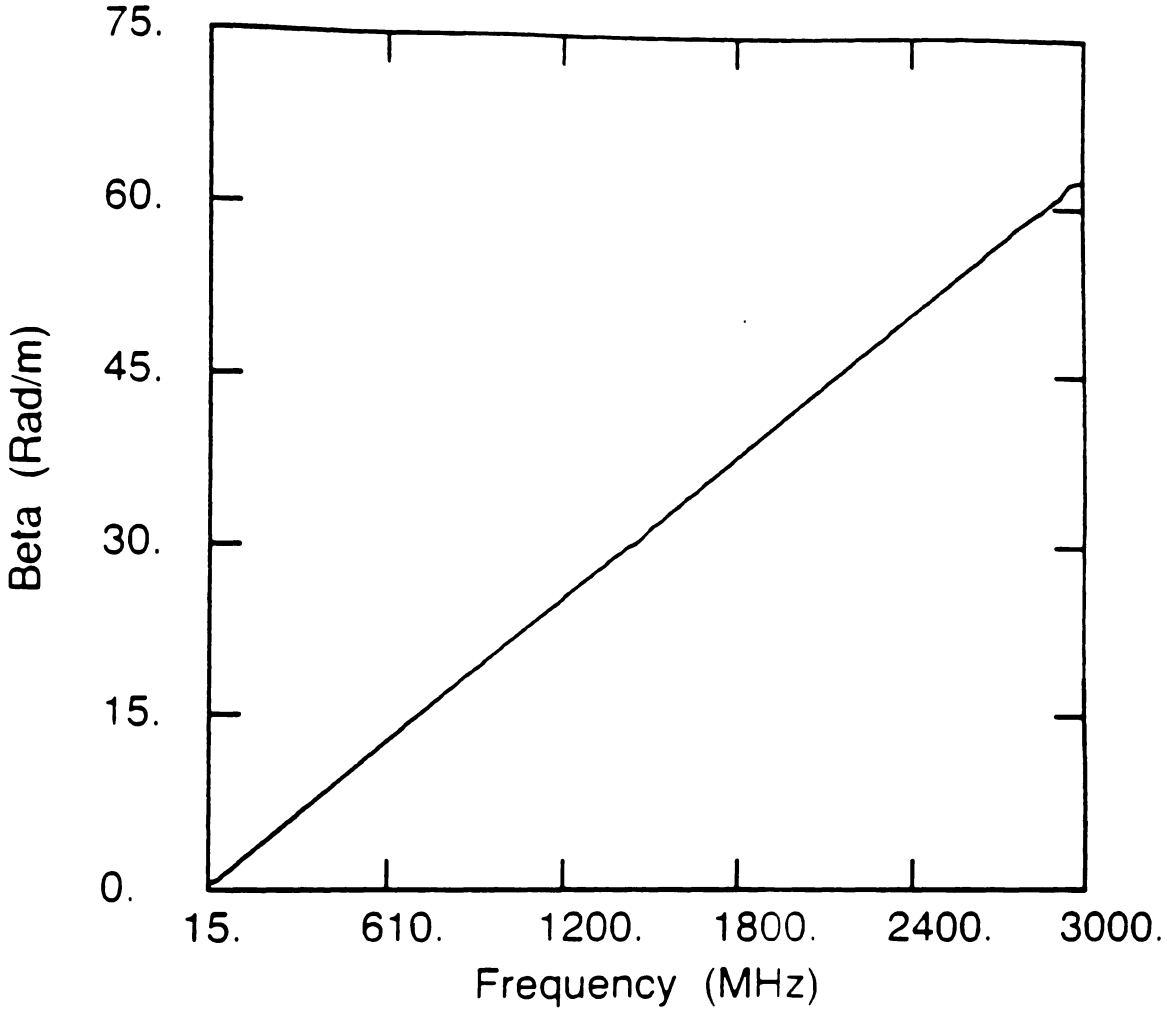

Figure 5.3.3: Normalized beta for the precision air line. Calculated using 3.6.4.

Relative Dielectric Constant (ϵ_r)

Using the propagation constant, $\gamma = \alpha + j\beta$, and equation 3.6.3 we have calculated the relative dielectric constant shown in Fig. 5.3.4. The figure shows that we are calculating the constant correctly since it is nearly unity over much of the frequency range. Naturally, an air dielectric coaxial line should have a unity relative dielectric constant. Up to this point, these results have been derived using previous authors work. Building on their work, we can take the process further by calculating the characteristic impedance of the coaxial line as developed in Chapter 3. Given the propagation constant and the coaxial free-space capacitance we calculate the coaxial characteristic impedance and compare it with the designed 50 ohm value.

Characteristic Impedance (Z_c)

For the reader's convenience we have re-written the characteristic impedance equation from Chapter 3 equation 3.6.8.

$$Z_c = \frac{j\omega}{c^2 C_0 \gamma} \tag{5.3.1}$$

The free-space capacitance, C_0, is a function of the inner and outer radii of the conductors. Measuring these radii is difficult and we chose not to attempt their meaurement. The capacitance can be calculated assuming the coaxial line impedance to be 50 ohms. This is valid because the coaxial designers would have chosen the radii to give a 50 ohm impedance. We have seen that the capacitance is

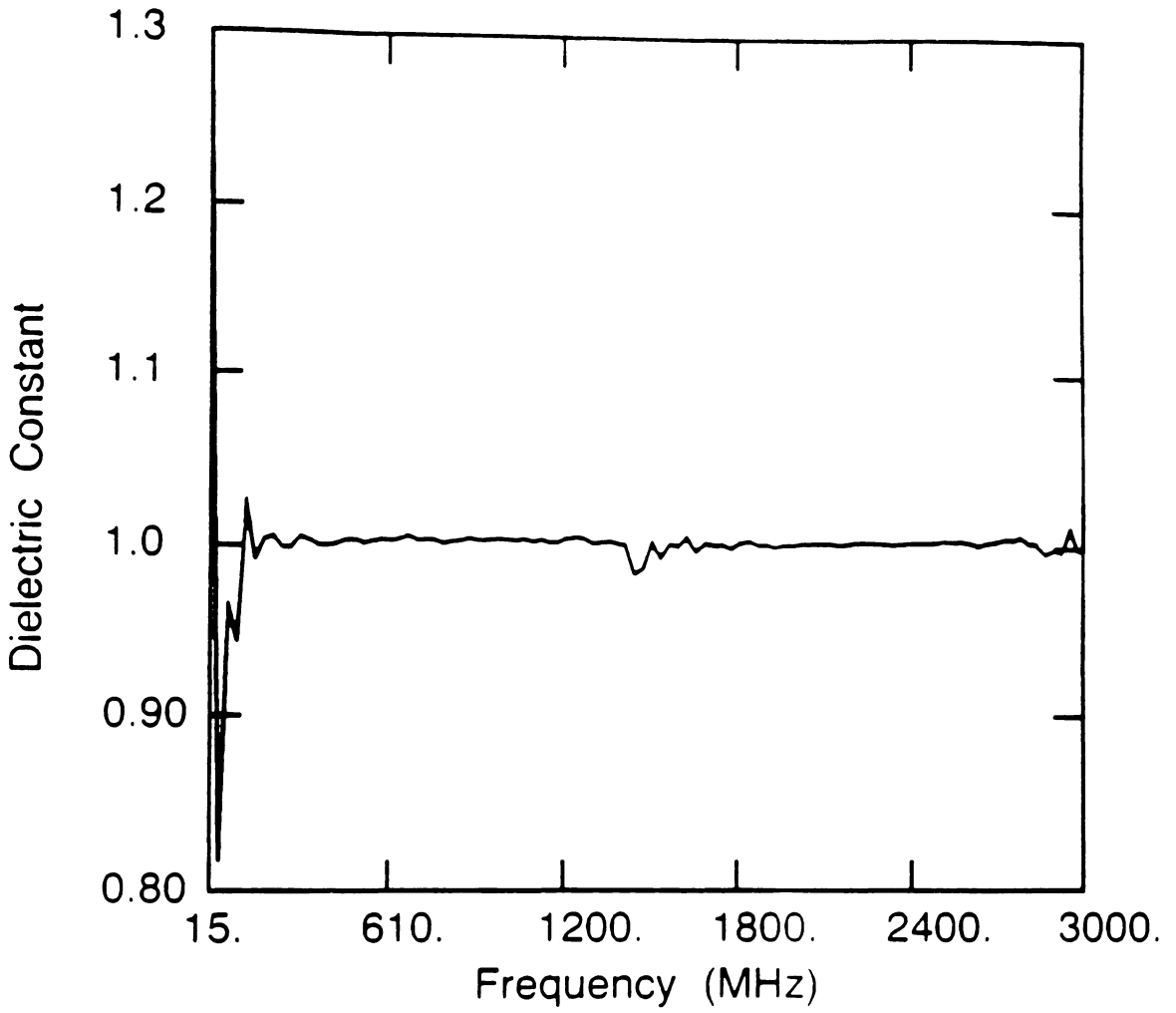

Figure 5.3.4: Relative dielectric constant for the precision air line. Calculated using 3.6.3.

a function of the impedance in Chapter 3 and using equation 3.6.2 we calculate the coaxial free-space capacitance to be 66.71 pico Farads per meter. Applying this to equation 5.3.1 yields the characteristic impedance. Fig. 5.3.5 and 5.3.6 show the real and imaginary values of the coaxial characteristic impedance. The real value is within one tenth of an ohm to 50 ohms and the imaginary is esentially zero showing good agreement with expected values. Now we can apply this impedance calculation to the embedded microstrip fixture used in the TSL results.

5.3.3 Embedded Microstrip Transmission Line Parameters

This section presents transmission line results calculated in the same manner as the coaxial example above. The fixturing used here is identical to the TSL fixture. With TSL, we determined the characteristic impedance of the line standards using TDR and here we will see that the impedance is complex and that the embedded microstrip lines are dispersive. The Δl used in this section is five cm. This value is necessary to extract reliable results at the lowest measurent frequency, 45 MHz yet it does increase the number of invalid regions. The results show that these regions exist but have little effect on calculating the embedded microstrip transmission line parameters.

Attenuation and Propagation Constants (α and β)

Embedded microstrip attenuation constant is shown in Fig. 5.3.7, with units

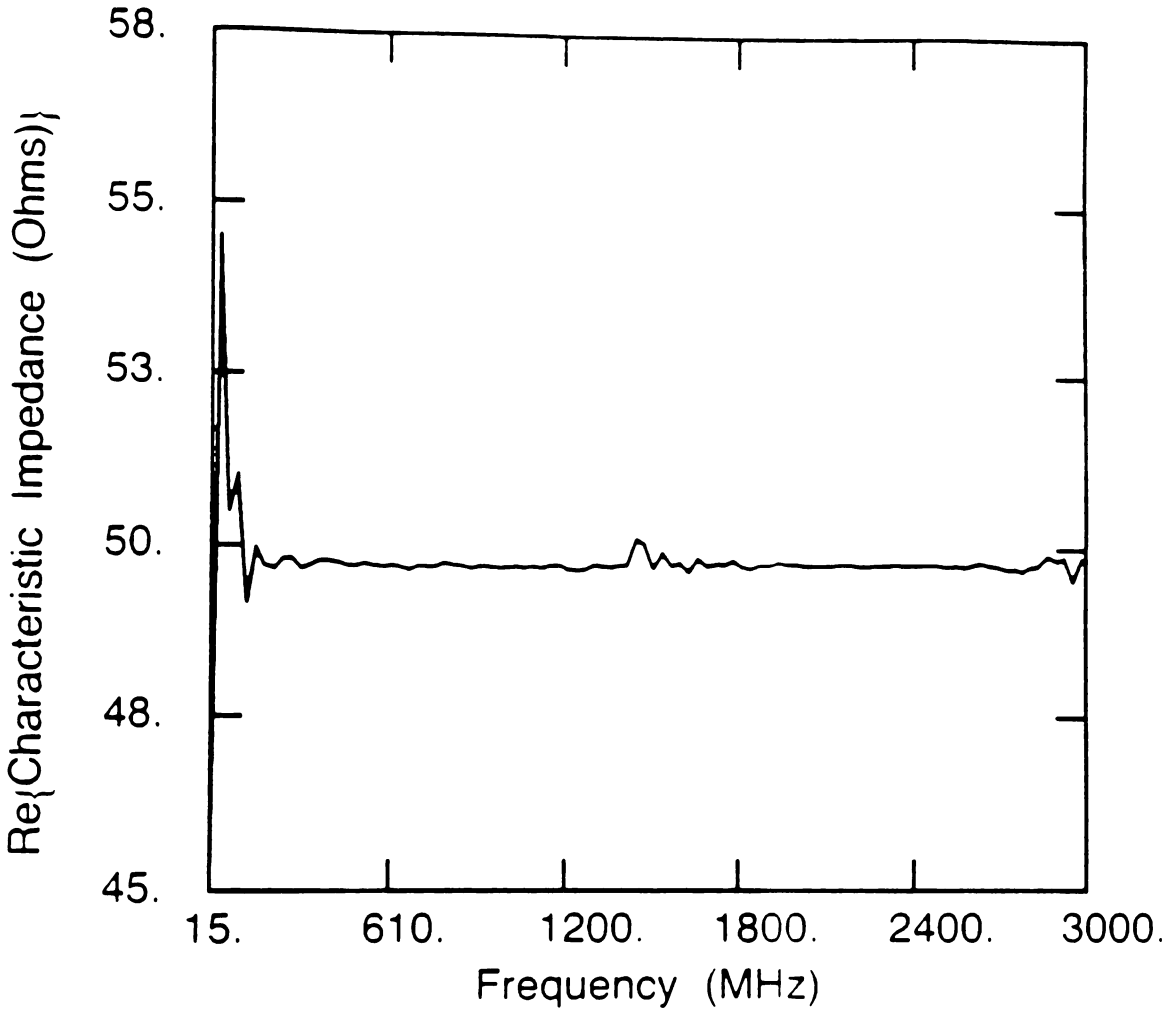

Figure 5.3.5: Real portion of the coaxial characteristic impedance. Calculated using the free-space capacitance and equation 5.3.1.

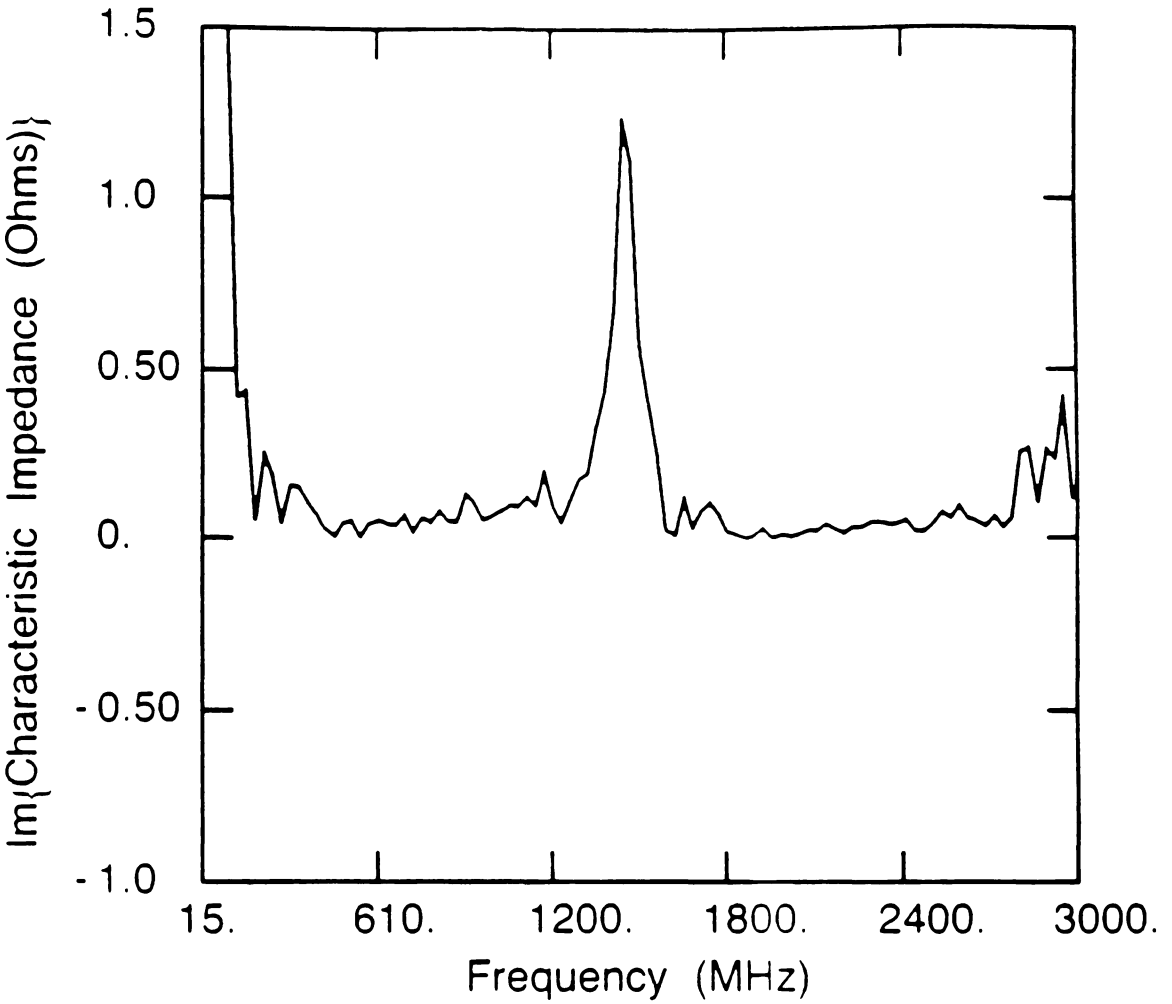

Figure 5.3.6: Imaginary portion of the coaxial characteristic impedance. Calculated using the free-space capacitance and equation 5.3.1.

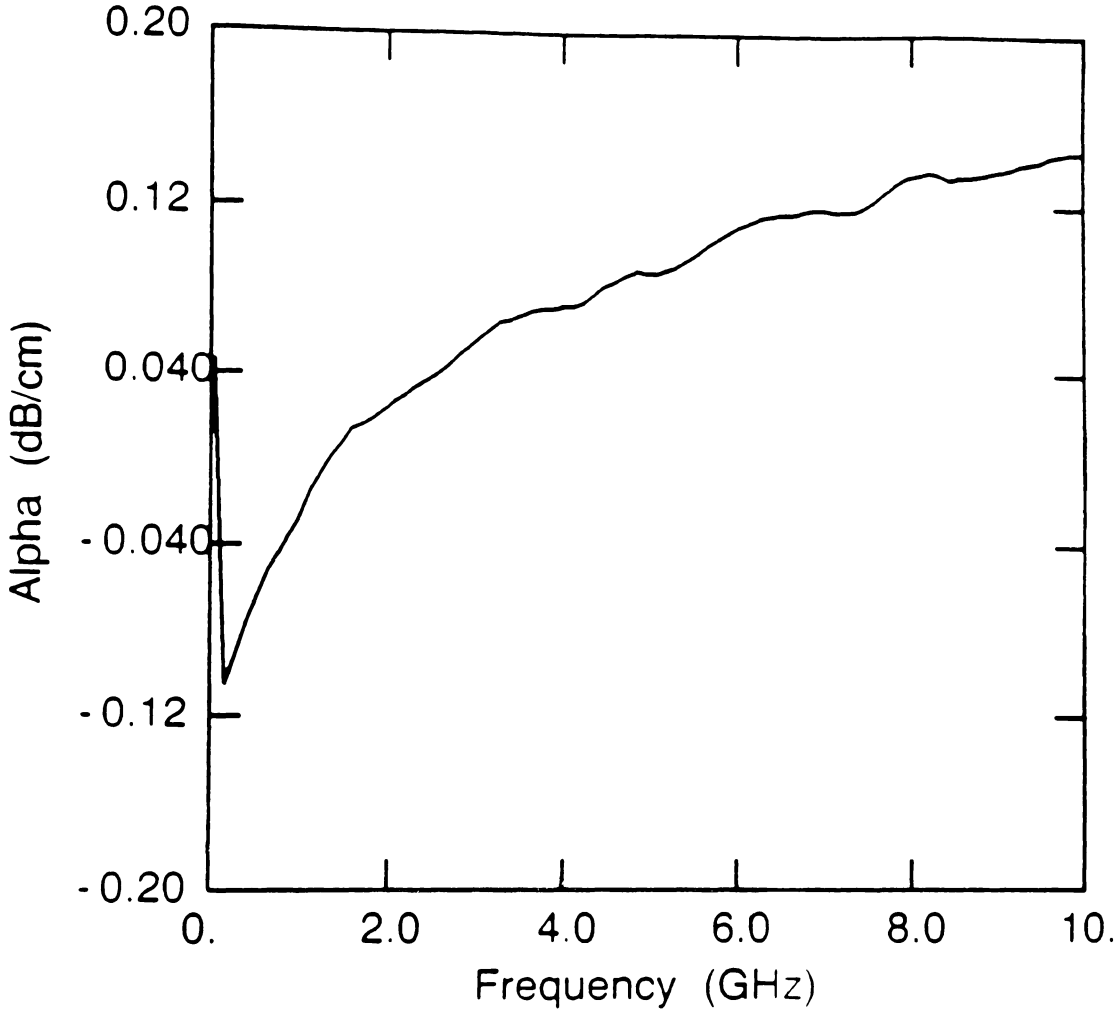

Figure 5.3.7: Attenuation constant, α, for a 5 cm embedded microstrip. Calculated using 3.6.4.

of dB/cm. Also, Fig. 5.3.8 shows the normalized propagation factor for the transmission line. The normalized β is a decreasing function of frequency therefore the line is dispersive. Additionally, values are greater than unity therefore the effective dielectric constant must also be greater than one.

Effective Dielectric Constant (ϵ_r)

As with the coaxial line, we calculate the real and imaginary parts of the embedded microstrip effective dielectric constant, $Re(\epsilon_{eff})$ and $Im(\epsilon_{eff})$ Fig. 5.3.9 and 5.3.10 respectively. The singularity effects are more pronounced here but they are still not significant. The decreasing $Re(\epsilon_{eff})$ represents dispersion and is intuitively clear since the amount of electric field contained in the air above the microstrip increases with frequency therefore lowering the effective dielectric constant. Moreover, $Im(\epsilon_{eff})$ increases to a constant value for similar reasons. Note, $Im(\epsilon_{eff}) = 0.1$ corresponds to a loss tangent of 0.03.

Characteristic Impedance (Z_c)

The free-space capacitance has been calculated as described by Bahl and Stuchly [33] and for this study has been found to be 31.59 pico Farads per meter. Given this and the propagation constant we calculate the complex characteristic impedance Z_c with results given in Fig. 5.3.11, and Fig. 5.3.12 imaginary impedance. The characteristic impedance is complex with increasing real and decreasing imaginary parts. These relationships are caused by the dielectric covering which effectively

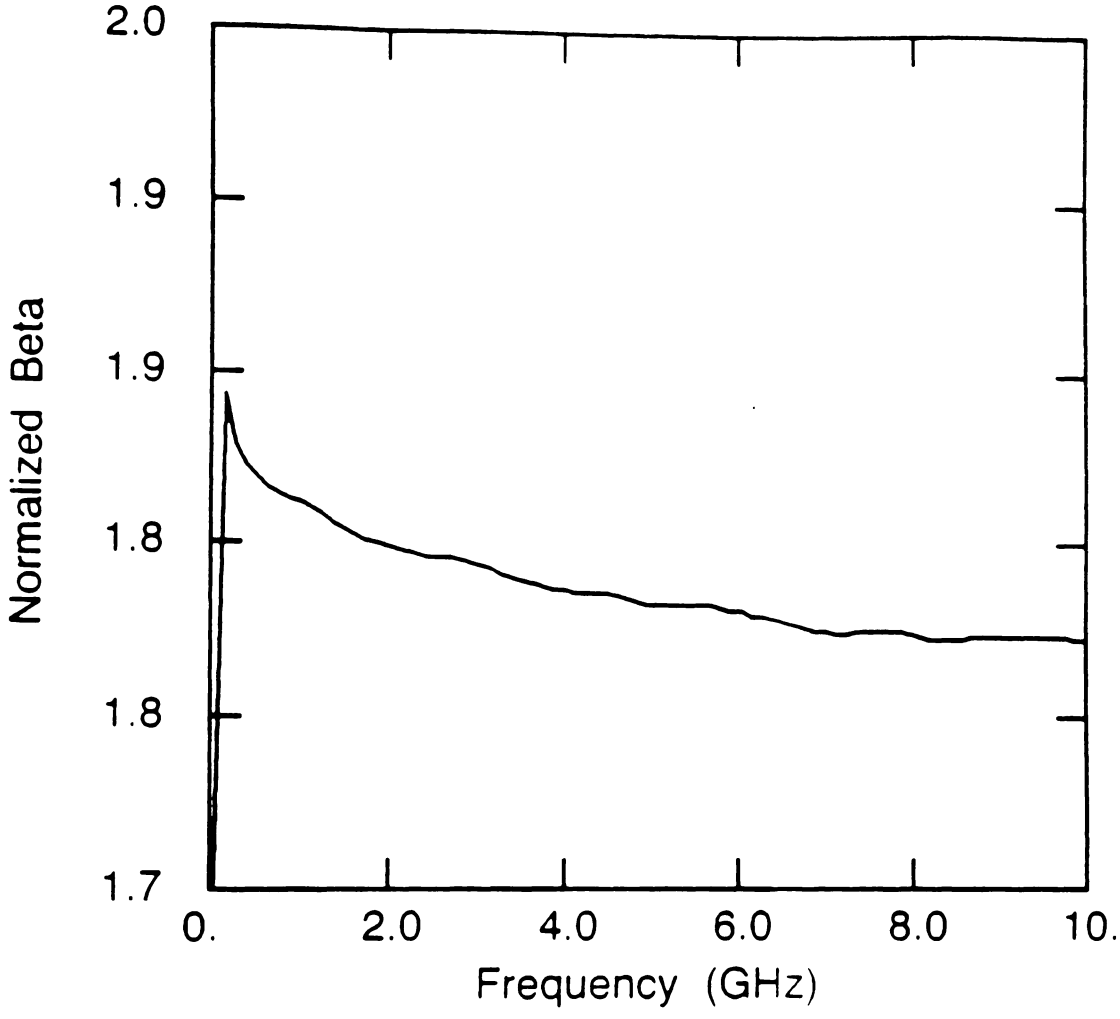

Figure 5.3.8: Normalized propagation factor for a 5 cm embedded microstrip. The decreasing value indicates dispersion. Calculated using 3.6.4.

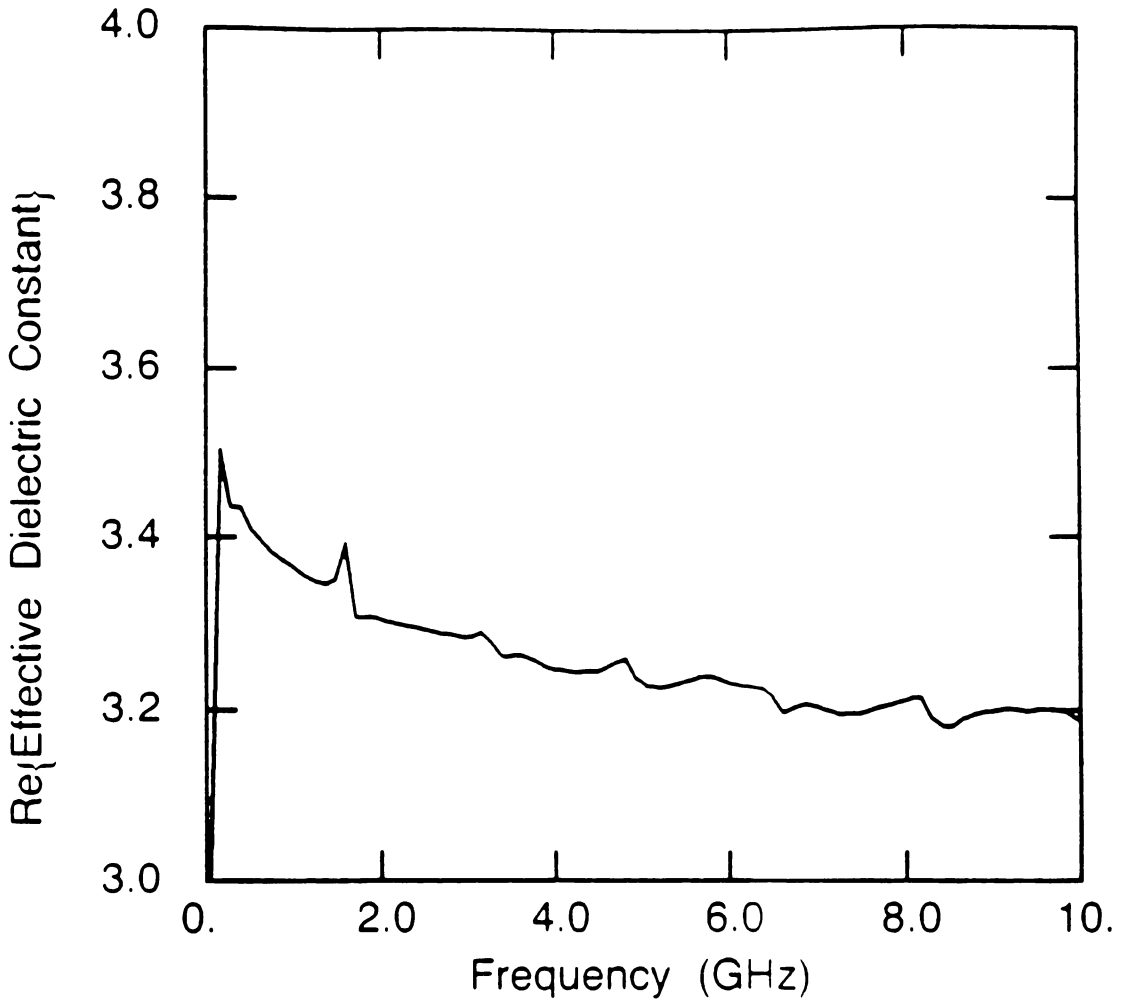

Figure 5.3.9: Real portion of the effective dielectric constant for a 5 cm embedded microstrip. Again, a decreasing value indicates dispersion. Calculated using 3.6.3.

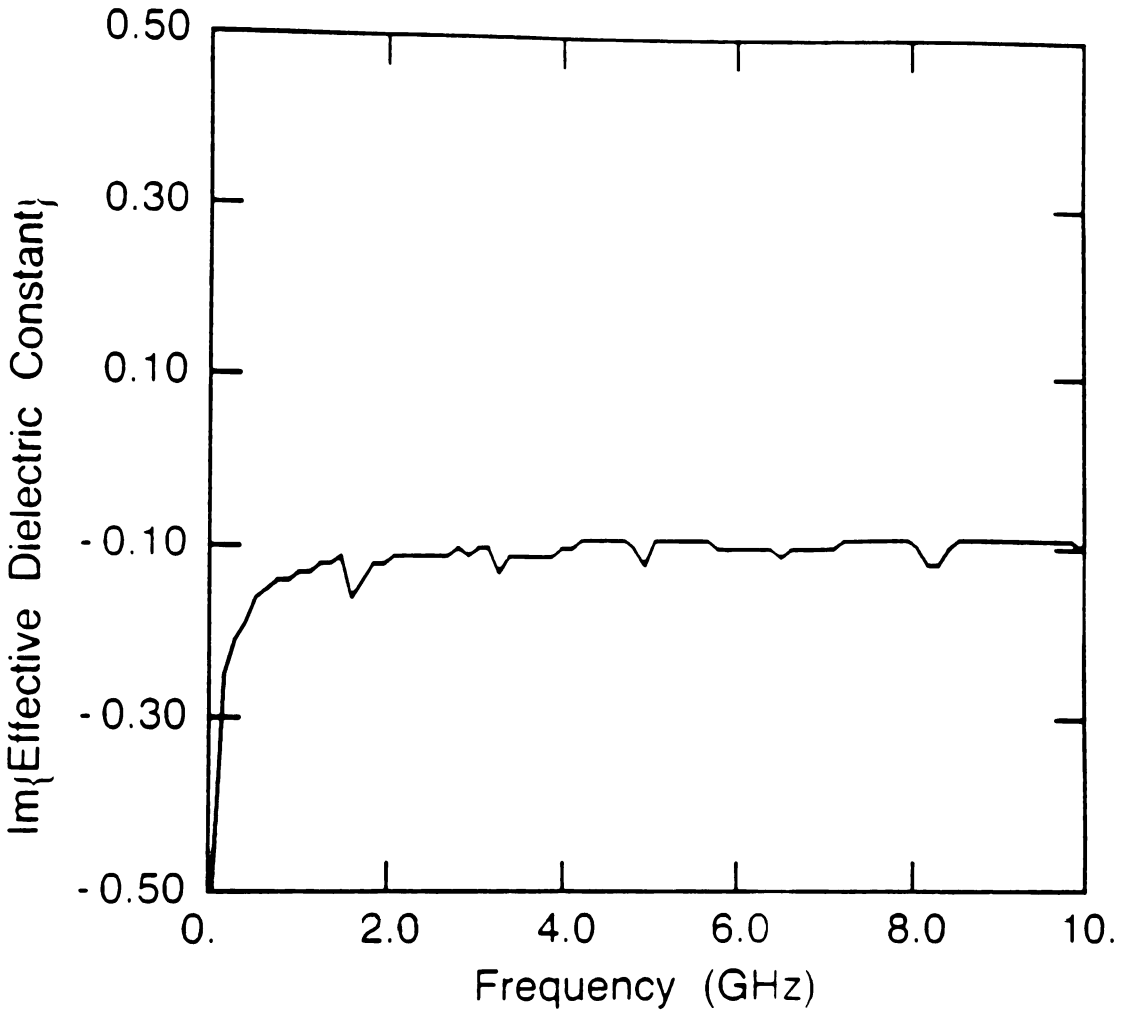

Figure 5.3.10: Imaginary portion of the effective dielectric constant for a 5 cm embedded microstrip. Calculated using 3.6.3.

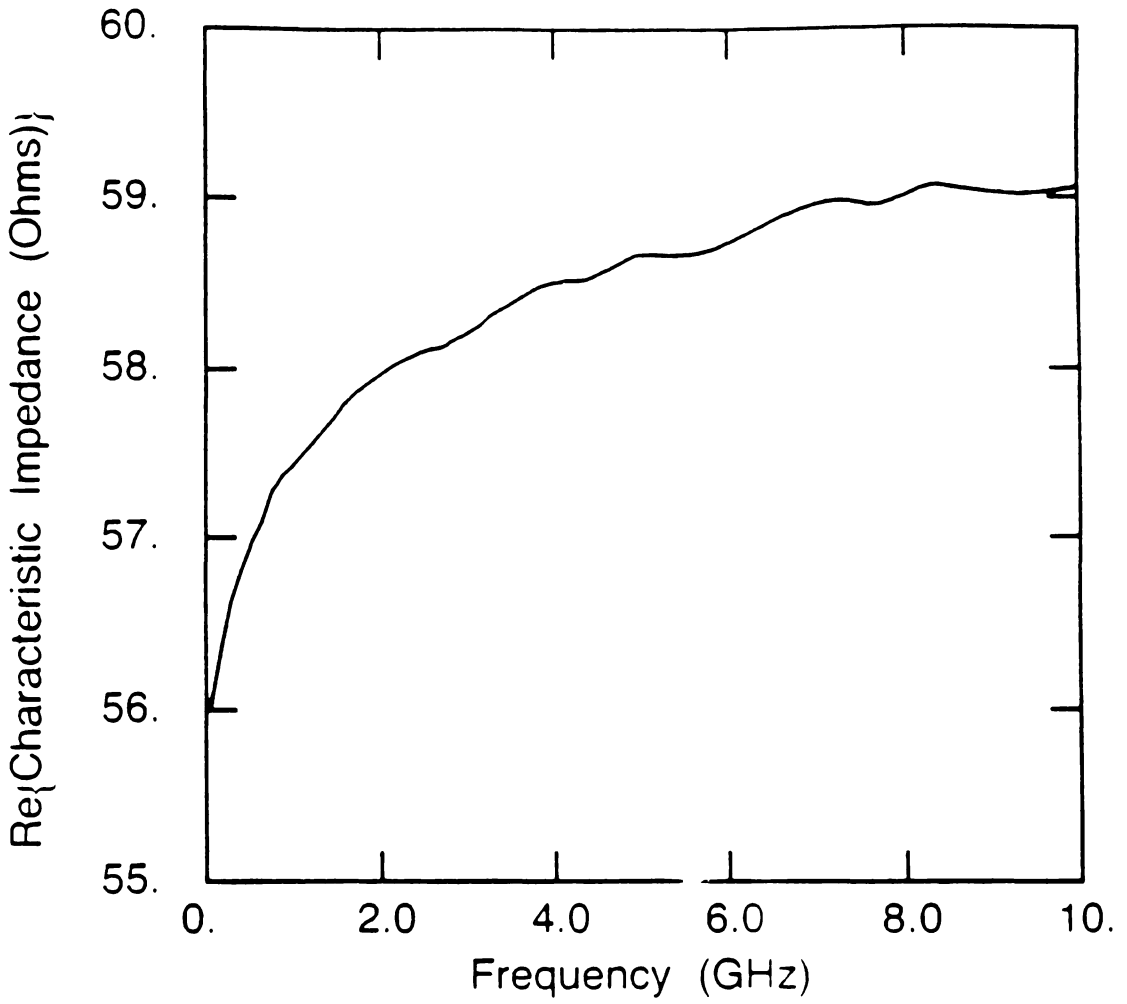

Figure 5.3.11: Real portion of the characteristic impedance for a 5 cm embedded microstrip. Calculated using the free-space capacitance and equation 5.3.1. TDR result for this line is 57 ohms.

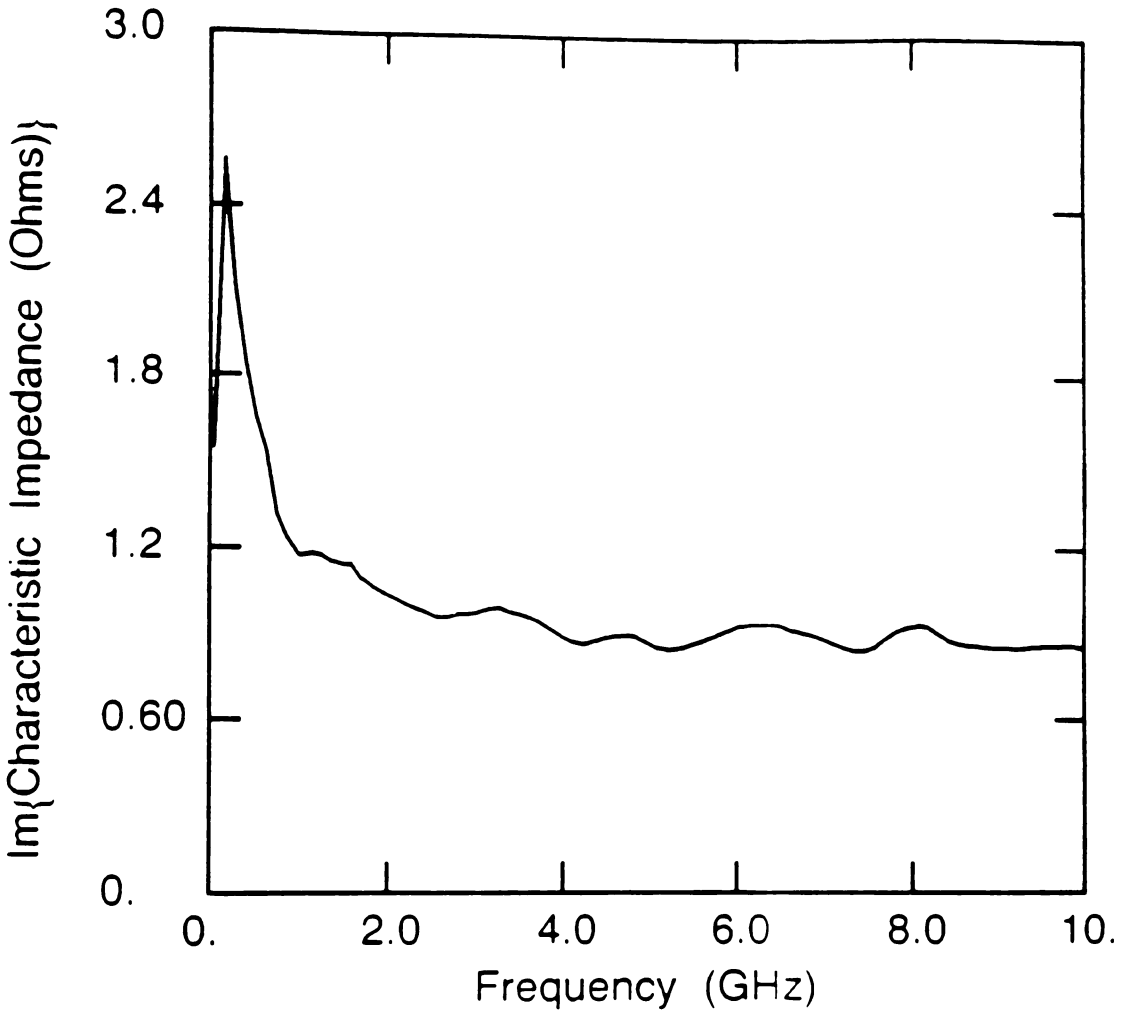

Figure 5.3.12: Imaginary portion of the characteristic impedance for a 5 cm embedded microstrip. Calculated using the free-space capacitance and equation 5.3.1.

contains much of the fringe electric field. At higher frequencies, the electric field occupies more of the free-space above the cover layer and the embedded microstrip exhibits microstrip behavior.

5.3.4 ETSL De-embedding Results

Finally, we apply this characteristic impedance profile to the line standard used in TSL and de-embed the same PCB via. Shunt capacitance and series inductive reactance are shown in Fig. 5.3.13 and Fig. 5.3.14 respectively.

5.3.5 Conclusion

The calculation of transmission line parameters for a precision 50 ohm coaxial line indicates that it is possible to determine the impedance using a free-space capacitance. Application of this calculation to the embedded microstrip makes it possible to calculate the complex characteristic impedance and then use it to improve the TSL algorithm. Enhanced Through-Symmetry-Line has been used to de-embed a PCB via from a symmetric fixture.

The effect of loss in transmission lines is indicated by dispersion and complex characteristic impedances. Also, loss reduces the effect of TRL singularities associated with half wavelength line standards. Up to now we have refered to these invalid regions as singularities yet the results only show minor pertibations in these regions. In fact, they are not mathematical singularities because the line standard

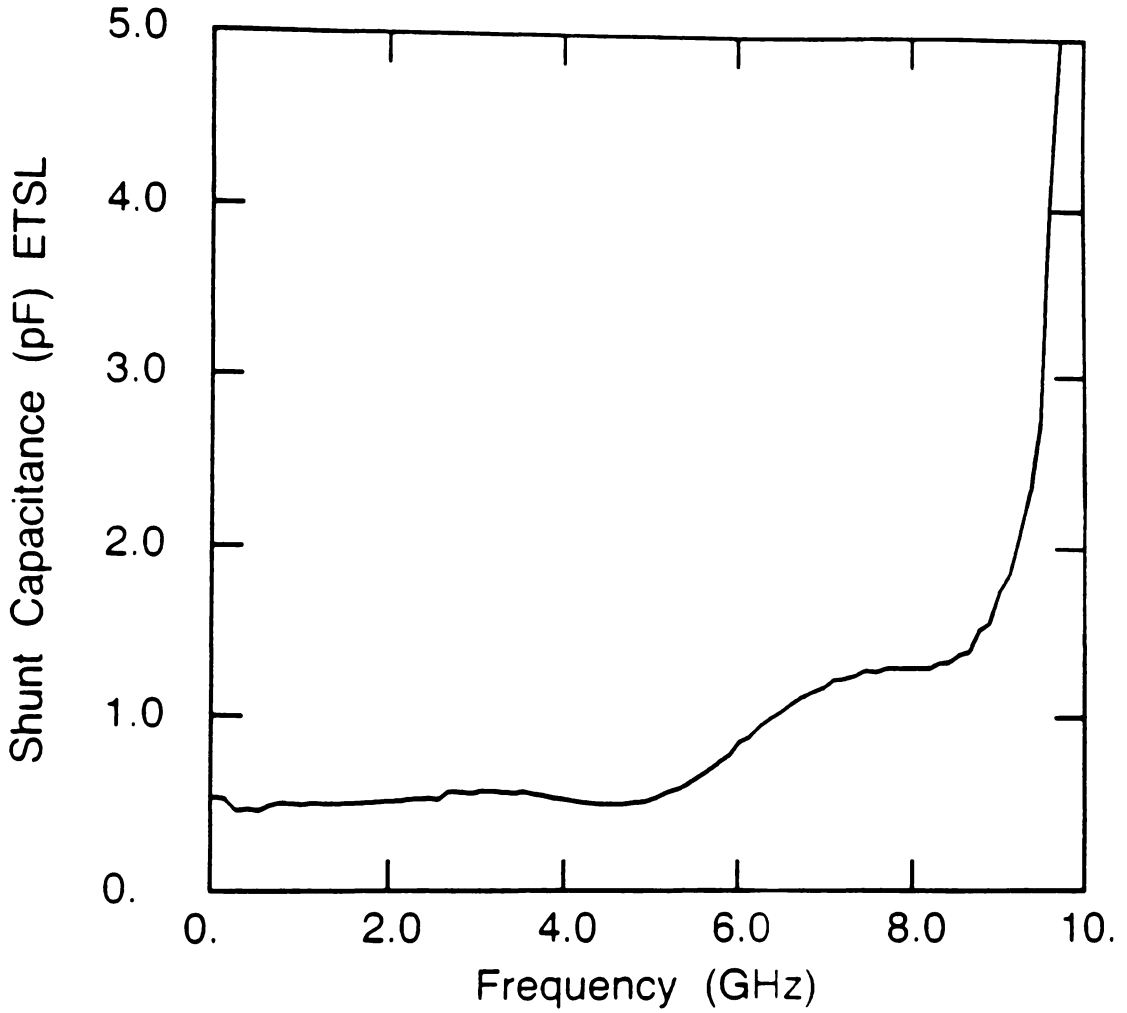

Figure 5.3.13: Shunt capacitance for a via pi equivalent circuit.

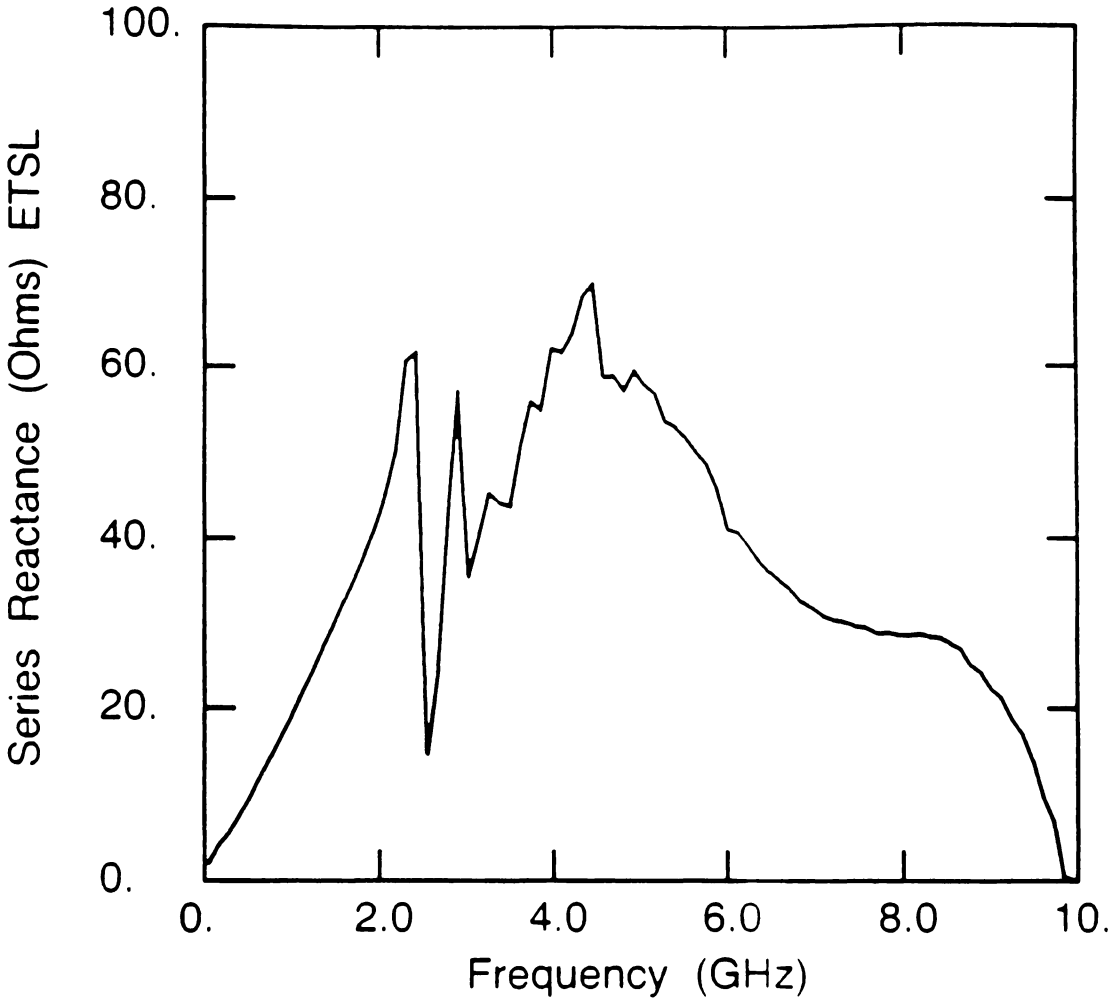

Figure 5.3.14: Series inductive reactance for a via pi equivalent circuit.

has higher per unit length loss than the through standard. At half wavelength frequencies, the line appears transparent only contributing an additional attenuation above that of the through.

A direct comparison of the via inductive reactance between TSL and ETSL is shown in Fig. 5.3.15. There is difference over the middle to upper frequency range. It is in this region that the complex impedance is farthest from the TDR 57 ohm value. More important than this comparison is that we can calculate the complex impedance of a uniform transmission line and include dispersion.

5.4 Results of the Through-Symmetric Fixture De-embedding Method

5.4.1 Introduction

This section contains verification of the TSF algorithm over a frequency range of 45 to 800 MHz. Also, TSF uses different fixturing so we will discuss its design and measurement. Verification is done by direct measurement of both the fixture halves and a de-embedded low pass filter.

5.4.2 Measurement and Fixture Design

It was shown in Chapter 3, that TSF requires a second order symmetric fixture. This forces the fixture halves to be symmetric and identical. The fixture was

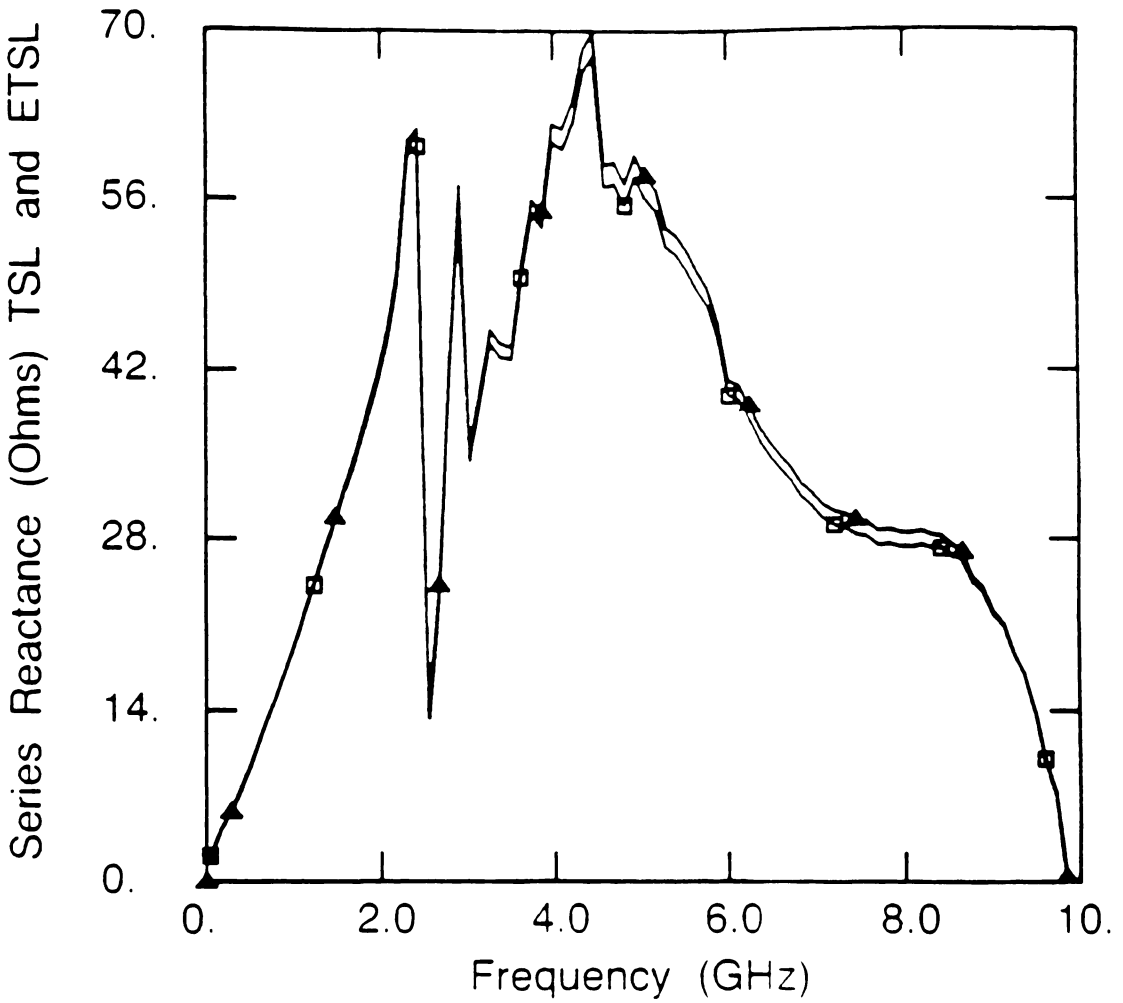

Figure 5.3.15: Comparison of via inductive reactance calculated with (□) TSL and (△) ETSL.

design to introduce significant error in the embedded measurement and still maintain the symmetry requirement. This was accomplished with an shunt inductive discontinuity placed between an APC-7 to female SMA adaptor and a male SMA to APC-7 adaptor, see Fig. 5.4.1. These connector combinations allow direct measurement and subsequent comparison with the error networks calculated with TSF.

The approximate inductance is ten nano Henries and connected as a shunt element appears as a short circuit at low frequencies and open at higher frequencies. This creates significant error yet it is possible to construct two of these fixture halves and satisfy the symmetrical requirements. Fig. 5.4.2 and 5.4.3 show the magnitude and phase of S_{ijf} respectively for the fixture s parameters. Only S_{11f} and S_{21f} need be shown because $S_{22f} = S_{11f}$ and $S_{12f} = S_{21f}$; the fixture is symmetric. The next section presents results of the TSF algorithm.

5.4.3 TSF De-embedding Results

TSF was applied to the embedded low pass filter (DUT) and results are shown in Fig. 5.4.4- 5.4.11. These graphs show the significant effect the fixture error networks impose and comparison, in magnitude and phase, between direct measurement and the TSF de-embedded filter.

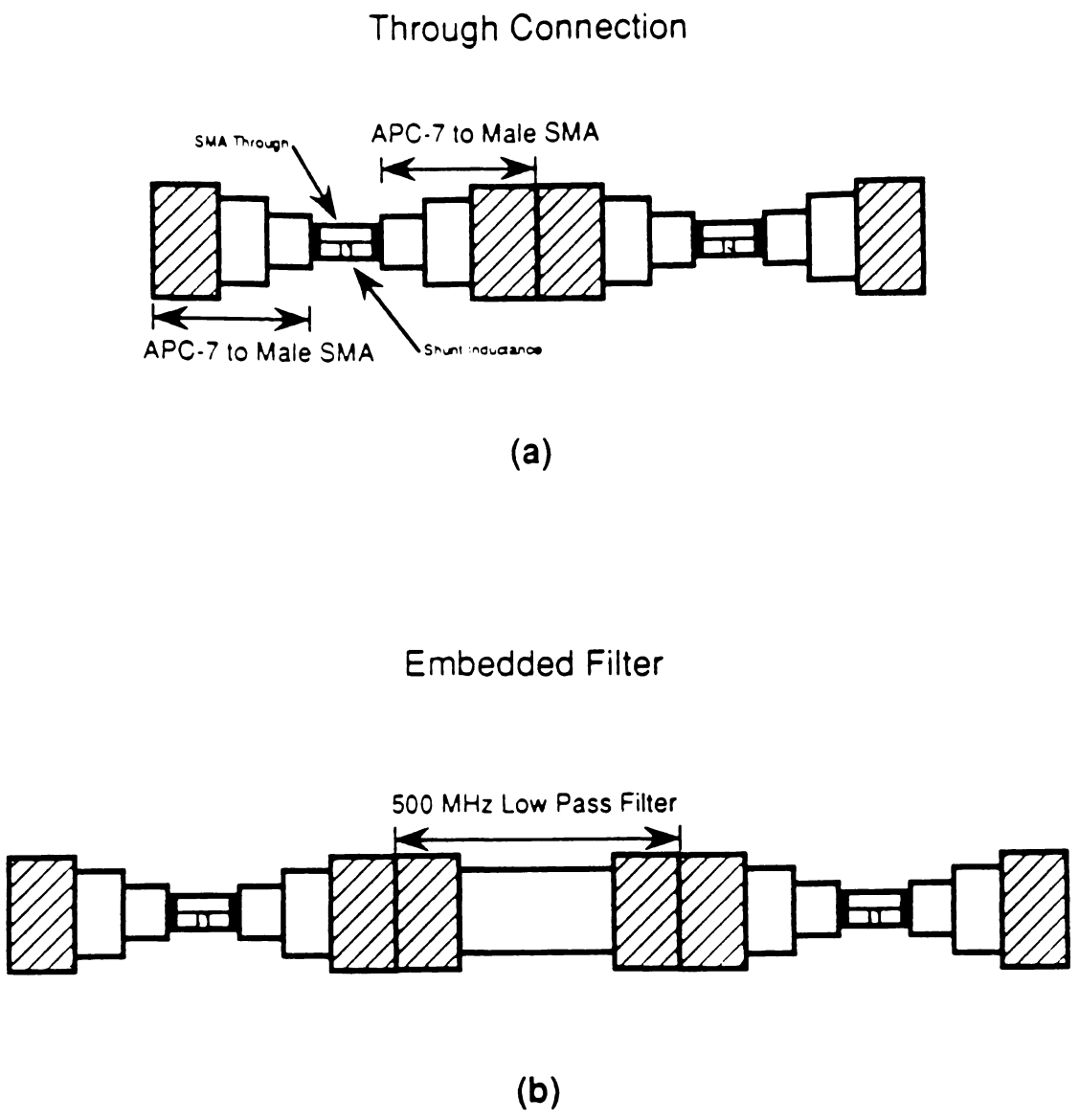

Figure 5.4.1: Fixturing for verification of TSF. (a) Fixture through connection and (b) embedded 500 MHz low pass filter. The fixture halve is composed of two adaptors (APC-7 to male SMA) and the shunt inductor (10 nano henries) mounted in a SMA through.

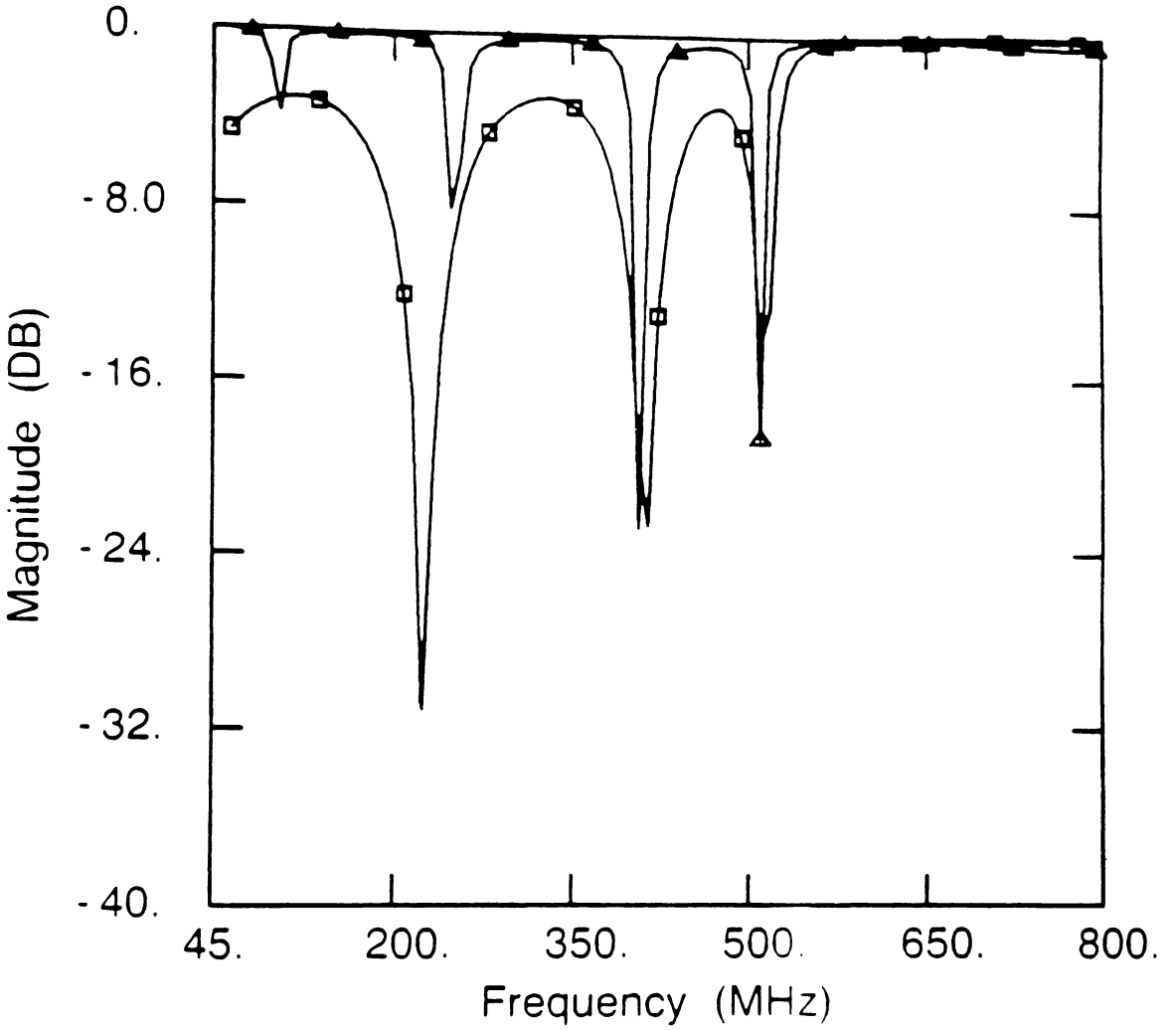

Figure 5.4.2: Magnitude of the TSF fixture s parameters, (□) S_{11f} and (△) S_{21f}.

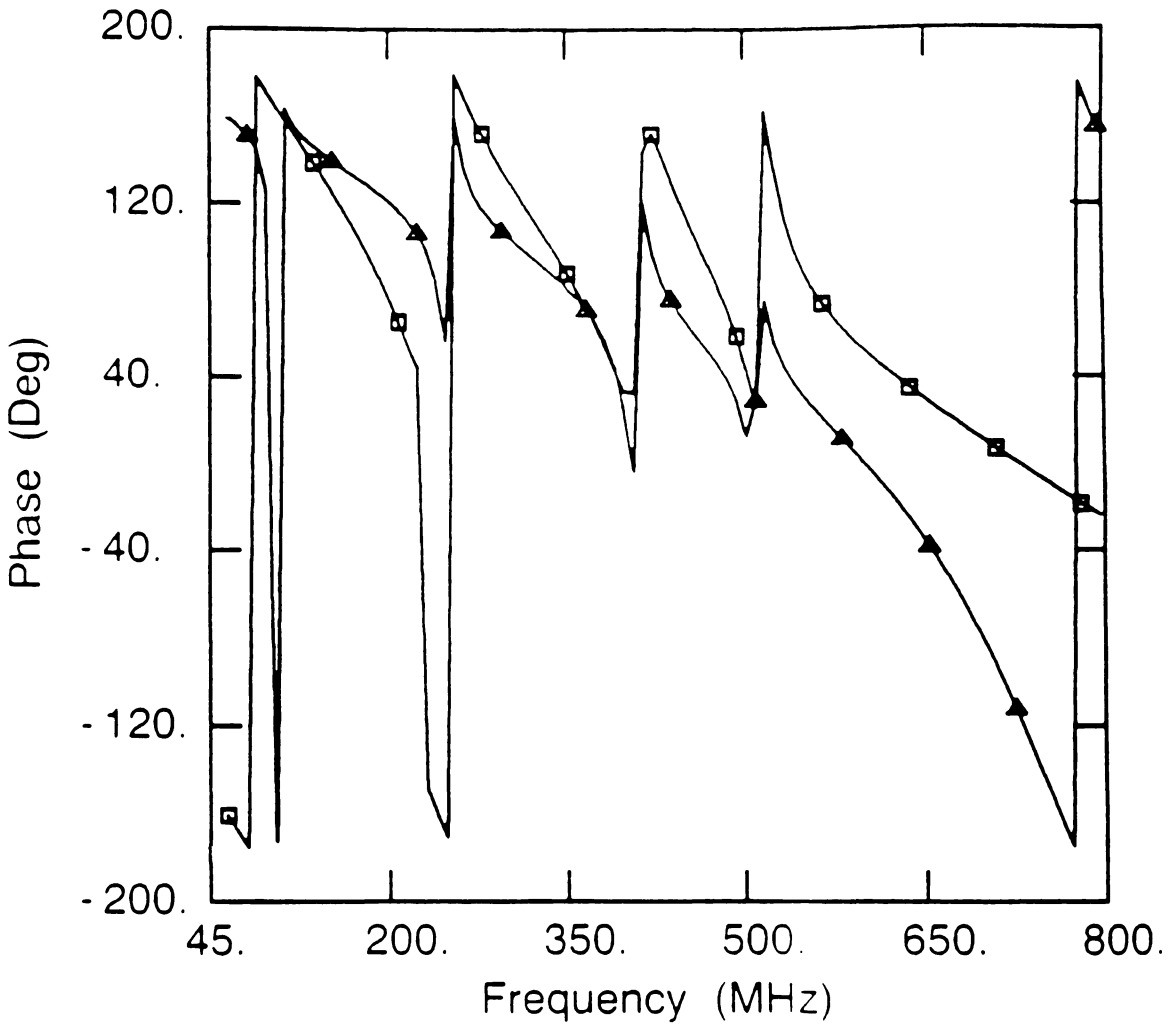

Figure 5.4.3: Phase of the TSF fixture s parameters, (□) S_{11f} and (△) S_{21f}.

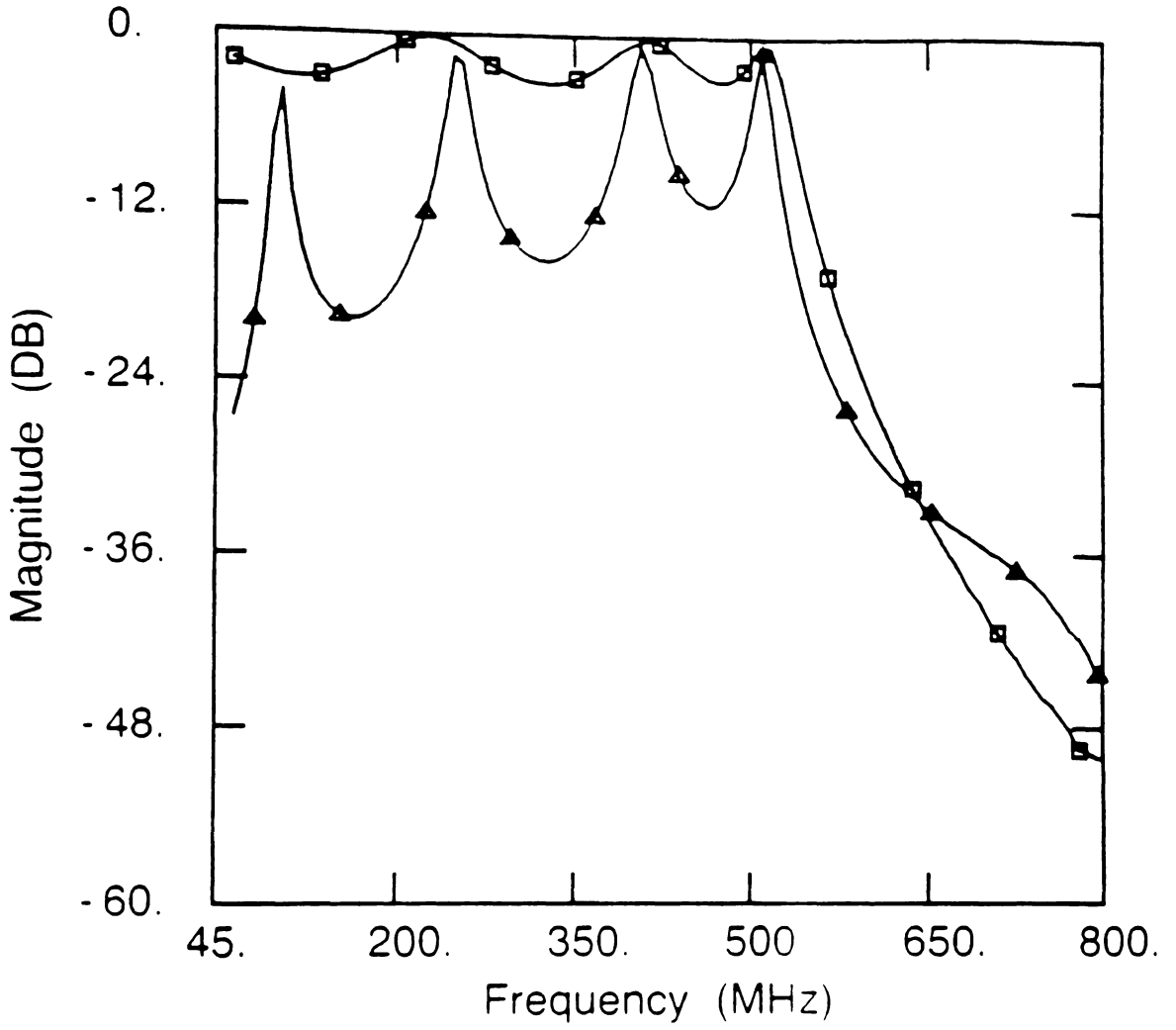

Figure 5.4.4: Magnitude of the filter S_{21}, (□) direct measurement and (△) embedded. The fixture error significantly alters the filter measurement.

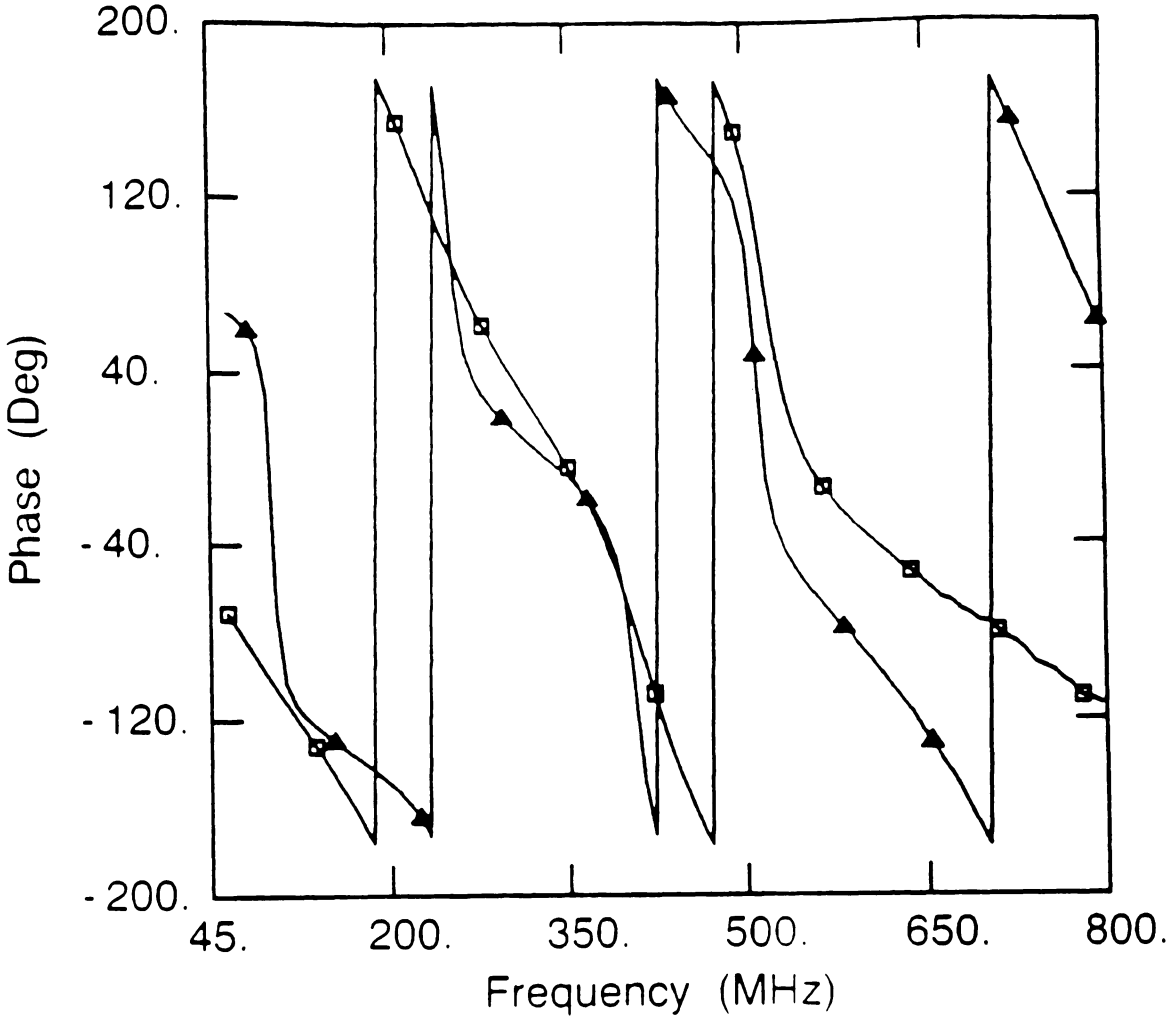

Figure 5.4.5: Phase of the filter S_{21}, (□) direct measurement and (△) embedded.

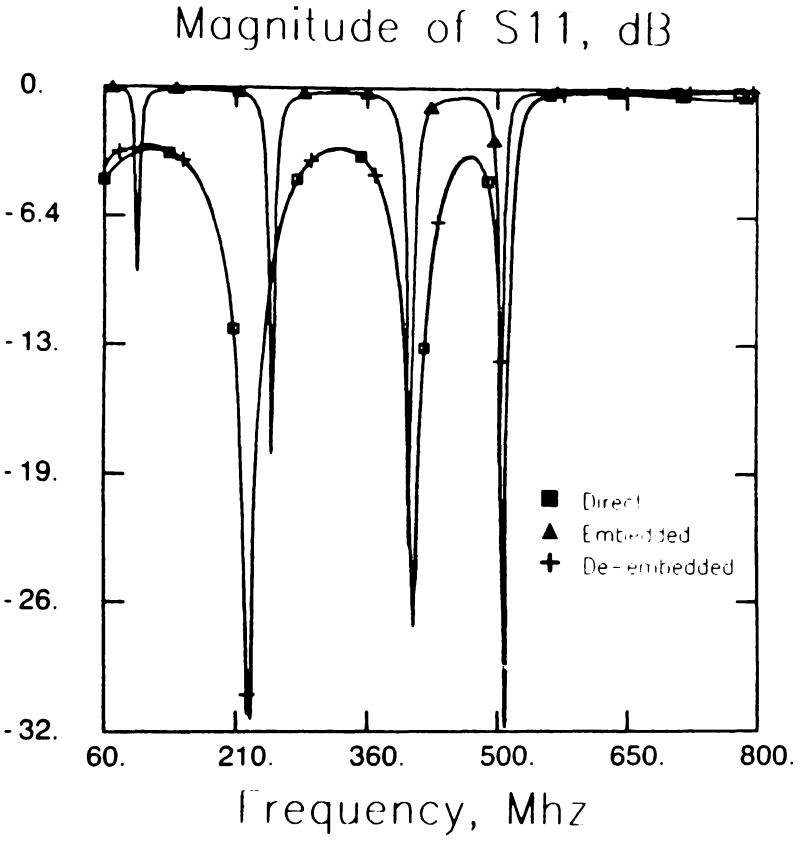

Figure 5.4.6: Magnitude of the filter S_{11}, ($\square$) direct measurement and ($\triangle$) embedded.

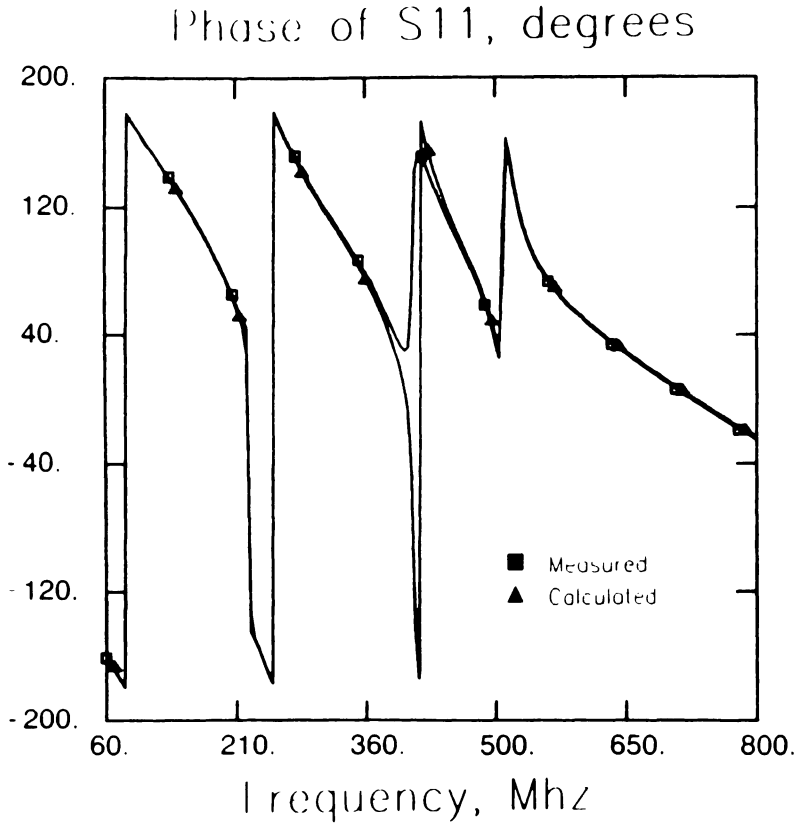

Figure 5.4.7: Phase of the filter S_{11}, (□) direct measurement and (△) embedded.

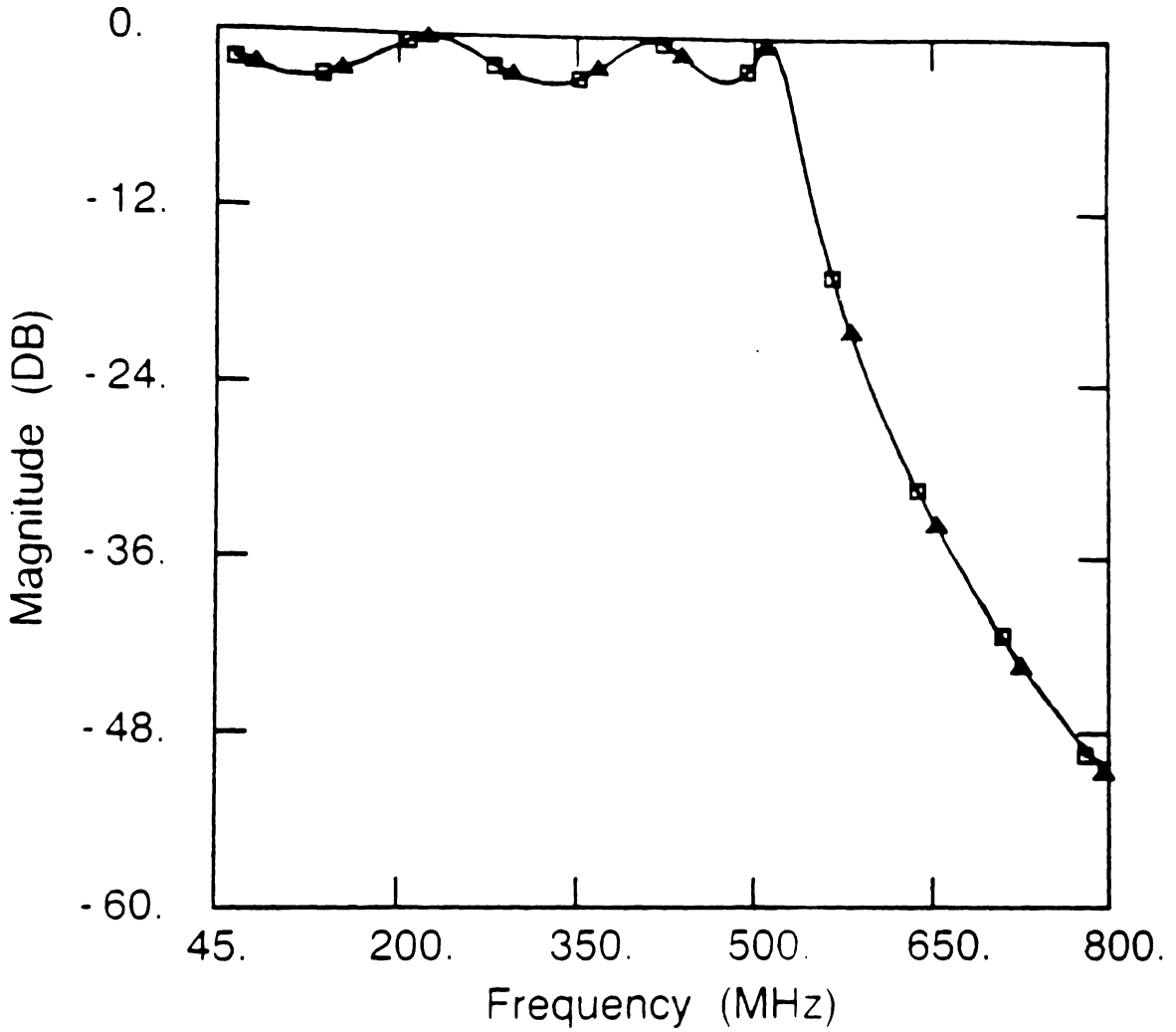

Figure 5.4.8: Magnitude of the filter S_{21}, (□) direct measurement and (△) de-embedded.

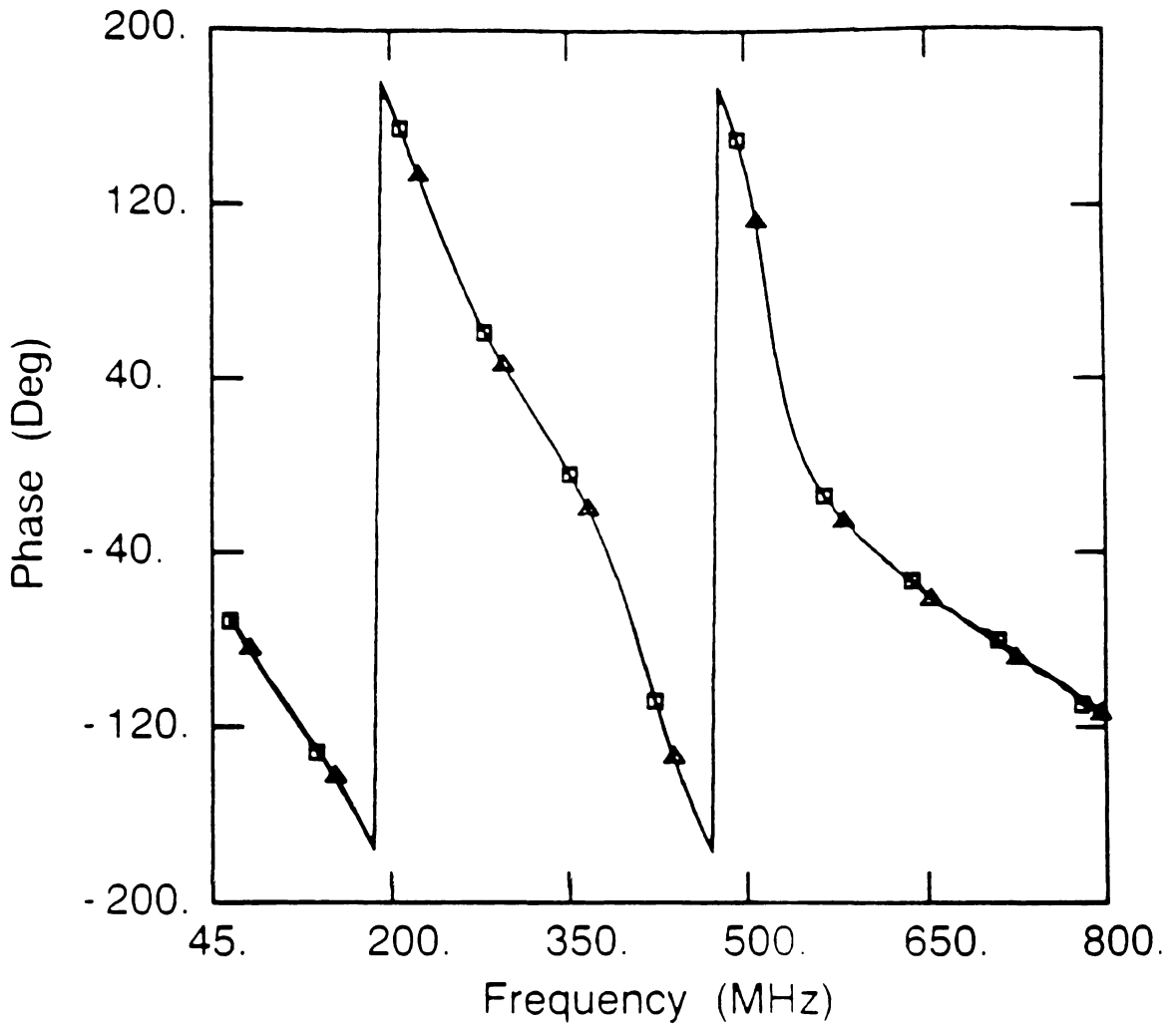

Figure 5.4.9: Phase of the filter S_{21}, (□) direct measurement and (△) de-embedded.

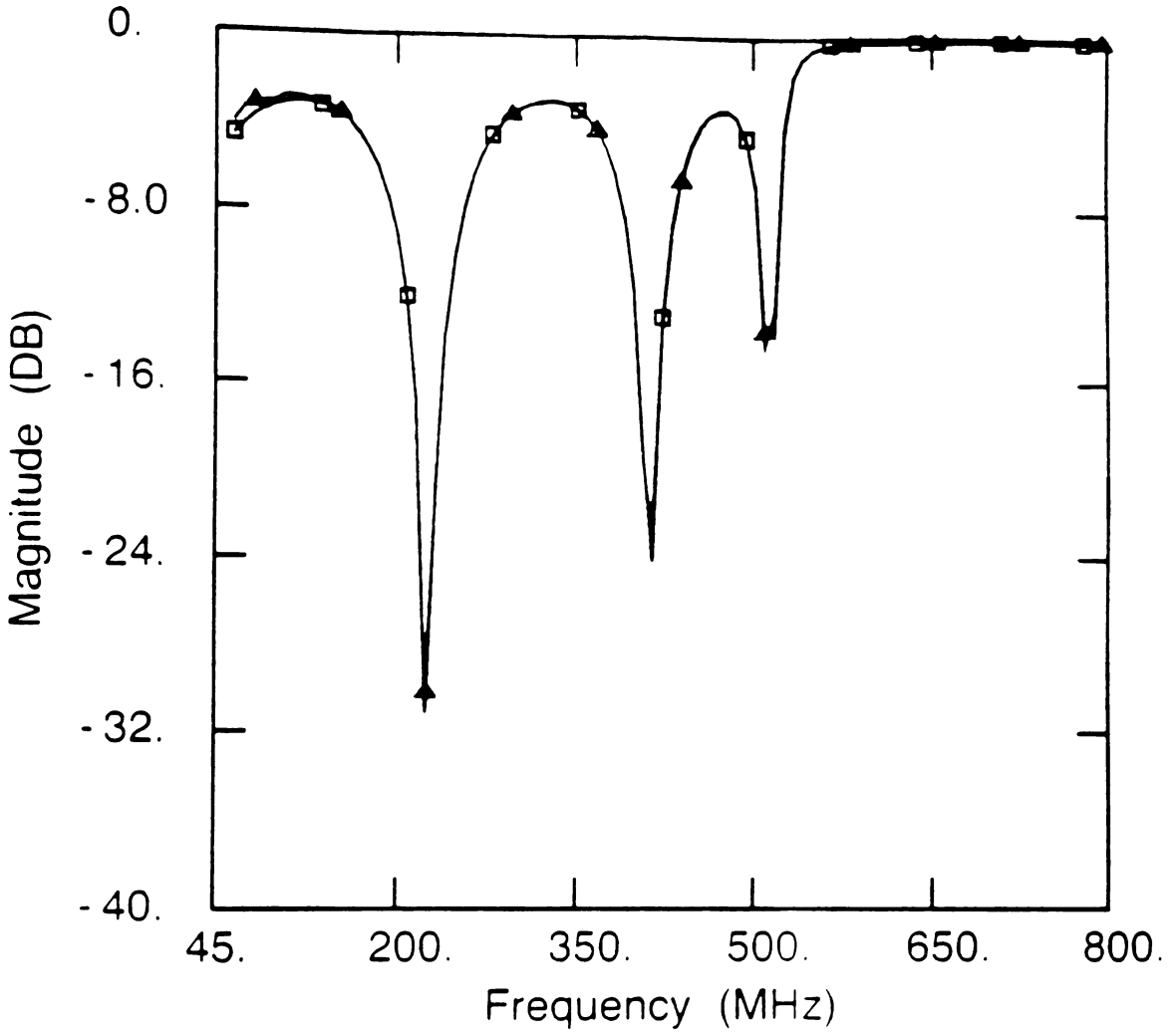

Figure 5.4.10: Magnitude of the filter S_{11}, (□) direct measurement and (△) de-embedded.

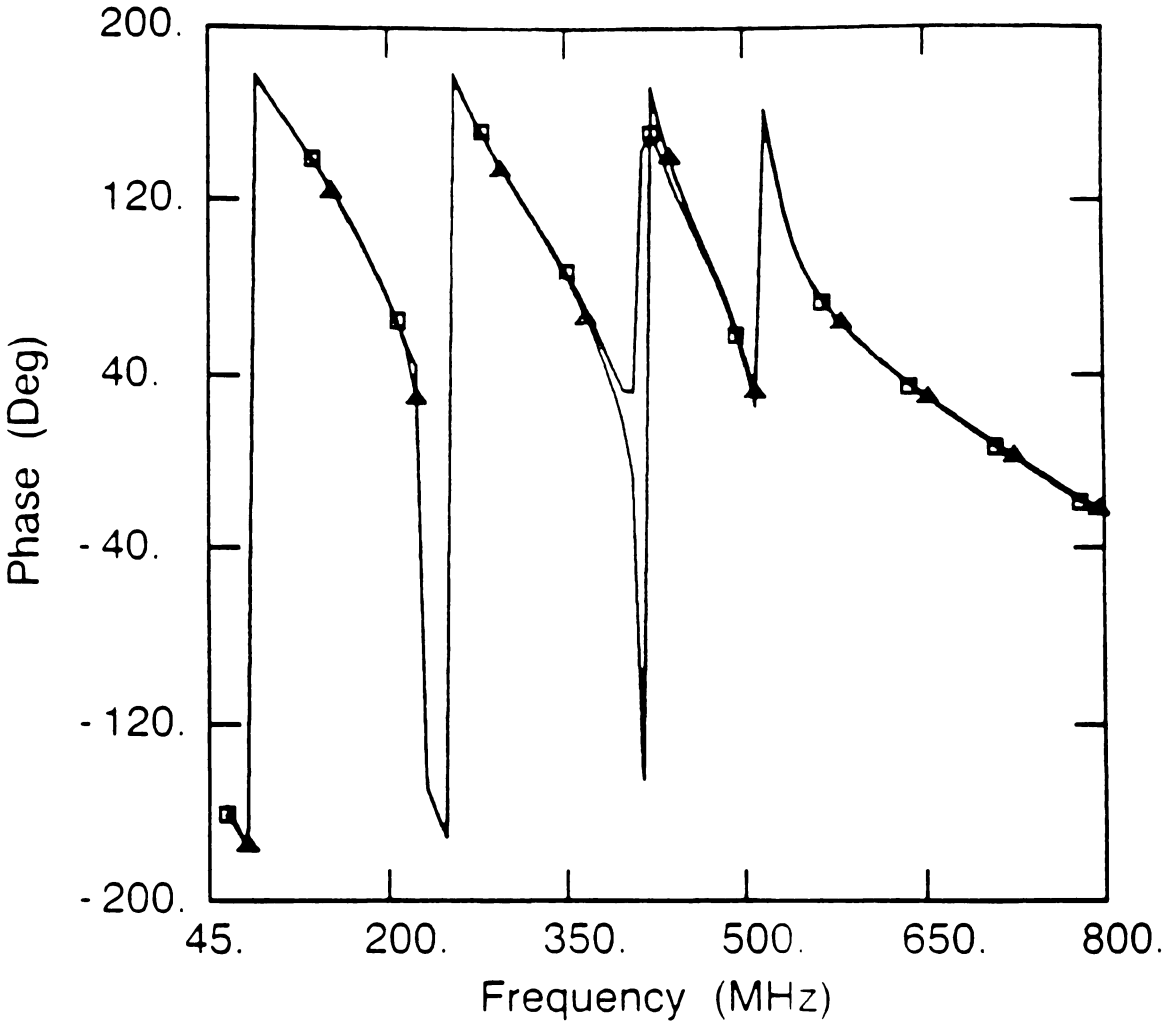

Figure 5.4.11: Phase of the filter S_{11}, (□) direct measurement and (△) de-embedded.

5.4.4 Conclusion

This section has shown that when a fixture is second order symmetric, TSF can be used to remove the fixture error from a DUT. TSF algorithm is not with out singularities however they did not influence this measurement because they existed beyond the measurement range.

5.5 conclusion

In this chapter we have presented experimental results for each of the symmetrical de-embedding methods developed in Chapter 3. TSL and ETSL were applied to a embedded microstrip fixture and the impedance enhancement to TSL was verified with a 50 ohm coaxial example. The complex characteristic impedance of an embedded microstrip was calculated and this result is not a function of symmetry and is directly applicable to TRL and LRL de-embedding methods.

It was also shown that TSF can be used to de-embed a second order symmetric fixture. This was accomplished by designing a second order fixture with essentially a lumped element. The next chapter concludes the work done here and hopes to encourage others to pursue symmetrical arguments when considering fixture design.

Chapter 6

Conclusion

6.1 Summary

The objective of this study was to study calibration of automatic network analysis. This work consists of two parts: the organization of existing calibration methods, and development of fixture calibration methods that address printed circuit board concerns.

In the first part, the exiting methods were organized by categorizing calibration methods into one or two port error models. Two port error models were further divided to automatic network analyzer models and fixture models. To complete the categorization calibration standards used for by previous authors were presented and discussion of their motivation was given.

In the second part of this study, symmetrical calibration methods were developed to combat the non-insertable nature of printed circuit board measurement, i.e. use a minimum number of standards and do so without physically inserting them. Through-Symmetry-Line was possible because the PCB fixture was symmetric allowing a third standard to be synthesized from two standards namely the through and line. The synthesized short circuit was experimentally verified

indicating that symmetry can be used to reduce the number of standards.

TSL was enhanced by calculating the complex characteristic impedance of the line standards. In order to verify this enhancement, a precision 50 ohm coaxial air line was measured and its transmission line parameters were calculated. Excellent agreement between expected coaxial parameters an calculated validate the enhancement. The transmission line parameters for an embedded microstrip were subsequently determined. This enhancement is not a function of the symmetry and can be applied to TRL and LRL de-embedding methods. Both TSL and ETSL were used to de- embed the pi equivalent circuit of a PCB via. Finally, their result was compared and the difference noted.

The final symmetrical method, Through-Symmetric Fixture was applied to directly measurable fixtures and embedded device (low pass filter). Again excellent agreement between measured and calculated responses show that TSF is successful at removing error from a second order fixture. In all cases, SPANA was used to implement the algorithms and present the data for this report.

6.2 Discussion

In general, calibration of network analysis models the systematic error of the measurement system. Under most circumstances the random measurement error is negligible but random process that effect the uniformity of transmission lines should be considered. This further strengthens the desirability to reduce the

standards needed.

Most new methods have been developed out of need. If a matched load cannot be fabricated then consider another standard to replace it. Having a review of existing techniques allows one to chose the most accurate method. When investigating a new measurement system it is valuable to keep a "what if we use a ..." attitude when selecting standards. In addition, by using a two tier calibration method the choice of algorithms is bountiful.

6.3 Suggestion for Further Study

Additional areas of study include:

i) effect of random variation of transmission line parameters on de- embedding results, and

ii) applying symmetrical de-embedding methods to wafer probe calibration.

References

[1] G. A. Deschamps, "Determination of reflection coefficients and insertion loss of a waveguide junction," *J. Appl. Phys.*, vol. 24, pp. 1046–1050, August 1953.

[2] J. E. Storer, L. S. Sheingold, and S. Stein, "A simplified calibration of two-port transmission line devices," *Proc. of the IRE*, vol. 41, pp. 1004–1013, August 1953.

[3] F. L. Wentworth and D. R. Barthel, "A simplified calibration of two-port transmission line devices," *IRE Trans. Microwave Theory Tech.*, pp. 173–175, July 1956.

[4] S. J. Mason, "Feedback theory – further properties of signal flow graphs," *Proc. of the IRE*, vol. 44, pp. 920–926, 1956.

[5] R. A. Hackborn, "An automatic vetwork analyzer system," *Microwave J.*, pp. 45–52, May 1968.

[6] I. Kasa, "Closed-form mathematical solutions to some network analyzer calibration equations," *IEEE Trans. Instrum. Meas.*, vol. IM-23, no. 4, pp. 399–402, December 1974.

[7] H. C. Heyker, "The choice of sliding load positions to improve network analyser calibration," *Proc. 17th European Microwave Conf.*, pp. 429–434, 1987.

[8] W. Kruppa and K. F. Sodomsky, "An explicit solution for the scattering parameters of a linear two-port measured with an imperfect test set," *IEEE Trans. Microwave Theory and Tech.*, vol. MTT-19, no. 1, pp. 122–123, January 1971.

[9] R. F. Bauer and P. Penfield Jr., "De-embedding and unterminating," *IEEE Trans. Microwave Theory Tech.*, vol. MTT-22, no. 3, pp. 282–288, March 1974.

[10] M. S. Hodgart, "Microwave impedance determination by reflection-coefficient measurement through an arbitrary linear 2 port system," *Electron. Lett.*, vol. 12, no. 8, pp. 184–186, April 1976.

[11] E. F. Da Silva and M. K. McPhun, "Calibration of microwave network analyser for computer-corrected s-parameter measurements," *Electron. Lett.*, vol. 9, no. 14, pp. 126–128, March 1973.

[12] H. V. Shurmer, "Calibration procedure for computer corrected s parameter characterization of devices mounted in microstrip," *Electron. Lett.*, vol. 9, no. 14, pp. 323–324, July 1973.

[13] J. W. Gould and G. M. Rhodes, "Computer correction of a microwave network analyser without accurate frequency measurment," *Electron. Lett.*, vol. 9, no. 21, pp. 494–495, October 1973.

[14] E. F. Da Silva and M. K. McPhun, "Calibration of an automatic network analyser system using transmission lines of unknown characteristic impedance, loss and dispersion," *Radio Electron. Eng.*, vol. 48, no. 5, pp. 227–234, May 1978.

[15] S. Rehnmark, "On the calibration process of automatic network analyzer systems," *IEEE Trans. Microwave Theory Tech.*, vol. MTT-22, no. 4, pp. 457–458, April 1974.

[16] J. Fitzpatrick, "Error models for systems measurement," *Microwave J.*, pp. 63–66, May 1978.

[17] A. M. Saleh, "Explicit formulas for error correction in microwave measuring sets with switching-dependent port mismatches," *IEEE Trans. Instrum. Meas.*, vol. IM-28, no. 1, pp. 67–71, March 1979.

[18] N. R. Franzen and R. A. Spaciale, "A new proceedure for system calibration and error removal in automated s-parameter measurements," *Proc. 5th European Microwave Conf.*, pp. 69–73, 1975.

[19] B. Bianco, M. Parodi, S. Ridella and F. Selvaggi, "Launcher and microstrip characterization," *IEEE Trans. Instrum. Meas.*, vol. IM-25, no. 4, pp. 320–323, December 1976.

[20] G. F. Engen and C. A. Hoer, "Thru-reflect-line: an improved technique for calibrating the dual six-port automatic network analyzer," *IEEE Trans. Microwave Theory Tech.*, vol. MTT-27, no. 12, pp. 987–993, December 1979.

[21] J. A. Benet, "The design and calibration of a universal mmic test fixture," *IEEE MTT-S International Microwave Symposium Dig.*, pp. 36–41, 1982.

[22] R. Vaitkus and D. Scheitlin, "A two-tier deembedding technique for packaged transistors," *IEEE MTT-S International Microwave Symposium Dig.*, pp. 328–330, 1982.

[23] R. L. Vaitkus, "Wide-band de-embedding with a short, an open, and a through line," *Proc. of the IEEE*, vol. 74, no. 1, pp. 71–74, January 1986.

[24] S. R. Pennock, C. M. D. Rycroft, P. R. Shepherd and T. Rozzi, "Transition characterisation for de-embedding purposes," *Proc. 17th European Microwave Conf.*, pp. 355–360, 1987.

[25] R. P. Meys, "A triple-through method for characterizing test fixtures," *IEEE Trans. Microwave Theory Tech.*, vol. MTT-36, no. 6, pp. 1043–1046, June 1988.

[26] H. J. Eul and B. Schiek, "Thru-match-reflect: one result of a rigorous theory for de-embedding and network analyzer calibration," *Proc. 18th. Europ. Microwave Conf.*, pp. 909–914, 1988.

[27] J. R. Souza and E. C. Talboys, "S-parameter characterisation of coaxial to microstrip transition," *IEE Proc.*, vol. 129, Pt. H, no. 1, pp. 37–40, February 1982.

[28] B. Bianco, A. Corana, S. Ridella and C. Simicich, "Evaluation of errors in calibration procedures for measurements of reflection coefficient," *IEEE Trans. Instrum. Meas.*, vol. IM-27, no. 4, pp. 354–358, December 1978.

[29] J. P. Mondal and T. H. Chen, "Propagation constant determination in microwave fixture de-embedding procedure," *IEEE Trans. Microwave Theory Tech.*, vol. MTT-36, no. 4, pp. 706–714, April 1988.

[30] Hewlett Packard, "Network analysis: applying the HP 8510B trl calibration for non-coaxial measurements," *Product Note 8510-8*, pp. 1–22, 1987.

[31] A. R. Martin and M. Dukeman, "Measurement of device parameters using a symmetric ixture," *Microwave J.*, pp. 299–306, May 1987.

[32] W.J. Getsinger, "Measurement and modeling of the apparent characteristic impedance of microstrip," *IEEE Trans. Microwave Theory Tech.*, vol. MTT-31, pp. 624–632, August 1983.

[33] I. Bahl and S. Stuchly, "Analysis of a microstrip covered with a lossy dielectric," *IEEE Trans. Microwave Theory Tech.*, vol. MTT-28, pp. 104–109, February 1980.

[34] T. Wang, R.F. Harrington and J.R. Mautz, "Quasi-static analysis of a microstrip via through a hole in a ground plane," *IEEE Trans. Microwave Theory Tech.*, vol. MTT-36, pp. 1008–1013, June 1988.

[35] R. D. Pollard and R. Q. Lane, "The calibration of a universal test fixture," *IEEE MTT-S International Microwave Symposium Dig.*, pp. 498–500, 1983.

[36] A. Enders, "An Accurate Measurement Technique for Line Properties, Junction Effects, and Dielectric and Magnetic Material Parameters," *IEEE Trans. Microwave Theory Tech.*, vol. MTT-37, no. 3, pp. 598–605, March 1989.

[37] E. R. Ehlers, "Symmetric Test Fixture Calibration," *IEEE MTT-S International Microwave Symposium Dig.*, pp. 275–278, 1986.

[38] S.J. Mason, "Power gain in feedback amplifiers," *I.R.E. Trans. Circuit Theory*, Vol. CT-1, June 1954, pp. 20–25.

RELATED REFERENCES NOT REFERRED TO IN TEXT:

[39] H. V. Shurmer, "New method of calibrating a network analyser," *Elect. Letters, vol. 6, no. 23, November 1970*, pp. 733–734.

[40] G. F. Engen, "Calibration technique for automated network analyzers with application to adapter evaluation," *IEEE Trans. Microwave Theory Tech., vol. MTT-22, no. 12, December 1974*, pp. 1255–1260.

[41] D. Woods, "Rigorous derivation of computer-corrected network-analyser calibration equations," *Elect. Letters, vol. 11, no. 17, August 1975*, pp. 403–405.

[42] R. A. Speciale, "A Generalization of the tsd network-analyzer calibration procedure, covering n-port scattering-parameter measurements, affected by leakage errors," *IEEE Trans. Microwave Theory Tech., vol MTT-25, no. 12, December 1977*, pp. 1100–1115.

[43] G. F. Engen, "Calibrating the six-port reflectometer by means of sliding termination," *IEEE Trans. Microwave Theory Tech., vol MTT-26, no. 12, December 1978*, pp. 951–957.

[44] A. Baranyi and J. Ladvanszky, "On the Exact S-Parameter Measurement of Active Devices," *Proc. 10th European Microwave Conf., 1980*, pp. 278–282.

[45] L. Gruner, "The Determination of the Scattering Parameters of Microwave N-Port Networks," *IEEE Trans. Instrum. Meas., vol. IM-30, no. 3, September 1981*, pp. 198–201.

[46] J. Dibeneditto and A. Uhlir Jr., "Frequency Dependence of 50-(ohm) Coaxial Open-Circuit Reflection Standard," *IEEE Trans. Instrum. Meas., vol. IM-30, no. 3, September 1981*, pp. 228–229.

[47] P. C. Sharma and K. C. Gupta, "A Generalized Method for De-embedding of Multiport Networks," *IEEE Trans. Instrum. Meas., vol. IM-30, no. 4, December 1981*, pp. 305–307.

[48] K. Brantervik and E. L. Kollberg, "A New Four-Port Automatic Network Analyzer: Part I–Description and Performance," *IEEE Trans. Instrum. Meas., vol. IM-33, no. 7, July 1985*, pp. 563–568.

[49] H. E. Stinehelfer Sr., "Discussion of De-Embedding Techniques Using Time-Domain Analysis," *Proc. of the IEEE, vol. 74, no. 1, January 1986*, pp. 90–94.

[50] P.R. Shepherd and R. D. Pollard, "Direct Calibration and Measurement of Microstrip Structures on Gallium Arsenide," *IEEE Trans. Microwave Theory Tech., vol MTT-34, no. 12, December 1986*, pp. 1421–1426.

[51] J. Curran, "Applying TRL Calibration for Noncoaxial Measurements," *Microwave Systems News & Communication Technology, vol., no., March 1988*, pp. 91-92, 94, 97–98.
8

[52] G. J. Scalzi, A. J. Slobodnik Jr. and G. A. Roberts, "Network Analyzer Calibration Using Offset Shorts," *IEEE Trans. Microwave Theory Tech., vol MTT-36, no. 6, June 1988*, pp. 1097–1100.

[53] D. F. Williams and T. H. Miers, "De-embedding Coplanar Probes with Planar Distributed Standards," *IEEE Trans. Microwave Theory Tech., vol MTT-36, no. 12, December 1988*, pp. 1876-1880.

[54] K. Brantervik, "A New Four-Port Automatic Network Analyzer: Part II–Theory," *IEEE Trans. Microwave Theory Tech., vol. MTT-33, no. 7, July 1985*, pp. 569-575.

[55] L. Dunleavy and P. B. Katehi, "Eliminate Suprises When De-Embedding Microstrip Launchers," *Microwaves & RF, vol., no., August 1987*, pp. 117-118, 120-122.

[56] Hewlet Packard, "Accuracy Enhancement Fundementals," *HP8510 Network Analyser Operating and Programm Manual, 1987*, pp. 165-180, 207-208. **8**

[57] D. Brubaker and J. Eisenberg, "Measuring S-Parameters with the TSD Technique," *Microwaves & RF, vol., no., November 1985*, pp. 97-98, 100-101, 159. **159**

[58] G. Elmore, "De-Embedding Device Data with a Network Analzer," *Microwaves & RF, vol., no., November 1985*, pp. 145-146.

[59] J. G. Evans, "Measuring Frequency Characteristics of Linear Two-Port Networks Automatically," *Bell System Technical Journal, vol., no., May-June 1969*, pp. 1313-1338.

[60] D. Woods, "Reappraisal of Computer-Corrected Network Analyser Design and Calibration," *Proc. IEE, vol. 124, no. 3, March 1977*, pp. 205-211.

[61] S. F. Adam, "A New Precision Automatic Microwave Measurement System," *IEEE Trans. Instrum. Meas., vol. IM-17, no. 4, December 1968*, pp. 308-313.

[62] O. J. Davies, R. B. Doshi and B. Nagenthiram, "Correction of Microwave-Network-Analyser Measurements of 2-Port Devices," *Electron. Lett., vol., no., November 1973*, pp. 543-544.

[63] H. B. Sequeira, M. W. Trippe and R. Jakhete, "A Network Analyzer Calibration Using Redundancy," *Proc. 18th. Europ. Microwave Conf., 1988*, pp. 321-325.

[64] J. G. Evans, F. W. Kerfoot and R. L. Nichols, "Automated Network Analyzers for the 0.9- to 12.4-GHz Range," *Bell System Technical Journal, vol. 55, no. 6, July-August 1976*, pp. 691-721.

[65] V. G. Gelnovatch, "A Computer Program for the Direct Calibration of Two-Port Reflectometers for Automated Microwave Measurements," *IEEE Trans. Microwave Theory Tech., vol. MTT-24, no. 1, January 1976*, pp. 45-47.

[66] L. A. Glasser, "An Analysis of Microwave De-embedding Errors," *IEEE Trans. Microwave Theory Tech., vol MTT-26, no. 5, May 1978*, pp. 379-380.

[67] T. E. MacKenzie and A. E. Sanderson, "Some fundamental design principles for the development of precision coaxial standards and components," *IEEE Trans. Microwave Theory Tech., vol MTT-14, no. 1, January 1966*, pp. 29-39.

[68] R. Q. Lane and G. L. McCollum, "A new sel-calibrating transistor test fixture," *IEEE MTT-S International Microwave Symposium Dig., 1979*, pp. 99-101.

[69] B. Donecker, "Accuracy prediction for a new generation network analyzer," *Microwave J., June 1984*, pp. 127-128, 130-132, 134, 136, 138, 141.

[70] R. Lane, "De-embedding device scattering parameters," *Microwave J., August 1984*, pp. 149-150, 152, 154-156.
54-156

[71] G. R. Simpson and R. Q. Lane, "A microstrip chip carrier and insert for the transistor test fixture," *ARFTG ?? , June 1985*, pp. 144-157.

[72] J. Archer, "Implementing the tsd calibration technique," *Microwave Systems News & Communication Technology, May 1987*, pp. 54, 56, 58, 60-61.
61

[73] M. A. Maury, S. L. March and G. R. Simpson, "Lrl calibration of vector automatic network analyzers," *Microwave J., May 1987*, pp. 387-392.

[74] L. DuBois, "New microstrip fixture and method for de-embedding," *Microwave Systems News & Communication Technology, September 1987*, p. 96, 98, 100.

[75] C. Beccari and U. Pisani, "Automatic discontinuity de-embedding in s-parameter measurement system," *Alta Frequenza, Vol. LVII, No. 5, June 1988*, pp. 249-257.

Appendix A

De-cascading: Removal of fixture error

In this appendix, the equation necessary to remove the de- embed the device under test (DUT) from the fixture is given. All de-embedding results given in Chapter 5 were produced by de-cascading the error networks from the embedded device.

The DUT is inserted between the fixture halves and the embedded s parameters are measured, $[S_{emb}]$. De- embedding is carried out by using cascadable s parameters (t-parameters). These are obtained by application of the standard s to t transform

$$\begin{pmatrix} T_{11} & T_{12} \\ T_{21} & T_{22} \end{pmatrix} = \frac{1}{S_{21}} \begin{pmatrix} 1 & -S_{22} \\ S_{11} & -\Delta \end{pmatrix} \tag{A.1}$$

where,

$$\Delta = S_{11}S_{22} - S_{12}S_{21} \tag{A.2}$$

The error networks **A** and **B** and the embedded DUT are transformed so $[S_A]$ becomes $[T_A]$, $[S_B]$ becomes $[T_B]$, and $[S_{emb}]$ corresponds to $[T_{emb}]$.

After conversion the embedded DUT is given by the following equation.

$$[T_{emb}] = [T_A][T_{DUT}][T_B] \tag{A.3}$$

Pre and post multiplication of this equation with inverses of **A** and **B** yield the T-parameters of the DUT

$$[T_{DUT}] = [T_A]^{-1}[T_{emb}][T_B]^{-1} \tag{A.4}$$

and thus its S parameters

$$\begin{bmatrix} S_{11} & S_{12} \\ S_{21} & S_{22} \end{bmatrix} = \frac{1}{T_{11}} \begin{bmatrix} T_{21} & T_{11}T_{22} - T_{21}T_{12} \\ 1 & -T_{12} \end{bmatrix} \tag{A.5}$$

For first order symmetric fixtures $\mathbf{B} = A^R$ and second order $\mathbf{B} = \mathbf{A}$.

Appendix B

SPANA Semantic Command Description

This appendix is a user's manual for SPANA. Its purpose is to inform the user of the command syntax and the required command line parameters. SPANA is not case sensitive and for clarity this appendix will use bold face characters to indicate command syntax.

Some of the functions require command parameters in addition to the command itself for example.

***dmb2 meas**=1 **type**=1 **dest**=2 **stan**=3

The command parameters provide the function with information. Each command parameter is separated with a space and the argument to the right of the parameter is the data to be passed to the function. The order of command parameters is not important but a complete command line is required. The arguments can be delimited with any white space character. If a command syntax occurs the line will be aborted and a message given.

Help. Example: **help more**

Purpose. HELP is the on-line help facility for listing the commands that are available in SPANA as well as a brief description of each command. The possible help arguments are shown below.

Arguments.

more

page2

```
* help
############################ HELP ##########################

Commands Available:

COMMAND       KEYWORD  DESCRIPTION                 CONTACT

DISPLAY       DISP     Describes Data               Steer
EXTRAPOLATE   EXT      Extrapolates Data            Steer
FFT           FFT      Does FFT on Data             Steer
PLOT          PLOT     Plots data                   Kasten
GET           GET      Reads data from file         S/K
HELP          H or ?   Displays this help file      S/K
PUT           PUT      Outputs data                 Steer

For more information on a command type "keyword" HELP
More information is available by typing HELP MORE
or by typing HELP PAGE2

############################################################
```

```
* help page2
####################### HELP PAGE2 ########################

Commands Available:

COMMAND       KEYWORD  DESCRIPTION                  CONTACT

DE-EMBED     DMB2 or 3 De-embeds DUT data            S/K
BUILD        BLD       Makes standard from data     Kasten
POLAR>RECT   PTOR      Polar to rect conversion     Kasten
RECT>POLAR   RTOP      Rect to polar conversion     Kasten
SYMMETRIZE   SYM       Symmetrize data              Steer
WINDOW       WIN       Smooths Data                 Kasten

For more information on a command type "keyword" HELP
More information is available by typing HELP MORE

############################################################

* help more
####################### HELP MORE ########################

The following input/output commands are available:

read filename  : the file filename is opened for input
read           : the previously opened file is now used for
              input
write filename : the file filename is opened for output
eof            : the input data file is closed
end            : the input data file is temporarily closed
title          : write line to output file
prompt         : write line to terminal
echo on        : the flag prt is set
echo off       : the flag prt is cleared
           If prt is set all lines input are echoed.

############################################################
```

B.0.1 get

Example: **get meas**=1 **file**=dut.s2p **format**=**magang**

Purpose. GET is used to input a measurement set into SPANA.

Arguments.

help

meas = n1

file = filename

format = **magang**

= **a+jb**

MEAS designates the measurement set (n1) that the data will be loaded into. The argument must be less than the maximum number of measurement sets. GET will over write an existing measurement set.

FILE designates the filename from which the data will be read from. The filename can be any acceptable name including a directory path provided the total number of characters is less than thirty.

SPANA allows for text information to be placed above the data. Each line of this text must begin with a comment delimiter (! or #) in the first or second column however the first line in the file is taken as the data identifier and it is used in the PUT and DISPlay functions. Any subsequent comment lines will be ignored and GET will begin reading the data when it encounters the first uncommented line. The data is read in until the end of file is encountered. Below is an example file.

```
! S parameters for DUT (This is an example data identifier)
! This line will be ignored
⋮
1.500  0.015  35.5  0.995  95.4  0.995  95.4  0.02  20.5
⋮
```

If the data is in the frequency or time domain than the independent variable is assumed to be in megahertz or nanoseconds respectively.

FORMAT is an optional parameter that designates the data format in the file. It can be either magnitude-angle form (**magang**) or real-imaginary (**a+jb**). GET defaults to magnitude-angle form if format is not specified. ZC format is used when a characteristic impedance, gamma and permittivity file is to be read in. It is assumed that the input values are in real-imaginary form.

The command **get help** will give the on-line help information about the get function. Reprinted below.

```
############################ GET ##########################

Usage:

  GET HELP
    : This Message

  GET MEASurement_set = n1 FILE=ssssss FORMAT=a+jb
    : GETs MEASurement set n1 from FILE ssssss
    : Input is is Real-Imaginary format

  GET MEASurement_set = n1 FILE=ssssss FORMAT=time
    : GETs MEASurement set n1 from FILE ssssss
    : Input is Magnitude format

  GET MEASurement_set = n1 FILE=ssssss FORMAT=zc
    : GETs MEASurement set n1 from FILE ssssss
    : Input is is Magnitude-Angle format

Note: 1.  If no FORMAT is given magang is assumed
    : 2.  Default units are MHz and nanoseconds

#############################################################
```

B.0.2 put

Example: **put meas**=n **file**=dut.s2p

Purpose. PUT is used to output a measurement set to the terminal screen or to a specified filename.

Arguments.

help

meas = n1

file = filename

inline = n2

option = 1 for option

MEAS designates the measurement set (n1) that will be processed. The argument must be less than the maximum number of measurement sets. If MEAS is the only argument then the measurement set will be put to the terminal screen and attached to the beginning of the data will be the PUT banner.

FILE designates the filename to which the data will be written to. The filename just as for GET can be any acceptable name including a directory path provided the total number of characters is less than thirty. Below are two banners that PUT would attach to the beginning of PUT file.

```
! S parameters for DUT
!-------------------------------------------------
! MEASUREMENT SET   1
!   Two-port S parameters
!   Frequency-Domain Data: Magnitude-Angle Form
!   Number of Frequency points:   1
!   Frequency Interval:   0.   MHz
!   Low  Frequency:    1000.00   MHz
!   High Frequency:    1000.00   MHz
!   Valid Measurement Data
!   Characteristic Impedance:    50.0000
! Identifier:
!   S parameters for DUT
```

```
!
! FREQ          S11              S21              S12              S22
! (MHz)     Mag    Angle     Mag     Angle     Mag     Angle     Mag     Angle
!
1000.0 0.01944 -151.31 0.97351 -102.56 0.97470 -102.43 0.01784  136.54
```

```
! Three port de-embeded result (DMB3).  Part 1 of 3.
!-------------------------------------------------
! MEASUREMENT SET   9
!   Three-port S parameters
!   Frequency-Domain Data: Magnitude-Angle Form
!   Number of Frequency points:   1
!   Frequency Interval:   0.   MHz
!   Low  Frequency:    1000.00   MHz
!   High Frequency:    1000.00   MHz
!   Valid De-embeded Data
!   Characteristic Impedance:    50.0000
! Identifier:
!   Three port de-embeded result (DMB3).  Part 1 of 3.
! FREQ            S11              S12              S13
!                 S21              S22              S23
!                 S31              S32              S33
! (MHz)       Mag    Angle    Mag    Angle    Mag    Angle
!
1000.0000 0.59842 -169.85 0.22104  -33.48 0.21382  -33.49
          0.22104  -33.48 0.75168 -167.80 0.30034  -30.96
          0.21382  -33.49 0.30034  -30.96 0.72729 -168.10
```

The banner that preceds the data depends on measurement statistics (see **displ**ay command for information about possible statistics) with the above examples showing two and three port data. The file format (magang, a+jb, zc or time) is specified by the format type of the measurement set to be written out.

The INLINE argument is used to place the data on one line with the line containing all the data for one frequency or time point. This is default for two port data but may be used for three and four port data output.

OPTION can be used to reduce a ZC format measurement set to only the characteristic impedance and gamma. The option is default to zero and does not reduce if an option value of one is entered the option is executed.

The command **put help** will give the on-line help information about the put function. Reprinted below.

```
############################ PUT ##########################

Usage:

  PUT HELP
    : This Message

  PUT MEASurement_set = n1
    : Types MEASurement on terminal

  PUT MEASurement_set = n1 INLINE
    : Puts results on a single line used with three ports
      and higher

  PUT MEASurement_set = n1 OPTION = n2
    : Outputs results using special option

  PUT MEASurement_set = n1 FILE=ssssss
    : PUTs MEASurement set n1 in FILE ssssss

#############################################################
```

B.0.3 disp

Example: **disp**=1

Purpose. Display is used to list measurement parameters for one set or all.

Arguments.

help

all

n1

If a measurement set number (n1) is given then the measurement statistics will be displayed. Statistics available include the following.

1, 2, 3 or 4 port S or Y parameters

System characteristic impedance

Start/Stop frequency or time

Number of data points

Data status (measured, converted or de-embedded)

Domain of data (frequency or time)

Data format (magang, a+jb)

If the **all** argument is given then statistics will be displayed for all available measurement sets. Below is a sample display output and the on line help for disp (**disp help**).

```
 !-------------------------------------------------
 ! MEASUREMENT SET   1
 !   Two-port S parameters
 !   Frequency-Domain Data: Magnitude-Angle Form
 !   Number of Frequency points:   1
 !   Frequency Interval:   0.00   MHz
 !   Low  Frequency:    1000.00   MHz
 !   High Frequency:    1000.00   MHz
 !   Valid Measurement Data
 !   Characteristic Impedance:    50.0000
 ! Identifier:
 !   S parameters for DUT

#########################  DISPlay  ####################

Usage:

  DISP HELP
    : This Message
  DISP
    : DISPlay data about all Measurement sets
  DISP n
    : DISPlay data about Measurement set n

#############################################################
```

B.0.4 del

Example: **del meas**=1

Purpose. Delete is a house cleaning tool and is used to delete an exiting measurement set making it available for reuse.

Arguments.

help

meas= n1

SPANA will delete the measurement set designated by n1. This deletion is permanent and should be used with caution. Note: **del** does not delete files stored on disk. If **del help** is entered, the on-line help for delete will be displayed and is reprinted below.

```
############################ DEL ##########################

Usage:

  DEL HELP
    : This Message

  DEL MEASurement_set = n1
    : DELetes MEASurement set n1

###########################################################
```

B.0.5 ptor

Example: **ptor meas**=1

Purpose. PTOR is for conversion from polar to rectangular format.

Arguments.

help

meas = n1

MEAS designates the measurement set that is to be converted. This is destructive since the measurement set is overwritten. PTOR will not convert a measurement set if it is currently in magang format. Note: ZC format can be converted however time format can not.

On-line help is available for PTOR by entering **ptor help**. The help message is reprinted below.

```
######################## PTOR ######################
Usage:
  PTOR HELP
    : This Message
  PTOR MEAS_set = n1
#############################################################
```

B.0.6 rtop

Example: **rtop meas**=1

Purpose. RTOP is for conversion from rectangular to polar format.

Arguments.

help

meas = n1

MEAS designates the measurement set that is to be converted. This is destructive since the measurement set is overwritten. RTOP will not convert a measurement set if it is currently in a+jb format. Note: ZC format can be converted however time format can not.

On-line help is available for RTOP by entering **rtop help**. The help message is reprinted below.

```
######################## RTOP ######################

Usage:

  RTOP HELP
    : This Message

  RTOP MEAS_set = n1

#########################################################
```

B.0.7 stoy

Example: **stoy meas**=1 **dest**=2 **rect**

Purpose. STOY is used to convert S parameter sets to Y parameters.

Arguments.

help

meas = n1

dest = n2

rect

magang

MEAS designates the measurement set that is to be converted and the result is place in the DEST measurement set. The default format is that of the MEAS set however by using either RECT or MAGANG arguments the result format can be forced accordingly. Note: This conversion is only valid for S parameter measurement sets.

On-line help is availiable for STOY by entering **stoy help**. The help message is reprinted below.

```
######################## STOY ######################

Usage:

  STOY HELP
    : This Message

  STOY MEAS_set = n1 DEST_set = n2
    : Convert S parameters data to Y parameters
    :   using current format.

  STOY MEAS_set = n1 DEST_set = n2 RECTangular
    : Convert S parameters data to Y parameters
    :   outputing data in complex rectangular form.

  STOY MEAS_set = n1 DEST_set = n2 MAGANG
    : Convert S parameters data to Y parameters
```

```
    :   outputing data in magnitude-angle form.

##########################################################
```

B.0.8 sym

Example: **sym meas**=1 **dest**=2

Purpose. SYM is used to symmetrize the specified measurement set.

Arguments.

help

meas = n1

dest = n2

Symmetrization of a MEAS set is done by replacing 11 and 22 and 21 and 12 with the respective average of the two. The format of the DEST set will be that of the MEAS.

On-line help is availiable for SYM by entering **sym help**. The help message is reprinted below.

```
##################### SYMmetrize ####################

Usage:

  SYM HELP
    : This Message

  SYM MEAS_set = n1 DEST_set = n2
    : Averages data in measurement set n1 and puts
      output in measurement set n2
      Output in columns 1 and 4 = average of data in input
      columns 1 and 4
      Output in columns 2 and 3 = average of data in input
      columns 2 and 3
      Averaging is done in real imaginary form and data is
      returned in the input format.

#####################################################
```

B.0.9 pul

Example: **pul meas**=1 **dest**=2 **every**=10

Purpose. PUL is used to reduce the size of a measurement set.

Arguments.

help

meas= n1

dest= n2

every= n3

MEAS signifies the measurement set to be reduced and DEST set will contain the result. EVERY specifies which data points to take, ie. take EVERY 8th one. Number of DEST points equals integer(number/every).

```
######################## PUL1 ######################

Usage:

  PUL HELP
     : This Message

  PUL MEAS_set = n1 DEST_set = n2 EVERY = n3

############################################################
```

B.0.10 win

Example: **win meas**=1 **dest**=2 **parm**=11 **size**=81

Purpose. Windowing is used to smooth a parameter in an existing measurement set.

Arguments.

help

meas = n1

dest = n2

parm = **11**

= **21**

= **12**

= **22**

size = n3

MEAS designates the measurement set that will be smoothed with the result to be place in the DEST measurement set. Windowing is done on the a+jb form of the PARM that is specified so both real and imaginary or magnitude and phase are smoothed together. The argument PARM is needed to designate which columns of data within the measurement set are to be smoothed. 11, 21, 12, and 22 correspond respectively to columns 1-2, 3-4, 5-6, and 7-8 of the measurement set. This is done so that any data format can be windowed.

SIZE is the width of the window and it is a number of samples and needs to be odd.

On-line help is availiable for WIN by entering **win help**. The help message is reprinted below.

```
######################## WINdow ######################
Usage:

  WIN HELP
    : This Message

  WIN MEASurement_set = n1 DESTination_set = n2
      PARAmeter = ?? window SIZE = n3

  Note:  Window size is an odd number of samples.
#######################################################
```

B.0.11 strp

Example: **strp meas**=1 **type**=logmag **file**=temp.stp **parm**=21

Purpose. STRP is used to generate X-Y data from a specified measurement set.

Arguments.

help

meas = n1

parm = **11**

= **21**

= **12**

= **22**

file = filename

type = **logmag**

= **linmag**

= **ang**

= **real**

= **imag**

MEAS designates the measurement set where the Y data is located with the X data assumed frequency or time depending on the measurement set domain. PARM specifies which column pair to use 11, 21, 12 and 22 for 1-2, 3-4, 5-6 and 7-8 respectively and finally TYPE gives the output format of the Y data. Note: Linmag, logmag and ang types apply to magnitude-angle format data and real and imag types correspond to a+jb format. Time format is either linmag, logmag or real type.

On-line help is availiable for STRP by entering **strp help**. The help message is reprinted below.

```
########################## STRiP ##########################

Usage:

  STRP HELP
    : This Message

  STRP MEASurement_set = n1 FILE=ssssss
       PARM = n2 TYPE = n3
    : Strips parameter either magnitude or phase
      and places along with frequency (x,y) in the
      file designated

###########################################################
```

B.0.12 dmb2

Example: **dmb2 meas**=1 **dest**=2 **type**=4 **h**=5.6 **l**=2000 **w**=8 **t**=3.6

Purpose. DMB2 contains all the two port de-embedding routines and their purpose is to do error correction.

Arguments.

help

meas = n1

dest = n2

error = n3

stan = n4

thru = n5

line = n6

zmeas = n7

reflect = n7

type = **1**

= **2**

= **3**

= **4**

t = ?

w = ?

h = ?

l = ?

eps = ?

zc = ?

The de-embedding routines are executed by providing the required arguments and possibly some optional arguments. The de-embedding types 1-4 require the following; MEAS set, DEST set and TYPE choice and some form of standard

information. The MEAS set contains the raw S parameters of the device under test (dut) and the result or error corrected parameters are placed in the DEST set. If the ERROR set is specified the de-embedding routines will place the error two-port to this measurement set. Only argument semantics will be discussed here with a detail discussion of de-embedding techniques left to the De-embedding Theory section of this manual.

type 1 Microstrip Open-Short-Load

Required arguments.

stan = n4

Type 1 (Microstrip Open-Short-Load) requires a STAN measurement set that contains the reflection coefficients for the three standards (open, short and load or matched termination). This STAN set is generated using the BLD command (see BLD for further information). Of course the result is placed in the MEAS set.

type 2 Through-Symmetric-Fixture

Required arguments.

stan = n4

Type 2 (Through-Symmetric-Fixture) requires a STAN measurement set that contains the through connection measurement of the embedding fixture.

type 3 Through-Symmetric-Line [enhanced]

Required arguments			Optional arguments		
thru	=	n5			
line	=	n6			
			zmeas	=	n7
t	=	?			
			short	=	n7
w	=	?			
			zc	=	?
h	=	?			
eps	=	?			

Type 3 (Through-Symmetric-Line [enhanced]) is a combination of type 3 de-embedding routines. The combinations exist because of the optional arguments.

First the required arguments, type 3 needs two S parameter measurements, THRU set and LINE set, and some physical information; w=microstrip width, t=metal thickness, h=dielectric height and eps=dielectric constant. Note: All dimensions are in mils. The default type 3 calculates the microstrip characteristic impedance (zcmic) based on the physical parameters. This zcmic can be replaced by a fixed impedance ZC=?? or a measurement set ZMEAS. The ZMEAS characteristic impedance is contained in position 11 of the measurement set and is usually generated by type 4 de-embedding. If zcmic is not used w, t, h, eps need not be specified.

The SHORT argument specifies a measurement set that contains the measured reflection coefficient (in the S11 position) with a physical short placed at the microstrip port of the embedding fixture. If SHORT is not specified then the symmetrical option is used. See the De-embedding Theory section for more information.

type 4 Through-Symmetric-Line

Required arguments.

thru = n4

line = n5

t = ?

w = ?

h = ?

l = ?

Type 4 (Through-Symmetric-Line) is used generally to determine the characteristic impedance of the microstrip. This in turn is used with type 3 de-

embedding. Type 4 requires two S parameter measurement sets, THRU set and LINE set as well as the physical parameters w=microstrip width, t=metal thickness, h=dielectric height and l=difference between the physical lengths of the line and thru standards. Reminder, all dimensions are in mils. For example if the thru microstrip is 1000 mils long and the line strip is 3000 mils long one would use 2000 mils as the length (l).

The characteristic impedance, propagation factor (gamma) and effective dielectric constant are outputs of type 4 and are placed in the last available measurement set. Typing **disp all** will inform the user what measurement set this is. This measurement set is assumed empty at all times and any data that may exist there is overwritten by type 4. This measurement set can be PUT just as any normal measurement set however if it is subsequently read in by GET the user will have to specify the FORMAT=ZC option to correctly input the data. See the command descriptions for PUT and GET for further information about this I/O operation.

This finishes the argument semantics discussion and below is a reprint of the on-line help that is available for DMB2 (type **dmb2 help**).

```
############ Two Port De-embedding (DMB2) ############
Usage:

  DMB HELP
     : This Message
  DMB MEAS = n1 DEST = n2 TYPE = n3 ERROR = ?? (opt)

  Type 1:  Microstrip Open-Short-Load
       STAN = n4
  Type 2:  Through-Symmetric-Fixture
       STAN = n4
  Type 3:  Through-Symmetric-Line (enhanced)
       THRU = n4 LINE = n5 W(idth) = ? H(eight) = ?
       T(hicknes) = ? EPSilon = ? ZC = optional
       ZMEAS = n6 (optional) SHORT = n7 (optional)
  Type 4:  Through-Symmetric-Line
       THRU = n4 LINE = n5 W(idth) = ? H(eight) = ?
       T(hicknes) = ? L(ength) = ?
```

Note: All dimensions are in mils

##

B.0.13 bld

Example: **bld open**=1 **shor**=2 **term**=3 **dest**=4

Purpose. BLD is used to build the three termination standard needed for TYPE 1 de-embedding.

Arguments.

help

dest = n1

open = n2

shor = n3

term = n4

OPEN, SHOR and TERM designate the measurement sets that contain open, short and matched termination reflection coefficient measurements respectively. These measurements are located in the S11 position for all three standards.

```
######################## BuiLD ######################

Usage:

  BLD HELP
     : This Message

  BLD OPEN_set = n1 SHOR_set = n2 TERM_set = n3
       DEST_set = n4

#####################################################
```

B.0.14 stop

Example: **stop**

Purpose. Stop is used to exit SPANA

B.0.15 dmb3

Example: Incomplete write up.

Purpose. Three port de-embedding.

```
 ####### DMB3  De-embedding of Three Ports ##############
Usage:

     DMB3 HELP
          : This Message
     DMB3 MEASA1 = n1 MEASB1 = n2 MEASC1 = n3 LOAD1 = n4
          MEASA2 = n5 MEASB2 = n6 MEASC2 = n7 LOAD2 = n8
          DEST   = n9
     Note:  The output will be a three port. Three
          measurement sets are required to store all
          of the parameters.  n9, (n9+1) and (n9+2) are
          used to store the output

 ########################################################

DMB3

PURPOSE:
De-embeds a three port.
```

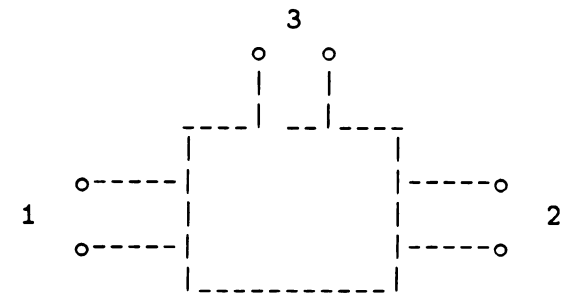

Six two port measurements are required for maximum accuracy.

measa1: Two port between ports 2 and 3 with a termination at port 1
of reflection coefficient fgama.
Port 2 of the three port is connected to port 1 of the network analyzer.

measa2: Two port between ports 2 and 3 with a termination at port 1
of reflection coefficient sgama.
Port 2 of the three port is connected to port 1 of the network analyzer.

```
measb1:   Two port between ports 1 and 3 with  a termination at port
2
      of reflection coefficient fgamb.
      Port 1 of the three port is connected to port 1 of the
      network analyzer.

measa2:   Two port between ports 1 and 3 with  a termination at port
2
      of reflection coefficient sgamb.
      Port 1 of the three port is connected to port 1 of the
      network analyzer.

measc1:   Two port between ports 1 and 2 with  a termination at port
3
      of reflection coefficient fgamc.
      Port 1 of the three port is connected to port 1 of the
      network analyzer.

measc2:   Two port between ports 1 and 2 with  a termination at port
3
      of reflection coefficient sgamc.
      Port 1 of the three port is connected to port 1 of the
      network analyzer.

   The reflection coefficient is passed in two 2 port measurement sets
   arranged as follows.

     load1:
           freq.  |fgama| /_fgama |fgamb| /_fgamb |fgamc| /_fgamc
     load2:
           freq.  |sgama| /_sgama |sgamb| /_sgamb |sgamc| /_sgamc
       e.g.
           1000. 0.090909 0. -0.666666 0. -0.7857 0. 0. 0.

     example:
     files:

 load1.s2p:
 1000. 0.090909 0. -0.666666 0. -0.7857 0. 0. 0.

 load2.s2p:
 1000. 0.16666 0. -0.818181 0. -0.05263 0. 0. 0.

 measa1.s2p:
  1000.00 0.752 -167.520 0.303 -31.421 0.303 -31.421 0.727 -167.821

 measa2.s2p:
  1000.00 0.751 -167.280 0.305 -31.770 0.305 -31.770 0.726 -167.587

 measb1.s2p:
 1000.00 0.627 -175.038 0.137 -21.762 0.137 -21.762 0.788 -175.525
```

```
measb2.s2p:
1000.00 0.653 -177.033 0.093 -15.439 0.093 -15.439 0.839 -178.065

measc1.s2p:
 1000.00 0.639 -176.141 0.118 -18.531 0.118 -18.531 0.842 -176.896

measc2.s2p:
1000.00 0.599 -170.085 0.218 -33.007 0.218 -33.007 0.754 -168.193

-------------------------------------------------------------------
Script of spana session:

spana

 ########################## SPANA ##########################

get meas 1 file=load1.s2p
get meas 2 file=load2.s2p
get meas 3 file=measa1.s2p
get meas 4 file=measa2.s2p
get meas 5 file=measb1.s2p
get meas 6 file=measb2.s2p
get meas 7 file=measc1.s2p
get meas 8 file=measc2.s2p
dmb3 measa1=3 measa2=4 measb1=5 measb2=6 measc1=7 measc2=8 \
load1=1 load2=2 dest=9

 * put meas 9

 ! Three port de-embeded result (DMB3).  Part 1 of 3.
 !-------------------------------------------------
 ! MEASUREMENT SET   9
 !   Three-port S parameters
 !   Frequency-Domain Data: Magnitude-Angle Form
 !   Number of Frequency points:   1
 !   Frequency Interval:   0.   MHz
 !   Low  Frequency:    1000.00   MHz
 !   High Frequency:    1000.00   MHz
 !   Valid De-embeded Data
 !   Characteristic Impedance:    50.0000
 ! Identifier:
 !   Three port de-embeded result (DMB3).  Part 1 of 3.
 ! FREQ            S11              S12              S13
 !                 S21              S22              S23
 !                 S31              S32              S33
 ! (MHz)       Mag    Angle    Mag    Angle    Mag    Angle
 !
 1000.0000 0.59842 -169.85 0.22104  -33.48 0.21382  -33.49
         0.22104  -33.48 0.75168 -167.80 0.30034  -30.96
         0.21382  -33.49 0.30034  -30.96 0.72729 -168.10
```

B.0.16 gain

Example: Incomplete write up.

```
######################## GAIN ######################

Usage:

  GAIN HELP
     : This Message

  GAIN MEAS_set = n1 [GAIN = n2] [MERIT = n3] [NOISE = n4]
     : Get gain, noise and figure of merit information
     : of a decie described by the two-port measurement
     : S parameters in measurement set n1.
     : The gain information is put in set n2 and the
     : figure of merit information in set n3 and the
     : noise information in set n4.
     : The parameters in [] s are optional.

#############################################################
```

B.0.17 sigma

Example: Incomplete write up.

```
###################### SIGMA ######################

Usage:

  SIGMA HELP
     : This Message

  SIGMA MEAS = n1 X = n2 XX = n3 mean = n4 stddev = n5
     : Each entry of measurement set n1 is added to set
       n2 and its square is added to set n3.  From these
       accumulated values the mean (put in set n4) and
       standard deviation (put in set n5) are calculated.
  SIGMA CLEAR X = n2 XX = n3
     : Clears measurement sets n2 and n3

#################################################
```

B.0.18 pie

Example: **pie meas**=1 **dest**=2

Purpose. PIE is used to calculate a pi equivalent circuit for a given S parameter measurement set.

Arguments.

help

meas = n1

dest = n2

MEAS specifies the S parameter measurement set to be converted and the result is placed in the DEST measurement set. It is important to note that the S parameters must be of a network that is accurately modeled by a pi circuit or the results will be erroneous. Below is a reprint of the on- line help that is availiable for PIE (**pie help**).

```
######################## PIE ##########################

Usage:

  PIE HELP
    : This Message

  PIE MEAS_set = n1 DEST_set = n2


#######################################################
```

Appendix C

SPANA "shell" Syntax

The SPANA shell feature is available to prototype user subprograms. The code follows.

```
c.....................................................................
c
c SPSHELL
c
c PURPOSE: Used to impliment special calculations
c
c.....................................................................
c
subroutine spshell(parmx,parmy,parmf,arg,noarg,ident)
c
real parmx(mxarg,mxparm,mxmeas),parmy(mxarg,mxparm,mxmeas)
real arg(mxarg,mxmeas),parmf(mxform,mxmeas)
integer noarg(mxmeas),tmparg
common/parmax/mxarg,mxmeas,mxparm,mxform
c
character*40 str
character*80 ident(mxmeas)
logical kf,fin,prt,ofile,rfile,pecho
common/freerd/nwrite,ntype,aval,ival,ich,kf,fin,prt
```

```
     +                ,ofile,rfile,pecho,str
c
logical lmeas,ldest
integer meas,dest
complex ptor,s11,s22,s21,s12,short,short1,short2
complex open,open1,open2
real ms11,ms22,as11,as22
call fread
c
if(str(1:4).eq.'HELP'.or.str(1:4).eq.'help')then
c   call qsmode(2)
write(ntype,50)
if(prt)write(nwrite,50)
50 format(
     +  ' ######################## SHELL ######################',//,
     +  ' Usage:',//,
     +  '   SHELL HELP',/,
     +  '     : This Message',//,
     +  '   SHELL MEAS_set = n1 DEST_set = n2',//,
     +  '   Options: X = ? Y = ? etc.  input parameters',//
     +  ' ##########################################################')
return
endif
c
c  Reset parameter flags (used to test that all parameters have been
input)
```

```
c
lmeas=.false.
ldest=.false.
c
c  Parse rest of command line
c
100 if(fin)goto 150
if(str(1:4).eq.'MEAS'.or.str(1:4).eq.'meas')then
  call fread
  meas=ival
  if(meas.lt.1.or.meas.gt.mxmeas.or.parmf(3,meas).eq.0.)then
    write(ntype,*)'  Measurment Set not available'
    goto 600
  endif
  lmeas=.true.
elseif(str(1:4).eq.'DEST'.or.str(1:4).eq.'dest')then
  call fread
  dest=ival
  if(dest.lt.1.or.dest.gt.mxmeas)then
    write(ntype,*)'  Destination Set not available'
    goto 600
  endif
  ldest=.true.
endif
call fread
goto 100
```

```
c
c  Check that all parameters have been specified
c
150 if(lmeas .eqv. .false..or.ldest .eqv. .false.)then
  write(ntype,*)' Not enough parameters specified in command line'
  goto 600
endif
c
do 10 n=1,noarg(meas)
c
c  Begin shell calculations here
c
  s11=ptor(parmx(n,1,meas),parmy(n,1,meas))
  s21=ptor(parmx(n,2,meas),parmy(n,2,meas))
  s12=ptor(parmx(n,3,meas),parmy(n,3,meas))
  s22=ptor(parmx(n,4,meas),parmy(n,4,meas))
  ms11=parmx(n,1,meas)
  ms22=parmx(n,4,meas)
  as11=parmy(n,1,meas)
  as22=parmy(n,4,meas)
  short1=s11-s21
  short2=s22-s21
  open1=s11+s21
  open2=s22+s21
  short=(short1+short2)/2.0
  open=(open2+open2)/2.0
```

```
  rtd=180./3.1415927
c
  parmx(n,1,dest)=cabs(short)
  parmy(n,1,dest)=atan2(aimag(short),real(short))*rtd
  parmx(n,2,dest)=cabs(open)
  parmy(n,2,dest)=atan2(aimag(open),real(open))*rtd
  parmx(n,3,dest)=abs(ms11-ms22)
  parmy(n,3,dest)=abs(as11-as22)
  parmx(n,4,dest)=cabs(short2)
  parmy(n,4,dest)=atan2(aimag(short2),real(short2))*rtd
c
  arg(n,dest)=arg(n,meas)
c
10 continue
noarg(dest)=noarg(meas)
c
c  Set-up descripter
c
do 20 i=1,mxform
  parmf(i,dest)=parmf(i,meas)
20 continue
c
c  Identifier
c
ident(dest)='GSC (avg), GOC (avg), Symmetry, GSC (S22)'
return
```

```
c
600 write(ntype,*)' Command Error -- Command Ignored'
return
end
```